

DESIGN AND TELE-IMPEDANCE  
CONTROL OF A VARIABLE STIFFNESS  
TRANSRADIAL HAND PROSTHESIS

by  
ELİF HOCAOĞLU

Submitted to the Graduate School of Sabancı University  
in partial fulfillment of the requirements for the degree of  
Doctor of Philosophy

Sabancı University

August, 2014

Design and Tele-Impedance Control of a  
Variable Stiffness Transradial Hand Prosthesis

APPROVED BY:

Assoc. Prof. Volkan Patođlu  
(Thesis Supervisor)



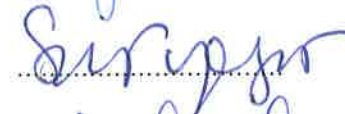
Assoc. Prof. Gll Kızıldaş



Assoc. Prof. Ayhan Bozkurt



Assoc. Prof. Serhat Yeşilyurt



Assoc. Prof. Duygun Erol Barkana



DATE OF APPROVAL:

06.08.2014

*To my parents,  
Leyla & Nurullah Hocaoglu*

© Elif Hocaoglu 2014

All Rights Reserved

DESIGN AND TELE-IMPEDANCE  
CONTROL OF A VARIABLE STIFFNESS  
TRANSRADIAL HAND PROSTHESIS

Elif Hocaoğlu

ME, Ph.D. Dissertation, 2014

Thesis Supervisor: Assoc. Prof. Volkan Patoğlu

Keywords: Transradial Prosthesis, Under-actuated Hand Design,  
Tele-Impedance Control, sEMG Interface, Variable Stiffness Actuation

**Abstract**

According to the World Health Organization, only about the half of upper extremity amputees receive prosthetic limbs and only the half of this group consistently use their prosthetic limbs. The prominent reasons that hinder widespread adaptation of prosthetic devices are their high cost, non-intuitive control interface and insufficient dexterity for performing activities of daily living. This dissertation aims to address these challenges and presents the design, implementation, experimental characterization and human subject studies of a low cost, customizable, variable stiffness transradial hand prosthesis controlled through a natural human-machine interface.

The transradial hand prosthesis features a low cost, robust, adaptive and lightweight design, thanks to its tendon-driven, under-actuated, compliant fingers and variable stiffness actuation. In particular, the under-actuated compliant fingers feature high dexterity by naturally adapting to different object geometries and provide impact resistance. Antagonistically arranged Bowden-cable based variable stiffness actuation enables independent modulation of the impedance and position of the main tendon of prosthesis. Moreover, Bowden-cable based transmission allows for the actuator/reduction/power module to be opportunistically placed remotely, away from the transradial hand prosthesis, helping significantly decrease the weight of the device. Furthermore, the transradial hand prosthesis, including the compliant fingers, can be implemented through simple and low-cost manufacturing processes, such as 3D printing, and each prosthesis can be customized to ensure an ideal fit to match the needs of the transradial amputee.

The tele-impedance control of the variable stiffness transradial hand prosthesis is performed through a natural human-machine interface based on surface electromyography (sEMG) signals. This interface, together with variable stiffness actuation, enables the amputee to modulate the impedance of the prosthetic limb to properly match the requirements of the task at hand, while performing activities of daily living. In particular, the regulation of the impedance is managed through the impedance estimations extracted from sEMG of intact muscle groups of the amputated arm; this control takes place naturally and automatically as the amputee interacts with the environment, while position of the prosthesis is regulated intentionally by the amputee through sEMG signals collected from the muscles placed under shoulder and chest. The proposed approach is advantageous, since the impedance regulation takes place naturally from task to task or during execution of a single task without requiring amputees' attention and diminishing their functional capability. Consequently, the proposed interface does not require long training periods or interfere with control of intact body segments, and provides amputee with ease of use. The performance of the transradial hand prosthesis under tele-impedance control is experimentally evaluated. Experimental results indicate that both position and stiffness can be adequately estimated using sEMG signals and rendered through variable stiffness actuator of the transradial hand prosthesis.

The effectiveness of task-dependent impedance modulation in increasing amputees' dexterity while interacting with a variety of environments is investigated through a set of human subject experiments. In particular, healthy volunteers are physically attached to the transradial hand prosthesis and are asked to perform several tasks using the prosthesis. The attachment of the prosthesis to the volunteer is designed to ensure realistic scenarios, by allowing interaction forces between the prosthesis and the environment to be appropriately transmitted through the physical couplings, while also ensuring consistent placement of the prosthesis for good hand-eye coordination. Three tasks that demand different levels of human arm impedance are administered: i) a contact force minimization task (low arm stiffness case), ii) a trajectory tracking task (high arm stiffness case), and iii) interaction with a variable impedance environment (modulated arm stiffness case). Experimental results provide evidence that enabling task-dependent impedance modulation significantly improves user performance; hence, the proposed variable stiffness transradial hand prosthesis holds high promise in increasing the dexterity of an amputees while executing activities of daily living, improving their quality of life.

DEĞİŞKEN ESNEKLİĞE SAHİP  
DİRSEK ALTI EL PROTEZİNİN  
TASARIMI VE UZAKTAN EMPEDANS KONTROLÜ

Elif Hocaođlu

ME, Doktora Tezi, 2014

Tez Danışmanı: Doç. Dr. Volkan Patoglu

Anahtar Kelimeler: Dirsek Altı El Protezi, Eksik Eyleyicili El Tasarımı,  
Uzaktan-Empedans Kontrolü, yEMG Arayüzü, Deđişken Esneklığe Sahip  
Eyleyiciler

**Özet**

Dünya Sağlık Örgütüncce yapılan arařtırmalara göre, dünya üzerinde üst ekstremite ampüte bireylerinin yarısı kadarı protez hizmeti alırken, bu grubun da sadece yarısı kadarı istikrarlı olarak protez kullanımını sürdürebilmektedir. Kullanım seviyesindeki düşüşün önde gelen sebepleri arasında, protezlerin günlük aktivitelerin gerçekleştirilmesi sırasında kullanımlarının kolay ve elverişli olmayışları, ve piyasada yüksek fiyatlarla satışı sunulmaları yer almaktadır. Belirtilen problemlerin çözümüne yönelik olarak bu doktora tez çalışmasında, düşük maliyetli, kişiye özel ölçülerde ayarlanabilen, doğal kontrol arayüzü ile kontrol edilebilen deđişken esneklığe sahip transradial el protezinin dizaynı, üretimi, deneysel deđerlendirmesinden bahsedilmiştir.

Transradial el protezi, tendon ile sürülebilen, eksik eyleyicili ve çevreye uyumlu parmaklara sahip olması sayesinde düşük maliyetli, gürbüz, adaptif ve hafiflik özellikleri ile ön plana çıkmaktadır. Özellikle, parmaklar tendon ile sürülen, eksik eyleyicili mekanizmalar olarak tasarlanmış olduğundan deđişik geometrideki objelere adapte olabilir, antagonistik olarak yerleřtirilen ve Bowden-kablo ile tahriklenen deđişken esneklığe sahip eyleyicinin (DESE) sağladığı empedans deđişimini herbir falanksa kolaylıkla aktarabilmektedirler. Kuvvet aktarımının Bowden-kablo yöntemi ile gerçekleştirilmesi eyleyicilerin, redüktör ve güç ünitesinin el protezinden ayrı olarak daha uzak bir bölgede

yerleřtirilmesine imkan sađladıđından, protezin ađırlıđını bđyđk lde azaltmaya yardımcı olur. Bununla birlikte, transradial el protezi, 3D yazıcı gibi retim prosesleri sayesinde kolay ve dđřđk maliyet ile ampute bireyin ihtiyalarına ynelik olarak llendirilerek retiler.

Deđiřken esnekliđe sahip transradial el protezinin uzaktan empedans kontrolđ, yEMG sinyallerinden faydalanılarak tasarlanıř olduđumuz dođal insan-makine ara yřzđ ile gerekleřtirilir. Bu arayřz ile DESE mekanizması, ampute bir bireyin protezin empedansını gđnlđk aktivitenin ihtiyacına ynelik olarak kontrol edebilmesine imkan sađlamaktadır. Protezin empedans deđiřimi ampute bireyin canlı kas grubundan algılanan yEMG sinyalleri tarafından dođal ve otomatik olarak kontrol edilirken, pozisyon deđiřimi ise gđs ve omuz altında yer alan kas gruplarından algılanan yEMG sinyalleri aracılıđı ile ampitenin istemine bađlı olarak kontrol edilir. Bylelikle, nerilen arayřz sayesinde empedans kontrolđ iin vřcudun sađlam kısımlarına mřdahale edilmemiř ve ampute iin kullanım kolaylıđı sađlanmış olur. Mekanik tasarım ve kontrol arayřzđnđn birbiri ile uyumu, ampitenin gđnlđk aktivitelerin ihtiyalarına kolaylıkla adapte olmasını sađlar ve bylelikle protezin kullanımının đrenilmesi iin uzun rehabilitasyon sřreleri gerektirmez. Transradial el protezinin uzaktan empedans kontrolđ deneysel olarak test edilmiřtir. Sonular, pozisyon ve empedans kontrol referanslarının yEMG sinyalleri aracılıđı ile bařarılı bir řekilde hesaplandıđını ve DESE ile transradial el protezinin bařarılı bir řekilde kontrol edildiđini gstermektedir.

Aktiviteye dayalı empedans deđiřiminin ampřtelerin yeteneklerindeki artıřa olan etkisi bir seri insanlı deneyler gerekleřtirilerek incelenmiřtir. Deneyler sırasında, transradial el protezi sađlıklı bireylerin n koluna fiziksel olarak bađlanır ve bađlanan bu protez ile belirlenen grevleri yerine getirmeleri beklenir. Protezin deneđin koluna bađlanması, ampute bir bireyin yařadıđı kořullara yakın bir durumun sađlanması, vre ile etkileřim sırasında dođan kuvvetlerin protez aracılıđı ile bireye aktarılmasına, ve deney sırasında sađlıklı bir el-gz koordinasyonunun sađlanması olanak tanır. Deneyde farklı seviyelerde insan kolunun empedans deđiřimine ihtiya duyan  grev talep edilmiřtir: i) temas kuvvetini křcřltme grevi (yřksek esneklik seviyesi durumu) ii) gidiřizi takibi grevi (dđřđk esneklik seviyesi durumu), ve iii) deđiřken esnekliđe sahip vre ile etkileřim grevi (ayarlanabilir kol esnekliđi durumu). Deneysel sonular greve dayalı empedans deđiřiminin kullanıcının performansını iyileřtirdiđine iřaret etmektedir. nerilen deđiřken esnekliđe sahip transradial el protezi, ampitenin gđnlđk aktivitelerini daha yřksek bir kabiliyet ile gerekleřtirmesi ve yařam standartını iyileřtirmesi ynünden umut vaadedici bir tasarım niteliđi tařımaktadır.

## Acknowledgements

First and foremost, I would like to thank my advisor Volkan Patoglu. It has been an honor to be his first Ph.D. student. I appreciate his throughout support, ideas and funding that made my Ph.D. experience productive as well as stimulating. I am also thankful to him for being an excellent role model as a successful academician and an accomplished engineer.

For this dissertation I would like to thank my dissertation committee members: Assoc. Prof. Gullu Kiziltas, Assoc. Prof. Ayhan Bozkurt, Assoc. Prof. Serhat Yesilyurt and Assoc. Prof. Duygun Erol Barkana for their time, interest, and insightful questions and helpful comments. I would also like to thank Assoc. Prof. Mujdat Cetin for his advice and collaboration for the study of EEG based Brain Computer Interface.

I would like to acknowledge the funding sources that made my Ph.D. possible. My research was partially supported by Tubitak Grants 107M337, 109M020, Marie Curie IRG Rehab-DUET and Sabanci University IRP.

I would like to thank my close friends, Burcu Atay, Rustu Umut Tok, Reyhan Ozerturk, Vildan Ozerturk, Ilknur and Yasser El-Kahlout, Kubra Karayagiz, Gulnihal Cevik, Atia Shafique, Vildan Bayram, Isil Berkun, Meltem Elitas, and Emrah Deniz for providing support and friendship. I would also like to thank my team members from Human Machine Interaction Laboratory, Ahmetcan Erdogan, Gokay Coruhlu, Hakan Ertas, Abdullah Kamadan, Mustafa Yalcin, Besir Celebi, Aykut Cihan Satici, Melda Ulusoy, Mine Sarac, Hammad Munawar and my colleague from Brain Computer Interface Group, Ela Koyas. I am in debt to many of my colleagues in the Mechatronics Laboratory for their friendship and support, especially Alper Yildirim, Omer Kemal Adak, Alperen Acemoglu, Ahmet Fatih Tabak, and Merve Acer. I want to thank to mechatronic laboratory intern, Ali Bayraktar to help me during my human subject experiments.

Lastly, I would like to thank my family for their love, support, patience and encouragement. My parents, Leyla and Nurullah Hocaoglu who raised me with love and taught me the importance of empathy and supported me in all my pursuits. I am grateful to my brother, Assoc. Prof. Emre Hocaoglu for all the support, encouragement and medical guidance. I would like to thank my spouse, Ertugrul Cetinsoy for his love and support during my Ph.D. I would also like to thank my twin nephews, Omer and Ali Hocaoglu to bring me good luck with their births by attending to my life during the hardest times in my Ph.D.

# Contents

<b>1</b>	<b>Introduction</b>	<b>1</b>
1.1	Contributions of this Dissertation . . . . .	7
1.2	Organization of the Dissertation . . . . .	10
<b>2</b>	<b>Mechanical Design of the Transradial Hand Prosthesis</b>	<b>12</b>
2.1	Mechanical Design of Antagonistic Variable Stiffness Actuator	18
2.2	Modeling of Expanding Contour Cam for Quadratic Stiffness .	19
2.3	Evaluation of VSA under Control . . . . .	23
2.4	Implementation of Transradial Hand Prosthesis . . . . .	26
2.5	Implementation of Compliant Fingers . . . . .	27
2.6	Fabrication of Transradial Hand Prosthesis . . . . .	28
2.7	Characterization of Transradial Hand Prosthesis . . . . .	31
<b>3</b>	<b>sEMG-based Tele-Impedance Control of the Transradial Hand Prosthesis</b>	<b>42</b>
3.1	Tele-Impedance Control of a Variable Stiffness Transradial Hand Prosthesis . . . . .	48
3.2	Joint Stiffness Model . . . . .	50
3.3	Stiffness Estimation through sEMG Signals . . . . .	54
3.4	Compensation against Muscle Fatigue . . . . .	60
<b>4</b>	<b>Experimental Evaluation of the Variable Stiffness Transradial Hand Prosthesis</b>	<b>67</b>
4.1	Setup and Experimental Procedure . . . . .	67
4.2	Illustrative Experimental Results . . . . .	71
4.3	Discussion . . . . .	72

<b>5</b>	<b>Human Subject Experiments to Investigate Efficacy of Stiffness Modulation</b>	<b>83</b>
5.1	State of the Art . . . . .	84
5.2	Overview of the Human Subject Experiments . . . . .	86
5.3	Experiment Design . . . . .	87
5.3.1	Experiment Setup . . . . .	87
5.3.2	Tasks . . . . .	94
5.3.3	Experimental Procedure . . . . .	99
5.4	Preliminary Results . . . . .	102
5.4.1	ANOVA Results of The Experiments . . . . .	103
5.4.2	Contact Force Minimization Performance . . . . .	104
5.4.3	Trajectory Tracking Task Performance . . . . .	105
5.4.4	Interaction with a Variable Impedance Environment Task Performance . . . . .	106
5.5	Discussions . . . . .	107
<b>6</b>	<b>Conclusions and Future Works</b>	<b>110</b>

## List of Figures

2.1	The expanding contour design in half size . . . . .	20
2.2	Solid model of Antagonistically driven VSA mechanism (a)The representation of VSA from angular perspective (b)Components of VSA Mechanism . . . . .	33
2.3	Schematic model of the antagonistically driven VSA finger mechanism . . . . .	34
2.4	This set-up is designed to verify the working principle of the VSA mechanisms. VSA mechanisms are connected to a simple pivot to control its stiffness and position independently and simultaneously. . . . .	34
2.5	This graph presents a response of the VSA mechanism to a sinusoidally changing position input when the stiffness reference is set to a constant level. . . . .	35
2.6	This graph presents a response of the VSA mechanism to a sinusoidally changing stiffness input when the position reference is set to a constant level. . . . .	35
2.7	This graph presents a response of the VSA mechanism to a sinusoidally changing stiffness input when the position reference gradually increases. . . . .	36
2.8	a)Movable pulleys transfer equal amount of tension on each tendon cable b)Schematic representation of the actuation in hand . . . . .	36
2.9	Solid modeling of the antagonistic VSA driven compliant transradial hand prosthesis . . . . .	37

2.10	Finger characteristics and responsible components are presented. (a) Top of (a) represents bone-like structures which provide stability of finger structure when stiffness is varying, namely prevent buckling towards outside palm. Bottom of (a) shows elastic joints which represents different stiffness characteristics by changing the joint width size (Jws). In (b), back view of the finger is demonstrated with soft fingerpads, which are placed on each phalanx of the finger to increase the stiffness between object and fingers and provide more stable grasping. .	38
2.11	A cross-section of a compliant finger design . . . . .	39
2.12	Actuation of the finger . . . . .	39
2.13	Fabrication process of the elastic joint fingers . . . . .	40
2.14	Assembly of hand prosthesis viewed from different perspectives (a) Top View of the Hand Prosthesis (b)Rear View of the Hand Prosthesis (c) The View of Inside of The Hand . . .	41
3.1	The control interface of the VSA prosthetic hand: In the first module, raw sEMG signals are measured from the intact forearm and relevant groups within the remaining thumb musculature and a series of filters are applied. In the second module, the desired position and stiffness levels are estimated from the filtered sEMG signals. Finally, the closed loop position and stiffness control of the variable stiffness prosthetic hand is handled by the third module. . . . .	49
3.2	Biomechanical system with the pivot at the elbow joint . . . .	55

3.3	The biceps and triceps muscles are employed for the stiffness regulation in (a), while trapezius and pectoralis major muscles are employed for position estimation in (b). . . . .	57
3.4	sEMG signal flow: Raw sEMG signals are bandpass filtered and full wave rectified. Then, these signals are averaged with 0.5 second moving window and an envelope detector is employed.	58
3.5	Signal processing of raw sEMG signals: On the top graph, the effect of bandpass filtering is presented. The graph in the middle shows rectified (red), moving averaged (green), enveloped (black) sEMG signals. The graph at the bottom depicts the normalized sEMG signal. . . . .	59
3.6	Result of linear regression analysis to estimate the indices of $\kappa$ and $\lambda$ . . . . .	61
3.7	Experimental results of average fatigue characteristics of biceps and triceps muscles . . . . .	64
3.8	Experimental results of average fatigue characteristics of biceps and triceps . . . . .	66
4.1	Schematic description of the experimental setup . . . . .	75
4.2	Stiffness Modulation of Hand through PC Workstation. Here, gray zone represents the results of each trial. The blue line represents the average value of ten trials. . . . .	76
4.3	Position Control of Hand through PC Workstation. Here, gray zone represents the results of each trial. The blue line represents the average value of ten trials. . . . .	77

4.4	Stiffness Modulation of Hand through sEMG Signals. Here, gray zone represents the results of each trial. The blue line represents the average value of ten trials. . . . .	78
4.5	Position Control of Hand through sEMG Signals. Here, gray zone represents the results of each trial. The blue line represents the average value of ten trials. . . . .	79
4.6	Grasping objects with different geometric properties . . . . .	80
4.7	Grasping objects with different geometric properties . . . . .	81
4.8	Grasping objects with different materials . . . . .	82
5.1	Schematic representation of the experimental setup . . . . .	88
5.2	a)Schematic representation of the interaction among prosthetic device, haptic interface and virtual environment b) The relation between haptic interface and the virtual environment . . .	90
5.3	The control interface of the VSA prosthetic hand: In the first module, raw sEMG signals are measured from the intact forearm and relevant groups within the remaining thumb musculature and a series of filters are applied. In the second module, the desired position and stiffness levels are estimated from the filtered sEMG signals. Finally, the closed loop position and stiffness control of the variable stiffness prosthetic hand is handled by the third module. . . . .	92
5.4	Representation of the Contact Force Minimization Task (a) Interaction between the hand prosthesis and haptic interface (b) Representation of physical (haptic interface) and virtual environment . . . . .	96
5.5	The Model of the Trajectory Tracking Task . . . . .	98

5.6	Representation of the Trajectory Tracking Task in Virtual Environment . . . . .	99
5.7	The Model of Interaction with a Variable Impedance Environment Task . . . . .	100
5.8	Representation of the Interaction with a Variable Impedance Environment Task in Virtual Environment . . . . .	101
5.9	Schematic representation of the experiment design. Experiment consisted of 4 sessions: Low Stiffness (LS) Level, Intermediate Stiffness (IS) Level, High Stiffness (HS) Level, and Varying Stiffness (VS) Level. Capital T represents the task training period before each session. Each session contains 5 subsessions, while each subsession has 5 trials. . . . .	103
5.10	Box Plot of the Contact Force Minimization Task Performance	105
5.11	Box Plot of the Trajectory Tracking Task Performance . . . .	106
5.12	Box Plot of the Interaction with a Variable Impedance Environment Task Performance . . . . .	107

## List of Tables

2.1	Material Specifications . . . . .	30
2.2	Energy Expenditure of the Transradial Hand Prosthesis . . . . .	31
2.3	Specifications of the Transradial Hand Prosthesis . . . . .	32
3.1	Estimation Results of Impedance Parameters . . . . .	60
5.1	Summary of significance measured by ANOVA for average RMS values . . . . .	104

# Chapter 1

## 1 Introduction

There are more than two million people in the world living with the limb loss. However, a rare percentage of this group uses prosthetic limbs in their daily lives. In particular, World Health Organization reports that only about the half of upper extremity amputees receive prosthetic limbs and only the half of this group consistently use their prosthetic limbs. Besides, many people with an upper-limb amputation prefer to use prosthesis only part time, for specific tasks, or not at all. The first reason discouraging amputees is that the commercially available prosthetic hands are both physically and mentally demanding. Their non-intuitive control interface and insufficient dexterity during the activities of daily living (ADL) are the major reasons for the regression in demand. Moreover, acquiring a relatively dexterous prosthetic hands is very costly and many amputees cannot afford such devices. The available low-cost designs could not satisfy the requirements of ADL. To address these challenges, currently several research groups are working towards developing low-cost but dexterous hand prosthesis, inspired by the biomechanical properties of the human hand and control architecture behind the neuromusculoskeletal system.

When we examine the human hand with a biomechanical perspective, one of its striking features is its underlying tendon drive mechanism. In a human

hand, each joint is driven by separate muscles. This allows hand to achieve a high level of dexterity. However, since design of fully-actuated hand prosthesis are complex and their control require high computational effort, this property cannot be effectively integrated into hand prosthesis. More importantly, more dexterity though many actuated degrees of freedom necessitates nonintuitive control interfaces that demand high level of intention from the amputee to control the each joint of the hand. Such non-intuitive control interfaces require long training periods such that amputees can learn the use of prosthetic hand. On the other hand, instead of full actuation, utilizing the property of tendon driven technique of the natural hand with under actuation can result in quite feasible prosthetic hand designs. Under-actuated designs can help diminish the learning period for prosthesis control, necessitate noteworthy less energy and thanks to their lightweight and ease of use, they can encourage the use of prosthetic hands by amputees.

The other remarkable property of hand biomechanics is its elastic nature. This feature helps the hand to be impact resistant and self-adaptive to the environment. Such compliance can be adapted to the hand prosthesis designs with the aid of today's manufacturing processes, such as 3D printing and deposition based manufacturing. Using elastic elements in design of prosthesis can help achieve robust, lightweight and low cost designs for amputees, while 3D printed parts can be easily customized for personalization of these devices for better fit to the needs of amputees.

Impedance modulation capability of human hand/limb is another aspect of human biomechanical system that helps achieve its high level of dexterity. The dexterity of the natural hands can be imitated by integrating the impedance modulation aspect of human limbs into prosthetic devices. In re-

cent studies, this idea has been embedded into the design of hand prosthesis using different approaches. Some research groups implemented varying impedance of hand prosthesis through active impedance control. However, this approach has limitations in terms of the control bandwidth, as the actuators and prosthesis behaves like a rigid body over this bandwidth. Besides, in this approach, controllers and actuators are continuously in use to regulate the interaction forces; therefore, the system is not energy efficient. More recently, it is observed that merely software based impedance modulation does not satisfy the demands of the amputees. Hence, hardware based modulation techniques based on *variable stiffness actuation (VSA)* are developed. VSA is promising technique to modulate impedance level of prosthetic limbs. By mimicking the working principle of antagonistic muscle groups in human hand, VSA can modulate the impedance and position of the joint independently and simultaneously.

The control strategy of the human neuromuscular system provides the ability to adjust mechanical impedance of the limbs to the required level based on various kind of tasks [1–6]. In particular, the desirable impedance for the task of discovery in unknown environments is regulated as low impedance. Multi-directional stiffness and damping levels of the limbs are changed through the antagonistic muscles to stabilize the limbs against perturbed or unbalanced environments. The reflexive response to unexpected situations is also a part of neuromotor control architecture to assist the stability of human-object interaction. These properties enable humans actively and naturally contribute to the effective control of interaction with a varying environment. Controlling mechanical impedance of hand makes various kinds of manipulations possible. For instance, drilling a hole or painting with brush

needs high level impedance of the limb, whereas holding an egg or a piece of cotton requires a low level of impedance to prevent damage [7]. Thus, the controllability of limb impedance bestows a privilege on humans to realize different human-environment interactions with respect to the available prosthetic hands.

In order to realize more natural prosthesis interface, impedance modulation of hand prosthesis should be performed by human in a natural manner. It is emphasized in the literature that human-based impedance modulation improves the amputee's performance during the ADL [8–10]. As performed in human neuromuscular system, impedance modulation can also be executed utilizing the surface electromyography (sEMG) signals through tele-impedance control [11].

Along these lines, in this dissertation, we present the design and tele-impedance control of a variable stiffness transradial hand prosthesis together with human subject experiments to investigate its efficacy. The variable stiffness transradial hand prosthesis features a low cost, robust, adaptive and lightweight design, thanks to its tendon-driven, under-actuated, compliant fingers and variable stiffness actuation. Thanks to under-actuated compliant fingers, hand prosthesis possesses high dexterity while interacting with the various geometry of objects and is robust against unexpected environment conditions, such as undesired impacts. Moreover, the compliant fingers of the transradial hand prosthesis are implemented with the use of 3D printers to allow for customization to guarantee an ideal fit to match the needs of the transradial amputee. Simple and flexible manufacturing processes used in design help with low-cost and accessibility of the device, while also allowing for personalization.

The tele-impedance control of the variable stiffness transradial hand prosthesis is performed through a natural human-machine interface based on the sEMG signals. The coherence of both variable stiffness actuation and tele-impedance control allows the amputee to naturally adapt to the requirements of ADL by modulating the impedance of the prosthetic hand. In particular, the regulation of the impedance is managed through the impedance estimations extracted from sEMG of intact muscle groups of the amputated arm; this control takes place naturally and automatically as the amputee interacts with the environment, while position of the prosthesis is regulated intentionally by the amputee through sEMG signals collected from the muscles placed under shoulder and chest. The proposed approach is advantageous, since the impedance regulation takes place naturally from task to task or during execution of a single task without requiring amputees' attention and diminishing their functional capability. Consequently, the proposed interface does not require long training periods or interfere with the control of intact body segments, and provides amputee with ease of use.

To investigate the effect of human-controlled impedance modulation on amputees' performance of conducting ADL, we have implemented a series of human subject experiments with the variable stiffness transradial hand prosthesis. Three tasks that demand different levels of human arm impedance are administered: i) a contact force minimization task (low arm stiffness case), ii) a trajectory tracking task (high arm stiffness case), and iii) interaction with a variable impedance environment (modulated arm stiffness case). The physical attachment of the variable stiffness transradial hand prosthesis to the human forearm reflects realistic conditions for an amputee during the ADL. Experimental results provide evidence that task-dependent impedance mod-

ulation significantly enhances participant's performance. The results also suggest that tele-impedance control of a variable stiffness hand prosthesis is a promising research direction to improve the amputee's performance during the ADL.

## 1.1 Contributions of this Dissertation

The contributions of this dissertation can be summarized as follows:

- A variable stiffness transradial hand prosthesis is designed and implemented. In particular, an under-actuated tendon based arrangement with compliant fingers is selected as the underlying kinematics of the prosthetic hand. Under-actuation and tendon based transmission provide adaptability to the device, while compliant fingers ensure coordinated closure of finger phalanges to adapt to object geometry. A Bowden-cable based variable stiffness actuator (VSA) featuring antagonistic quadratic springs realized through expanding contour cams is used for independent control of position and impedance of the main actuation tendon of the prosthetic hand. Bowden-cables simplifies power transmission and allow for remote placement of the actuator/reduction/power units to significantly reduce the weight of the device. Variable stiffness actuation allows for user-controlled impedance modulation of the hand together with its position control. Independent and simultaneous position and impedance control performance of VSA is experimentally characterized and successful achievement of independent impedance modulation is verified.
- A natural human-robot interface based on surface electromyography (sEMG) signals is designed and implemented for tele-impedance control of variable stiffness transradial hand prosthesis. In particular, firstly, the reference position and stiffness levels for the prosthesis are estimated through sEMG signals for tele-impedance control. Conse-

quently, the position of the hand prosthesis is regulated intentionally by the amputee through the estimated position of chest and shoulder muscles, extracted from sEMG signals of the trapezius and pectoralis major muscles. Regulation of hand impedance is managed through the impedance measurements of the biceps and triceps antagonistic muscle groups. The impedance regulation of the prosthesis takes place naturally and automatically as the amputee interacts with the environment, without requiring attention of amputees and diminishing their functional capability. Muscle fatigue effect is also compensated for during the real-time use of variable stiffness transradial hand prosthesis. The proposed interface does not require long training periods or interfere with control of intact body segments, and provides amputee with easiness in use. Feasibility studies are conducted and it is demonstrated that human-robot interface together with VSA enable the amputee to modulate the impedance of the prosthetic limb to properly match the requirements of the task at hand, while performing ADL.

- A set of healthy human subject experiments are designed and conducted to investigate the efficacy of user modulated stiffness in increasing performance of amputees while performing ADL. In particular, healthy volunteers are physically attached to the variable stiffness transradial hand prosthesis and are asked to perform several tasks requiring different levels of limb stiffness. Four different conditions are compared: Three of the test cases administered prosthetic hands with constant stiffness set to low, intermediate and high levels, while the last case featured user-modulated stiffness. Statistical evidence from these experiments suggests that the impedance match between the prosthesis

and the task has a significant effect on performance and enabling user-modulated stiffness to match the task requirements significantly improves user performance. Hence, the results provide evidence that proposed variable stiffness transradial hand prosthesis hold high promise in increasing the dexterity of an amputees while executing ADL.

## 1.2 Organization of the Dissertation

This dissertation addresses to design, fabrication, human interface and tele-impedance control of a variable stiffness transradial hand prosthesis. In addition, performance evaluation of the design is presented with a set of human subject experiments.

In Chapter 2, the mechanical design of the variable stiffness transradial hand prosthesis is detailed. Modeling of expanding contour cam for nonlinear spring implementation is formally expressed and its working principle is verified by a physical experiments. Performance of the variable stiffness actuator is evaluated under different experimental scenarios and performance evaluations are presented in this section. Moreover, compliant finger design and its fabrication are also explained in detail.

In Chapter 3, tele-impedance control of the variable stiffness transradial hand prosthesis is presented. Estimation of finger joint stiffness through sEMG signals to be used in the tele-impedance control architecture is explained. Moreover, muscle fatigue effect influencing the sEMG signal characterization and an approach to remedy this effect are detailed in this section.

In Chapter 4, experimental evaluation of tele-impedance controlled variable stiffness transradial hand prosthesis is presented. Two types of experiments are executed. The first one is realized to verify the desired working principle of variable stiffness transradial hand prosthesis. The second experiment provides illustrative studies to demonstrate the capability of the proposed hand.

In Chapter 5, a set of human subject experiments are presented to evaluate the efficacy of the user-modulated impedance on the performance of the

user's ability to perform ADL. In particular, physical and virtual experiment setups are introduced and important differences of this set-up compared to state-of-the-art in the literature are emphasized. Design of various type of tasks requiring different levels of human impedances are explained and the experimental procedure and analysis methods to evaluate performance are discussed. Finally, for each task category, the performance evaluations are presented and the results are discussed.

Finally, Chapter 6 concludes the dissertation with several remarks, discussions and the future research directions.

# Chapter 2

## 2 Mechanical Design of the Transradial Hand Prosthesis

Research and engineering focus on dexterous multi-fingered robot hands [12–27] has increased owing to their contributions on the various range and complexity of the tasks involved with dexterous manipulation over conventional grippers. The limelight of the versatile grasping and manipulation has become realization of their performance in unstructured and varying surroundings. Prehension and compliance of robot hands and prostheses are improved by emulating partially or completely human like hand shape, size, consistency, namely anthropomorphism and manipulation [28] to work even under defined conditions above. Anthropomorphism is an important criteria in the design of robotic end-effectors for the purpose of hand prostheses replaced by the loss of hand [29,30]. Since the tools around the environment, e.g. consoles, keys are designed for the human hand, the human-like hand is the best candidate for the tasks. Anthropomorphic hands, however, have some drawbacks, such as a complex kinematic structure, sophisticated sensing systems, and high cost. On the other hand, dexterity is a quite evident design goal for the hand prostheses as well as robotic hands functionality, prehension and apprehension. Current literature discusses a tradeoff between dexterity and anthropomorphism. Some end-effectors, dissimilar to anthropomor-

phic hands and represent a considerably high dexterity level, are capable of complicated manipulations [29]. As for the matter of hand prostheses, anthropomorphism and dexterity cannot be evaluated separately as they are combined in utilizing human hand functionality, its physical properties and successful manipulations with the environment by means of smart manufacturing techniques and control methodologies. In particular, commercially available hand prostheses are designed and manufactured in consideration of these two important phenomena, anthropomorphism and dexterous manipulation [13–17, 22]. In deed, realizing human manipulation taxonomies [31, 32] is qualified as dexterous if the manipulation is supported with the impedance modulation. In particular, the significant human like property behind successful physical interaction between human and environment arises from their adaptation ability. Compliance to the environmental conditions or activities of daily living that human physically interact with arise from modulating the impedance level based on the varying requirements. During some of the activities requiring high-accuracy position control such as writing, the stiffness level of the fingers increases considerably, likewise manipulation with a soft/fragile environment requires a decrease in the stiffness level of fingers, e.g., manipulating an egg.

Recently, the impedance modulation of human like hands has inspired novel research on the design and control strategies for robotic hands whose goal is to execute such tasks involving interaction with a dynamic environment, especially under unpredictable conditions. Specifically, prostheses can only be reliable and compliant for different characteristics of manipulations if the appropriate impedance level is matched with the task property [33–35]. It is evident that the prosthesis design has to be improved by including a

property of task-dependent impedance modulation in order to enhance amputees' performance throughout their use [8–10]. In literature, property of impedance modulation is integrated into robotic systems in two ways. At first, compliance to the environment can be accomplished through software based approach, such as impedance/admittance control. However, the impedance modulation ability of this approach is limited by the controllable bandwidth of the actuators and prosthesis behaves like a rigid body over this bandwidth [34, 35]. Moreover, software based impedance regulation requires continuous use of actuators and suffers from high energy expenditure. On the other hand, in recent years, impedance modulation is embedded into the robotic systems in passive ways. In this approach, impedance of the robotic manipulator is adjusted through the mechanisms including passive elastic elements, like springs. Series elastic actuators, in the group of hardware based impedance regulation, are designed to improve the compliance of the robotic systems and protect them against shock loads while interacted with environment. This mechanisms promise that output impedance of the artificial limb stays low above the control bandwidth [36]. However, actuators are continuously in use while controlling the interaction forces with SEA and therefore they are energetically inefficient. More recently, hardware based modulation is developed including another mechanism into this group, called *variable stiffness actuators (VSA)*. VSA is proposed to modulate desired impedance level of robotic system. These actuators are utilized for impedance modulation and/or joint rotations when it is required, hence this mechanisms provide energy efficiency. Moreover, the desired impedance can be enforced over the whole frequency spectrum, including frequencies well above the controllable bandwidth of the actuators.

In literature, robotic hands employed for such tasks requiring human machine interaction are designed with VSA mechanisms [18, 37, 38], whereas no such application has been noticed in the field of hand prostheses. In particular, each active degree of freedom of the DLR Hand Arm System is controlled antagonistically by two motors and two elastic elements [37, 38]. Since the joints of the DLR arm system have an adjustable wide impedance band, they can present variable dynamical conditions depending on environmental conditions. Similarly, a natural way of impedance modulation employed in a Shadow hand design which facilitates a smooth and soft motion is realized by antagonistically arranging and pneumatically moveable artificial muscles [18]. In particular, each joint in this system, however, needs respective actuators, that inevitably result in the requirement of huge volume of space. The system, inspired by an anthropomorphic hand mechanism, represents characteristics in common with a dexterous manipulation system ,e.g., a large number of active degrees of freedom, tactile and visual feedbacks, complex control architectures and advanced task planning algorithms. On the other hand, owing to their high cost, sophisticated mechanism design, complex control architecture, and high computational load, the system of the Shadow hand is not preferred in the field of prosthetics. Moreover, weight restrictions, high cost, and complex control design make the Shadow hand use improbable in hand prostheses.

Studies in this field have focused on the simplification of the mechanical design of robotic hands without losing functionality but increasing their compliance to the environment. Underactuation provides a remarkable feature for a new generation simplified design of hand prostheses. Even though certain parts of the research groups are inclined to develop control of many

degrees of freedom [39–41], the full actuation of each finger joint still requires more progress. In the literature, underactuation is first acquainted for the fingers employing a linkage mechanism [42–45]. Link mechanisms, however, bring together with a large scale in the finger design. In particular, this approach is not well suited to the anthropomorphic prosthetic hand structure. Underactuated mechanism allows fingers to only follow the line trajectory and; accordingly it restrains the dexterity of hand. Some research groups have developed underactuated hands with the integration of electromagnetic joint locking mechanisms and extra motors for each finger, which increase the dexterity of the hand to a certain extent and also provides high speed motion and large actuation force [46, 47]. However, adding more component results in an increase the weight of the hand, power consumption, load on every joint and risk of instability at each joint. In addition, more actuators and sensors require complex control systems, which might be a cumbersome learning period for the disabled person in controlling all of the actuators.

Reducing the number of actuators and employing light weight and compliant materials suitable for mechanical construction, integrating various sensors into the design are important steps in this field. Dollar *et al.* propose a compliant, underactuated, sensor integrated robotic hand whose manufacture is based on the support decomposition manufacturing (SDM) technique [48–50]. Proposed hand can adjust the finger’s shape depending on the geometry of grasping object with the aid of simple control methods, thanks to the underactuated mechanism and elastic joints integrated into the fingers. This system is advantageous in terms of ease of control, cost-effectiveness, functional manipulation even in the unknown environment. However, actuation systems of the proposed hand [48–50] do not modulate its impedance

depending on the environmental conditions.

In this chapter, we present the design, fabrication, and evaluation of a variable stiffness transradial hand prosthesis. VSA mechanisms are designed to serve as an antagonistically arranged artificial muscles which are responsible for the impedance and position modulation of the hand. This mechanism can regulate impedance and position itself independently under quasi-static conditions [51], and can also be opportunistically placed anywhere on the forearm. Mimicking the working principle of an antagonistically arranged muscle groups can be approximated by using spring elements moving on a designed second order surface [52]. Our proposed hand design ensures the compliance of the fingers utilizing the polyurethane material to fabricate compliant joints inside the finger design. Moreover, the compliant finger design provides benefits in terms of simplified manufacturing process, and enhancement in robustness in the event of uncertain conditions, such as impact. The use of silicon rubber instead of metal elements prevents the source of mechanical failures, such as screw blockage, gap in metal bearing and its bed, and elastic joints are not deprived of their functions after any type of contacts. Furthermore, the fingers are designed to be tendon driven, under-actuated mechanisms, which provides opportunity in terms of both adapting the fingers' position based on different object geometry and reflecting impedance modulation supplied by VSA into each phalanges. With these skills, our hand design gains an advantage over the currently available hand prosthesis. The proposed hand prosthesis provides also many benefits in terms of stiffness regulation while handling tasks, ease of control, low-cost manufacturing, light-weight design, and high dexterity in an unpredictable environment.

## 2.1 Mechanical Design of Antagonistic Variable Stiffness Actuator

The design criteria for the variable stiffness prosthetic hand are determined as follows: Variable stiffness hand prosthesis should reflect the both desired position change of human fingers and also impedance variation of human limb. Prosthesis should be capable of grasping a large variety of objects with different geometry (e.g., angled, spherical, cylindrical shapes) and various material properties (e.g., soft or fragile structures, smooth or ragged surfaces). The prosthetic hand should require low computational and mental load for control, but must be fast enough to properly respond to unexpected environmental conditions, such as impacts. The device should be low cost and possess light-weight and low energy consumption to enable long working periods.

In order to address all these requirements, a VSA integrated compliant hand prosthesis is proposed. This mechanism becomes prominent in terms of reflecting the same property of antagonistic muscle groups, i.e., working principle of position and stiffness regulation. The proposed hand consists of five fingers that are connected each other with pulley elements. Each of the tendon driven fingers has three compliant revolute joints. Highly under-actuated hand mechanism has a total of 15 rotational degree of freedom (DoF) controlled through main tendons attached to a Bowden cable based transmissions. Thanks to the Bowden cable based transmission, VSAs are located at remotely, away from the device. Extension, flexion and stiffness variations can be independently controlled through the VSA mechanisms actuated by two DC motor with harmonic drive reduction units. The under-actuated prosthetic hand provides an intermediate solution between dexterous hands

(versatile, high-cost, stable grasp, high computational load) and simple grippers (task-specific design, low-cost, unstable grasps, uncomplicated control). Since the under-actuated hand mechanism has quite less number of actuators than DoFs of the device, the design provides energy efficiency. Moreover, it is self-adaptive and hence does not require intricate control algorithms.

## **2.2 Modeling of Expanding Contour Cam for Quadratic Stiffness**

VSA mechanism preferred in this hand design [51] is proposed and mathematically modeled in literature [52]. It is mathematically proven that VSA mechanism can merely mimic the independent impedance and position control of human limb joint if the characteristics of spring elements inside the VSA are nonlinear [51]. The desired nonlinearity can be obtained using linear spring elements with the use of a cam mechanism representing nonlinearly characterized expanding surface, called expanding contour [52]. When the force is exerted on the linear springs, linear springs extend based on the nonlinear surface; hence, a nonlinear relationship between force and the spring deflection occurs as required. Expanding contour, represented as curve of the gradient of the force versus deflection, is a function of several parameters, including the linear spring constant, maximum and minimum joint stiffness.

As described at the beginning of this section, the idea is reflecting the stiffness variation at fingers's joint of human to that of fingers's joint of prosthesis. In order to match the change in impedance levels of human limb with the hand prosthesis, maximum and minimum joint stiffness values of human finger [53] are utilized. These two design parameters are essential to calculate the required second order equation of the expanding contour.

The prototype of the VSA mechanism is manufactured based on the design presented in [52] and satisfies the upper and lower bounds of the impedance limits of the fingers. However, to save space, rather than implementing the design in [52], expanding contour mechanism is redesigned in vertical direction as half size. This implementation of expanding contour design reduces the size of the mechanism, depends less number of design parameters, simplifying the contour equation, provides considerably more stable movement, enables linear springs to achieve extension without bending and can be easily connected to the hand part of the prosthesis, which are also beneficial to enable placement of the VSA mechanism into the forearm part of transradial amputees.

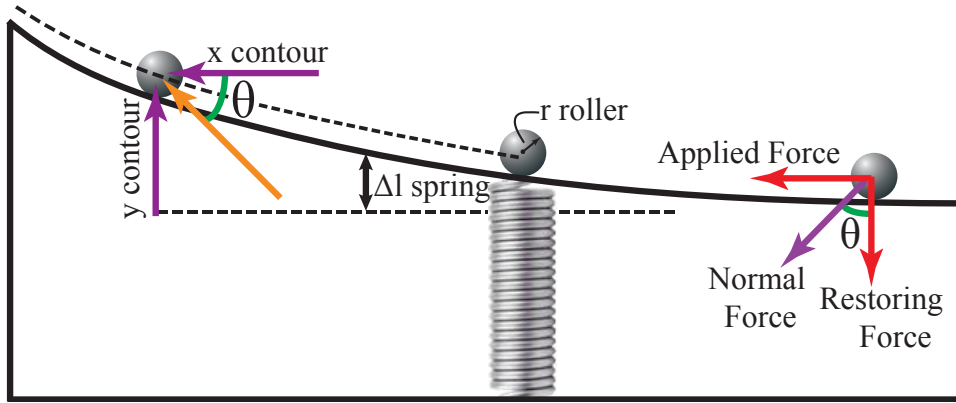


Figure 2.1: The expanding contour design in half size

At the beginning of the motion, preload force of the linear springs are set to zero. In addition, radius of the rollers is selected to be negligibly small compared to the whole mechanism; hence, their effect is neglected in the nonlinear contour equation. As presented in Figure 2.1,  $y$  contour defines the spring elongation during the motion. Hence, the free length of the spring is not taken into account. Here, force-length relationship of elastic elements

are chosen to be quadratic such that

$$F_{app} = ax_{contour}^2 + bx_{contour} + c \quad (2.1)$$

$$F_{restoringforce} = ky_{contour} \quad (2.2)$$

$$\tan(\theta) = \frac{\Delta y_{contour}}{\Delta x_{contour}} \quad (2.3)$$

$$F_{app} = y'_{contour}(x_{contour})F_{restoringforce} \quad (2.4)$$

$$ax_{contour}^2 + bx_{contour} + c = y'_c(x_{contour})(ky_c) \quad (2.5)$$

$$\frac{d(y_c(x_{contour}))}{dx_{contour}}(ky_{contour}) = ax_{contour}^2 + bx_{contour} + c \quad (2.6)$$

$$\int y_c dy_c(x_{contour}) = \int \left[ \left(\frac{a}{k}\right)x_{contour}^2 + \left(\frac{b}{k}\right)x_{contour} + \left(\frac{c}{k}\right) \right] dx_{contour} \quad (2.7)$$

Solution of the differential Eqn. (2.5) is expressed in Eqn. (2.8).

$$y_{contour}^2 - \left(\frac{2a}{3k}\right)x_{contour}^3 - \left(\frac{b}{k}\right)x_{contour}^2 - \left(\frac{2c}{k}\right)x_{contour} - m = 0 \quad (2.8)$$

When the linear springs are at the initial point of the expanding contour, the boundary conditions are introduced as in the expression (2.9).

$$x_{contour} = 0, y_{contour} = 0 \implies m = 0 \quad (2.9)$$

Hence, substituting  $m$  into the Eqn. (2.8) is represented as in Eqn. (2.10).

$$y_{contour}^2 - \left(\frac{2a}{3k}\right)x_{contour}^3 - \left(\frac{b}{k}\right)x_{contour}^2 - \left(\frac{2c}{k}\right)x_{contour} = 0 \quad (2.10)$$

In Eqn. (2.10), required parameters to calculate the expanding contour is  $a$ ,  $b$ ,  $c$  and spring constant of linear springs. Here, parameters of  $a$ ,  $b$  and  $c$  directly depend on maximum and minimum stiffness values of joint [51], which is expressed in Eqn. (2.11).

$$F_{app} = \underbrace{\left(\frac{S_{max} - S_{min}}{4r_j^2 \Delta x_{max}}\right)}_a x_{contour}^2 + \underbrace{\left(\frac{S_{min}}{2r_j^2}\right)}_b x_{contour} - \underbrace{\left(\frac{\Delta x_{max}(S_{max}^2 - 2S_{min}^2)}{8r_j^2(S_{max} - S_{min})}\right)}_c \quad (2.11)$$

In Eqn. (2.11),  $S_{min}$  and  $S_{max}$  represent the minimum and maximum stiffness value of finger joint simultaneously and related joint impedance results used in this study are referred in [53]. When linear springs are unstretched ( $x_{contour} = 0$ ), the joint stiffness is regulated at a minimum level, namely

$S_{min}$ . In addition to this, the time at which both of the linear springs reach maximum stretch, ( $x_{contour} = x_{max}$ ), the joint stiffness is arranged as maximum level, namely  $S_{min}$ . The range of maximum and minimum stiffness values are accepted to be 2177.2 N mm/rad and 527,12 N mm/rad according to literature [53] and the expanding contour is designed depending on the upper and lower bound limits.

Expanding contour design in half is validated through a series of experiments.

### 2.3 Evaluation of VSA under Control

VSA mechanism is employed for the actuation of the five-fingered, under-actuated compliant prosthetic hand via tendons. The hand prosthesis provides grasping and releasing of finger movements through a single main joint. Joint position is determined by two antagonist Bowden cables. Moreover, impedance level of the fingers are determined as a function of the location of linear springs on the expanding contour. Two parameters,  $\alpha$  and  $\beta$  represented in Figure 2.3 are assigned to express the position and impedance control equations of the VSA. Two brushed DC motors with harmonic drive reductions are connected to the VSA mechanisms to control the position and the stretch level of the linear springs. Angular positions of two DC motors,  $\alpha$  and  $\beta$ , are the control inputs responsible for the desired joint stiffness and joint angle,  $\theta$ .

System's control equations are derived under quasi-static conditions of the VSA mechanism. Equilibrium angle of the hand joint ( $\theta_{eq}$ ) is obtained parallel to derivations in [51, 52] and represented in Eqn. (2.12). In Eqn. (2.12),  $\alpha$  and  $\beta$  represent angular position of DC motors,  $\theta$  defines joint angles of

fingers,  $a$  and  $b$  indicate coefficients of second order function belonging to nonlinear spring. External torque,  $\tau_{load}$  applied to the fingers' joint is shown in Eqn. (2.12).

$$\theta_{eq} = \frac{r_m}{2r_j}(\alpha - \beta) - \frac{\tau_{load}}{2r_j^2(ar_m(\alpha + \beta) + b)} \quad (2.12)$$

Equation of joint impedance, namely resistance of joint against angular deviation, is represented in Eqn. (2.13).

$$S = 2ar_mr_j^2((\alpha + \beta) + 2br_j^2) \quad (2.13)$$

Two separate control references belonging to joint position and impedance (later on to be estimated through sEMG signals) are utilized to compute the angular position of the motors by means of the derived equations (Eqn. (2.12) and Eqn. (2.13) under quasi static conditions.

Expanding contour VSA mechanism in Figure 2.2 is connected to a simple pivot to experimentally verify the control performance of the mechanism. The aim is to validate the position and stiffness control of the pivot independently and simultaneously. All possible conditions are tested through the set-up to demonstrate VSA's capability under real-time control. During the experiment three conditions are evaluated sequentially: positions of the fingers are stationary while stiffness is changing; stiffness of the fingers is set to a constant level while the position is varying, and both control parameters are altering simultaneously. The closed loop system includes PD controller and VSA mechanism with the pivot as shown in Figure 2.4. The experimental results in Figure 2.5-2.7 represent the independent and simultaneous position and impedance control of the pivot. In Figure 2.5, the first two figures show that pivot stiffness is set to around a low level of impedance

while the position is changing. The last two graphs represent the behaviors of two actuators. Since motors are placed in parallel each other, as observed from the real-time experiment that when the angular position is controlled motors are rotated in opposite directions. Control reference is given in two different ranges,  $\pm\pi/2$  rad and  $\pm\pi/18$  rad. Both small and big variations, pivot position is successfully executed while independently control the stiffness keeping at a constant level. In Figure 2.6, the exact opposite situation is implemented. As seen from the top two graphs, angular position is kept at zero level while stiffness of the pivot is varying sinusoidally in the range between middle and high level. It is important to notice that DC motors are rotating in the same direction to be able to modulate the pivot stiffness. In Figure 2.7, both references concerning stiffness and angular position are variable. Motor behaviors are affected by both these variations.

## 2.4 Implementation of Transradial Hand Prosthesis

The most significant and distinguishing characteristics of VSA hand prosthesis with respect to the other designs in the literature is its ability to provide impedance modulation under various conditions. Impedance modulation is naturally executed with the aid of a human-machine interface based on sEMG signals. Designed interface allows amputees to adjust the impedance of VSA hand prosthesis to the requirements of activities of daily living. Required references of joint position and impedance are estimated through sEMG signals and employed in the control of VSA hand prosthesis.

In fully actuated robotic hands, the motion of each joint has to be planned and actively controlled to be able to adapt different shape of grasped objects [54]. In spite of this, under-actuated hands, i.e., mechanisms that have fewer number of actuators than degree of freedom, represent passive adaptation property. In this study, the hand prosthesis designed as an under-actuated mechanism and has self-adaptive fingers (in Figure 2.8). It includes 12 DoF elastic joints controlled by two variable stiffness actuators. Force transmission from VSA to the joints realized through the movable pulleys shown in Figure 2.8. Self adaptation makes hand prosthesis capable of enveloping the any shape of objects to grasp without requiring complex control architecture and also releasing object which is an reversible version of self adaptation. As seen from the solid model of the compliant hand prosthesis in Figure 2.9, all system is composed of two main parts. One half is the hand and other part is the arm includes VSA mechanisms. VSA mechanisms are moving backward and forward on the sliders which are hidden in the arm cabinet.

## 2.5 Implementation of Compliant Fingers

Grasping an object with human-like hand requires initial contact at proximal phalanx, following contact at middle phalanx and final interaction at distal phalanx. In order to satisfy this rule in our design, each joint is designed to represent different stiffness levels. Hence, this idea is implemented by using the same materials but different widths of silicone (Figure 2.10 (a)) in such a way that distinguishing stiffness property in each phalanges are obtained. Moreover, compliance of each joint is also provided by means of silicone based material. Utilizing under-actuation and elastic materials, i.e. silicone, our design is soft and self-adaptive. In particular, it is capable of naturally adapting to the shape of different objects. Light-weight is also at the forefront, expanding contour element of VSA mechanism and finger phalanges are produced with the material of ABS plastic. Each finger weighs 17.4 g.

Force transmission plays crucial role in a finger's grasping ability. In this design, flexion requires more effort with respect to the extension of tendons. In particular, one way of increasing force transmission on each phalanx to make finger's grasping easier is to increase the moment arm at phalanges where the force is applied. In Figure 2.11, the cross-section of the finger solid model is depicted. Tendon routing is designed to feature  $120^\circ$  angles instead of straight routing to increase the moment acting on phalanges.

Robustness in tendon driven hand manipulation mainly depends upon taking precautions against loss of force transmission during the extension and flexion of tendons. Desired force transmission on finger through tendons during grasping is presented in Figure 2.12. The amplitude of tension level on flexion tendon should be equal to amplitude of tension level on extension ten-

don during the no load action. However, during the transmission, force loss is inevitable due to friction and moment requirements of compliant fingers. If finger is not appropriately designed, cable slack may occur. To prevent loss of force transmission the moment effect on silicon rubber is increased by placing this elastic material to the upper level of the finger. Hence, when the finger is under the load, required force level to bend the rubber is diminished and force loss caused by friction is partially compensated.

## **2.6 Fabrication of Transradial Hand Prosthesis**

Variable stiffness compliant hand fabrication can be examined mainly in two parts: palm and fingers. Owing to the intricate design of phalanges and also second order surface of VSA expanding contour, simple and low-cost manufacturing solution is handled with the use of a 3D prototyping machine. Thanks to 3D printing technology, each prosthesis can be customized to ensure an ideal fit to match the needs of the transradial amputee. Prosthesis entitled the compliance property with the integration of elastic material is fabricated after several processes. Figure 2.13 details the main steps of the manufacturing process to produce the compliant hand fingers. Phalanges corresponding to stiff parts of the fingers and molds are produced in a 3D printer with 100 micron resolution as presented in Figure 2.13, Part-a. In Part-b of Figure 2.13, mold is employed both for providing precise position arrangement for phalanges and fingers, and for defining accurate location to be used for injecting a highly-adhesive silicone rubber in liquid form. Other component in the mold, carbon fiber strip is utilized for constraining the motion of twisting, while permitting the bending of the finger in one direction. In particular, during the stiffness variation of fingers, polyurethane materials

would like to move any weak resistance direction, such that fingers lose their anthropomorphic structure and also self-adaptive properties. Besides, carbon fiber is durable enough to resist buckling and is appropriate for requirement of light-weight material selection for finger structure. Thumb and the other fingers are produced in separate molds. Four fingers are produced in a mold to ensure good alignment of the fingers with respect to each other. Tendon holes on the phalanges are closed with a strip to prevent polyurethane flow inside them. Before pouring the silicon resin, a release agent is used to prevent cured polyurethane from bonding to mold surfaces and to help easy release of the part from crinkled-shaped mold. In Part-c, polyurethane material is injected into the mold. While pouring the silicon rubber, bubbles may be produced and cause inhomogeneous material distribution in the joints. If this problem is not prevented, elastic joints do not gain desired characteristics. Degassing process shown in Part-d is introduced to prevent such gaps in the silicon rubber and is realized inbetween  $-0.7$  and  $-0.2$  bar. The cure time for the resin is kept as about 12 hours at standard room temperature. The complete manufacturing process takes approximately 13 hours. In the fingers, three different materials are used: for stiff links (phalanges), a white ABS plastic; for elastic joints, SILASTOSIL® 28-700 FG (terrasilicone, Istanbul); for the motion limiter, epoxy resin infused with a single-layer of carbon fiber. Table 2.1 represents the material properties of the elastic joints. When rubber cure is completed, it is removed from the mold as shown in Part-e.

During the stiffness regulation of the fingers, both extension and flexion tendon work simultaneously. Because of the elastic joints inside the fingers when stiffness level reaches at high level, fingers tend to buckle into a side where the net force around the joint is positive. In order to prevent such

Table 2.1: Material Specifications

SILASTOSIL® 28-700 FG	
Hardness Shore A	
ISO 868	28
Tensile Strength ( $N/mm^2$ )	
ISO 37	6,5
Elongation at break (%)	
ISO 37	700
Tear Strength ( $N/mm^2$ )	
ASTM D 624 B	> 30
Viscosity at 23°C	
after stirring (mPa.s), ISO 3219	10,000

bending caused by stiffness modulation, especially towards the reverse side of the palm, bone-like structures are used on the finger surface as shown in Part-e. They allow bending towards the palm, and permit the opening of fingers until the constraints provided by the bone-like structures, mimicking human hand finger behavior. The fully assembled VSA mechanism and under-actuated hand mechanism is presented in Figure 2.14.

The touch surface of the fingers contains a soft finger pad produced with the same material as in elastic joints. The soft finger pad increases the friction and provides more stable grasps without slip [55, 56]. Since the mechanism is highly under-actuated, the same soft material is used in the elastic joints to allow grasping without requiring much force. Otherwise, closing the hand necessitate more effort if more viscous silicon rubber is used. More viscous

Table 2.2: Energy Expenditure of the Transradial Hand Prosthesis

Energy [J]		
	Low Impedance	High Impedance
Power Grasp	3,5	5,7
Pinch Grasp	2,6	5,1
Impedance Change (Low to High Impedance)	4,4	

silicon rubber also negatively effects the independent stiffness and position control performance of the hand. In our design, the drawbacks of soft elastic material choice are eliminated with the aid of carbon fiber strip and bone-like structure components used in fingers.

## 2.7 Characterization of Transradial Hand Prosthesis

The energy expenditure of the transradial hand prosthesis differs depending on the grasp types. In Table 2.2, the energy requirement of the hand prosthesis for different conditions is presented. Here, power grasp presents the grasping of cylindrical objects, which require the contacts of all phalanges of the hand. Moreover, the study of pinch grasp is realized grasping the object with the aid of distal phalanges only. The energy requirement of two commonly used conditions with this hand prosthesis is observed for two different impedance levels. Furthermore, the portion of the impedance variation on energy consumption is presented in the Table 2.2 and shows that energy is mostly consumed when the impedance is regulated from low to high level.

In Table 2.3, minimum and maximum force, speed requirement of the hand prosthesis are presented. The ranges are determined based on the difficulty levels of the task at hand. Moreover, the weight of the transradial hand prosthesis is the almost half weight of the natural human hand with

Table 2.3: Specifications of the Transradial Hand Prosthesis

Min Main Tendon Speed	3 mm/s
Max Main Tendon Speed	26 mm/s
Min Main Tendon Force	20 N
Max Main Tendon Force	157 N
Min Elastic Joint Stiffness	132 Nmm/rad
Max Elastic Joint Stiffness	544 Nmm/rad
Min Grasp Speed	0,19 Hz
Max Grasp Speed	1,64 Hz
Weight	1,1 kg

arm [57, 58]. It provides easiness in use for amputees while carrying the prosthesis. Since its size and configuration can be customized upon amputee's request, the battery unit can be embedded into the arm section in order to match the real arm weight.

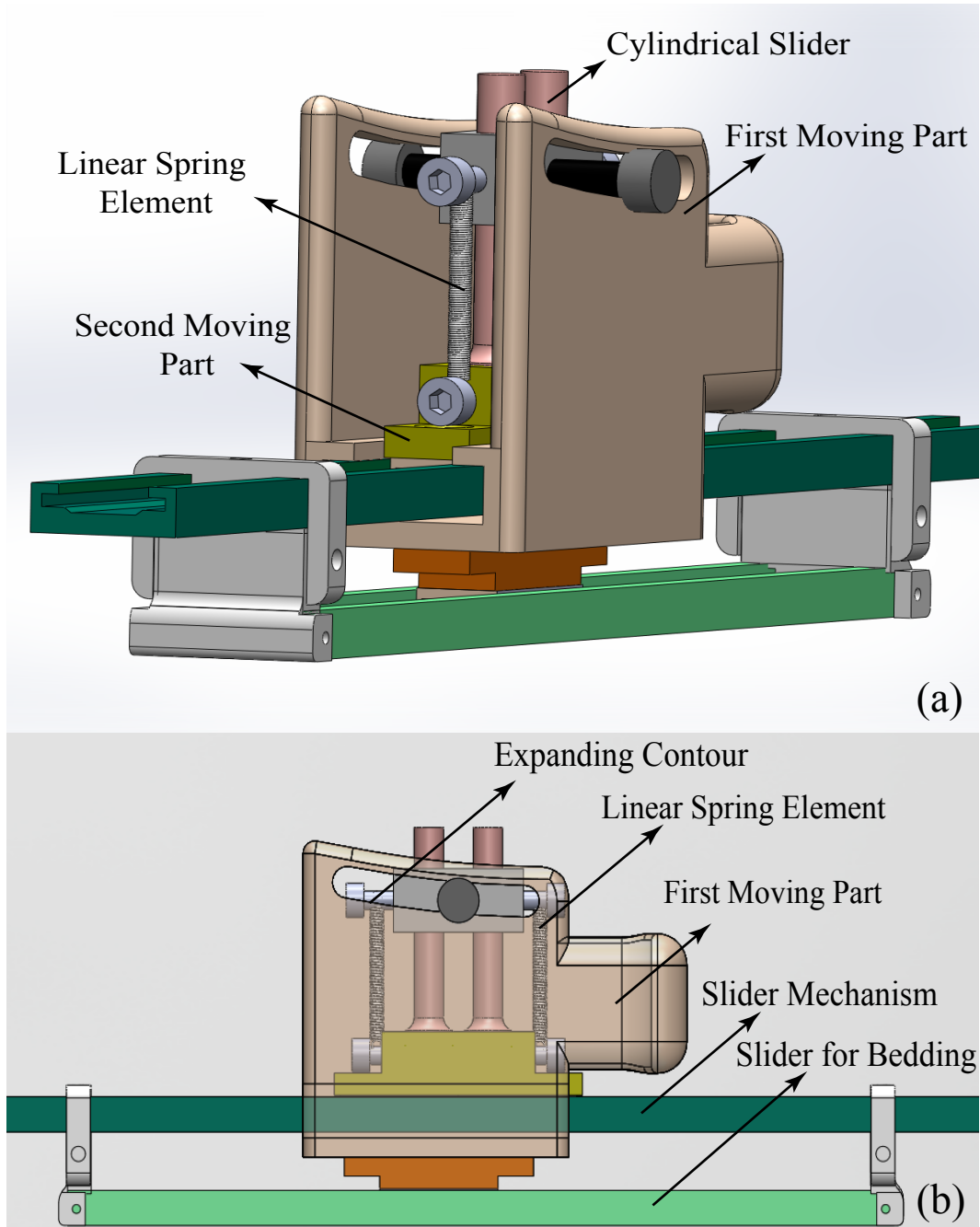


Figure 2.2: Solid model of Antagonistically driven VSA mechanism (a)The representation of VSA from angular perspective (b)Components of VSA Mechanism

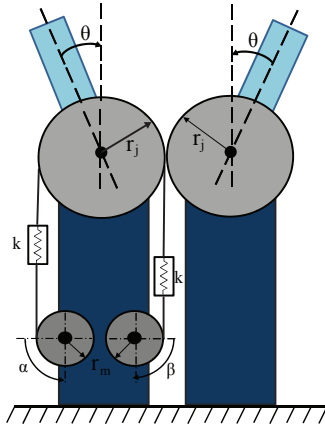


Figure 2.3: Schematic model of the antagonistically driven VSA finger mechanism

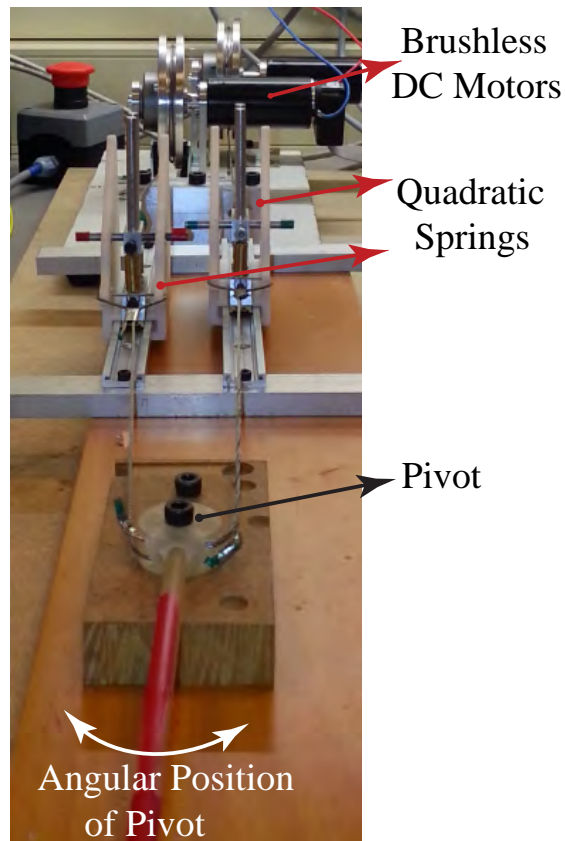


Figure 2.4: This set-up is designed to verify the working principle of the VSA mechanisms. VSA mechanisms are connected to a simple pivot to control its stiffness and position independently and simultaneously.

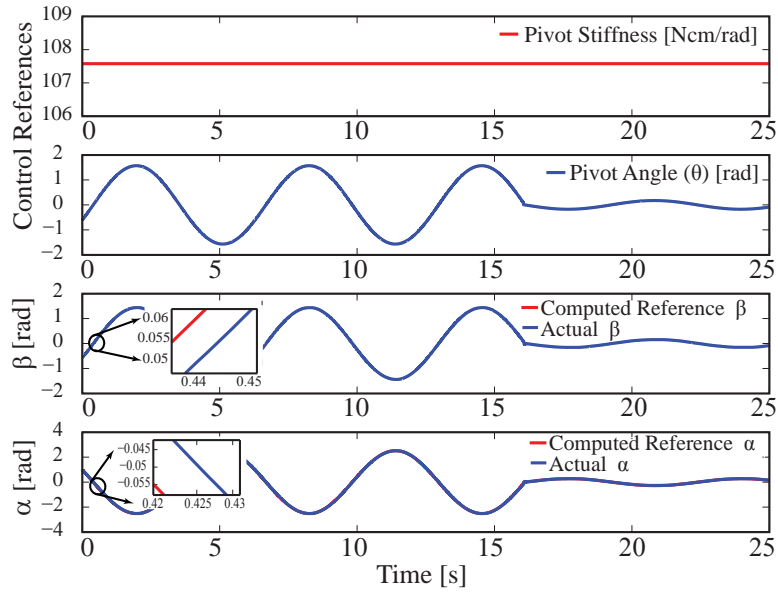


Figure 2.5: This graph presents a response of the VSA mechanism to a sinusoidally changing position input when the stiffness reference is set to a constant level.

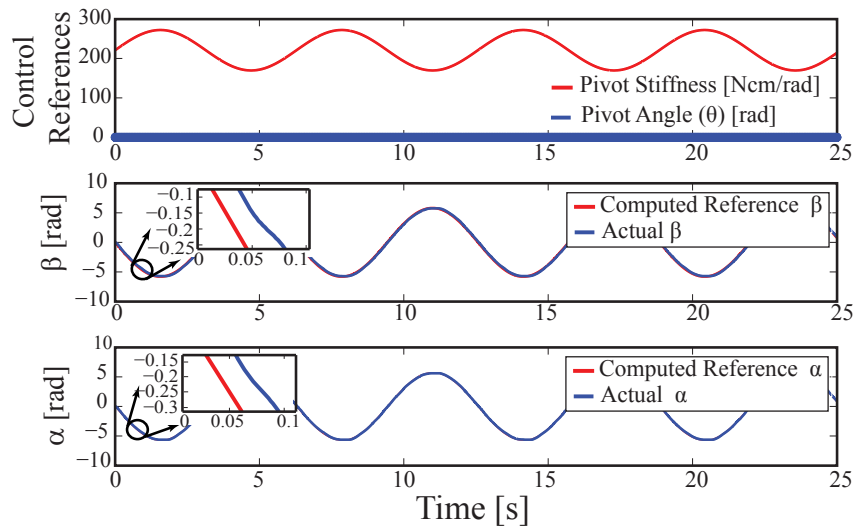


Figure 2.6: This graph presents a response of the VSA mechanism to a sinusoidally changing stiffness input when the position reference is set to a constant level.

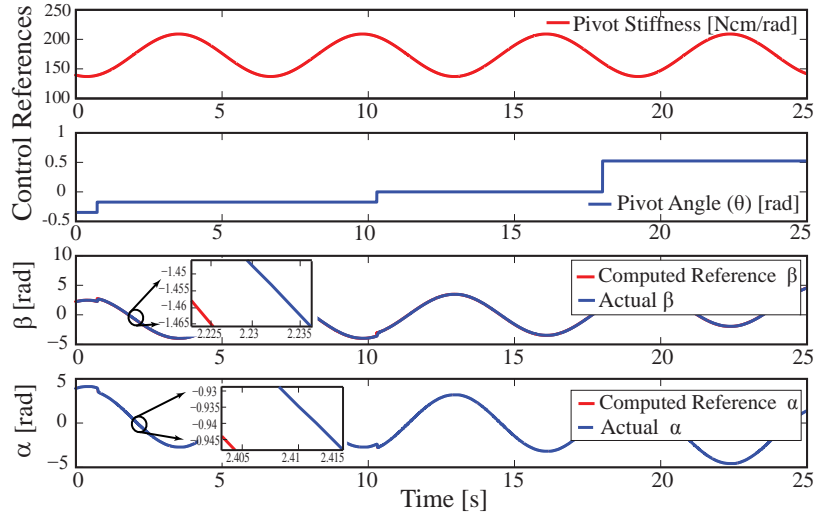


Figure 2.7: This graph presents a response of the VSA mechanism to a sinusoidally changing stiffness input when the position reference gradually increases.

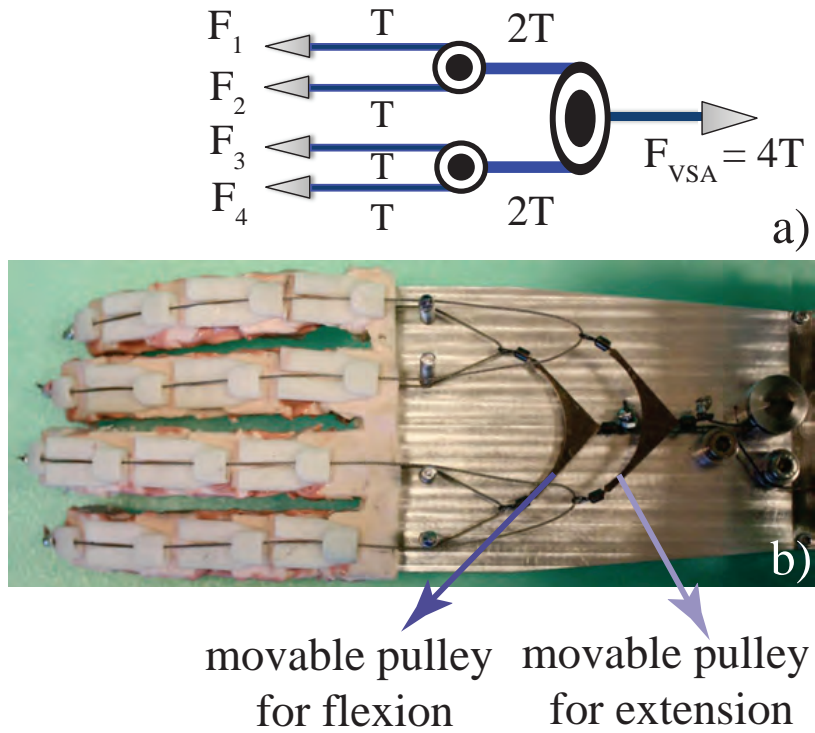


Figure 2.8: a) Movable pulleys transfer equal amount of tension on each tendon cable b) Schematic representation of the actuation in hand

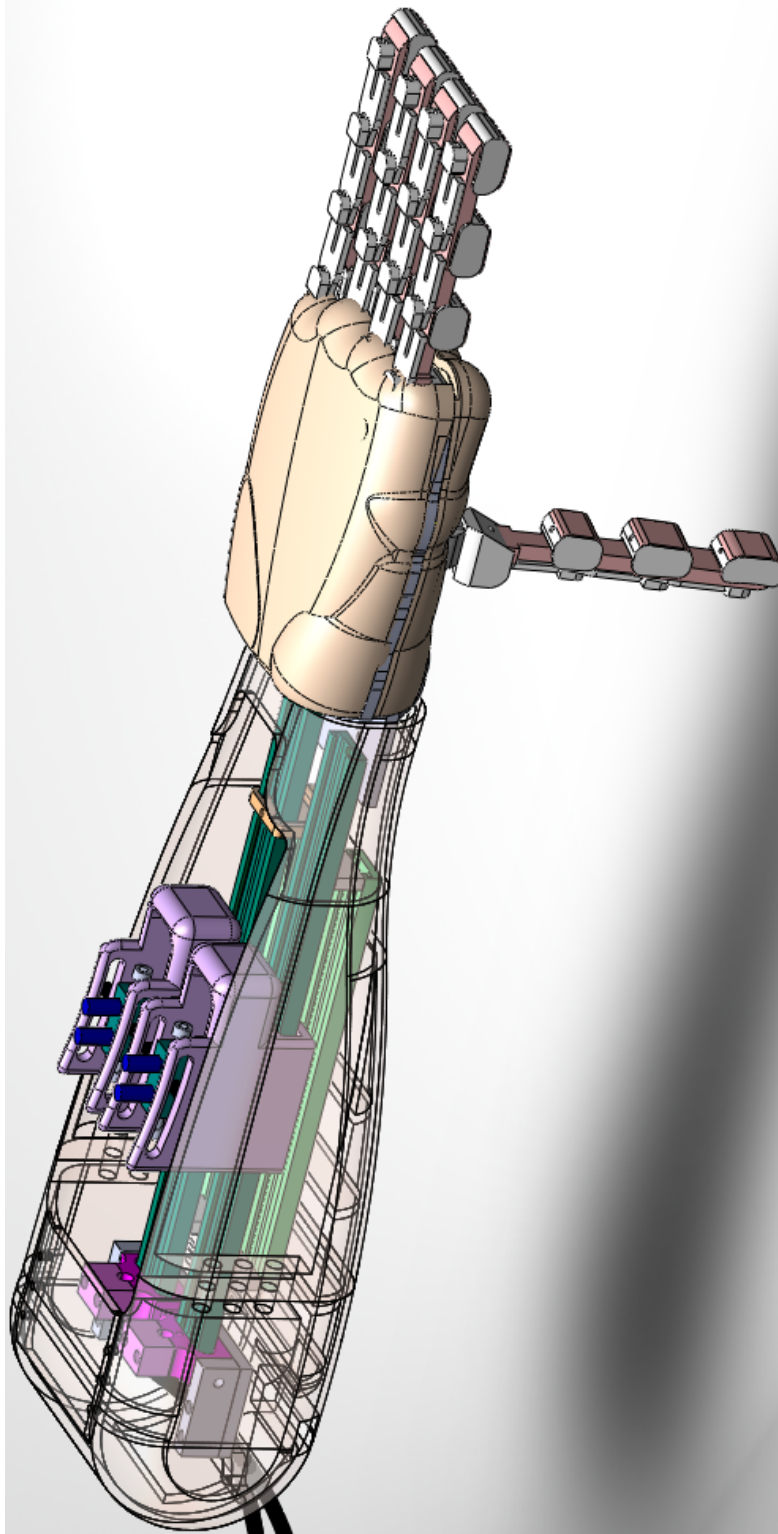


Figure 2.9: Solid modeling of the antagonistic VSA driven compliant transradial hand prosthesis

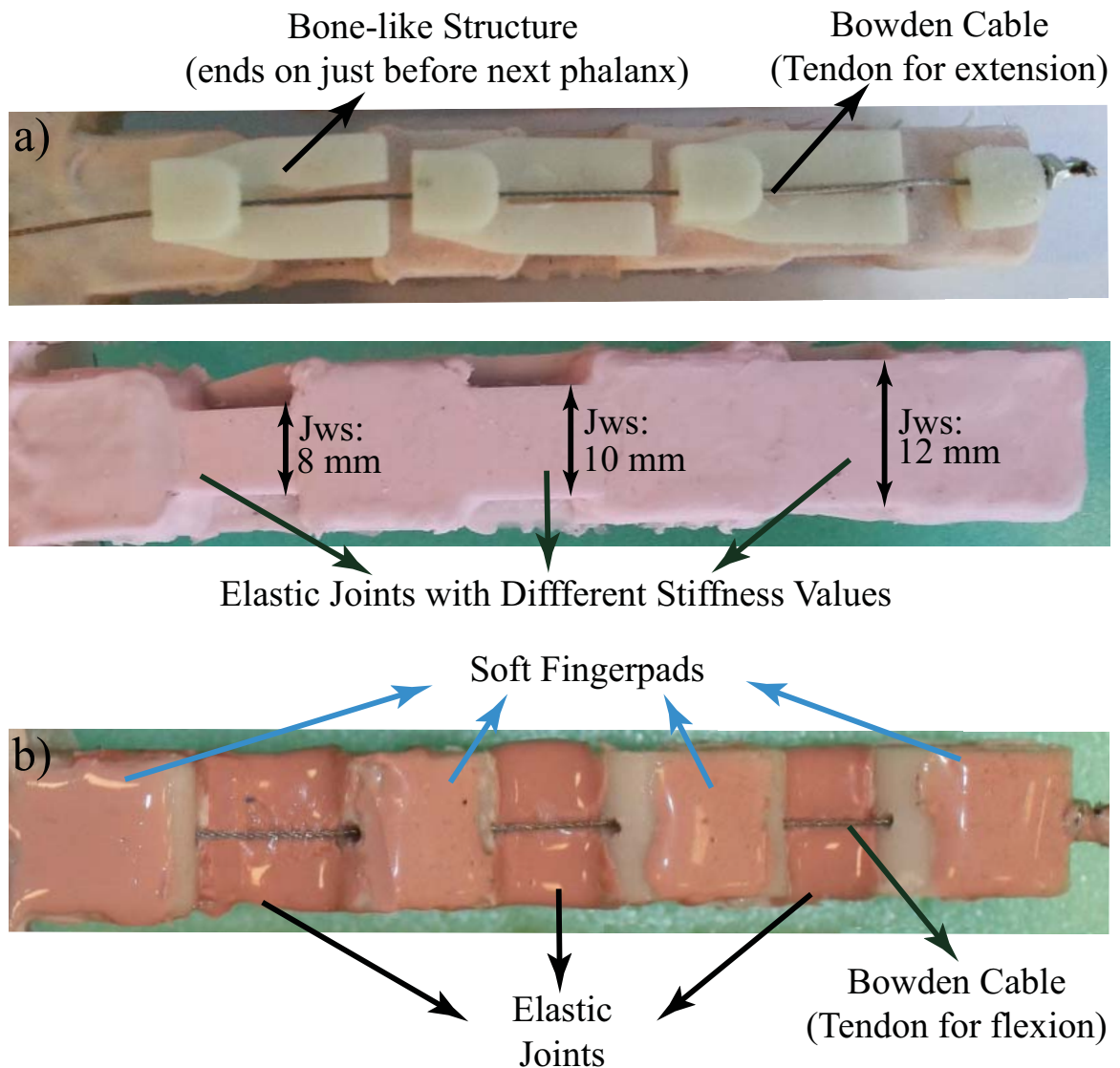


Figure 2.10: Finger characteristics and responsible components are presented. (a) Top of (a) represents bone-like structures which provide stability of finger structure when stiffness is varying, namely prevent buckling towards outside palm. Bottom of (a) shows elastic joints which represents different stiffness characteristics by changing the joint width size (Jws). In (b), back view of the finger is demonstrated with soft fingerpads, which are placed on each phalanx of the finger to increase the stiffness between object and fingers and provide more stable grasping.

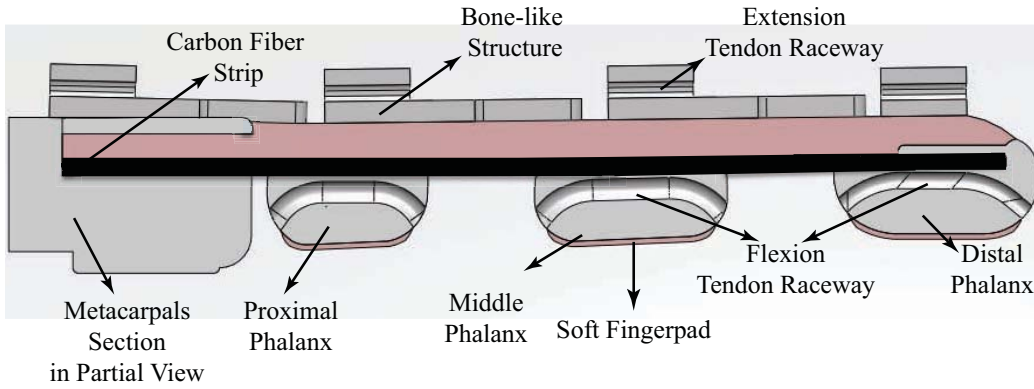


Figure 2.11: A cross-section of a compliant finger design

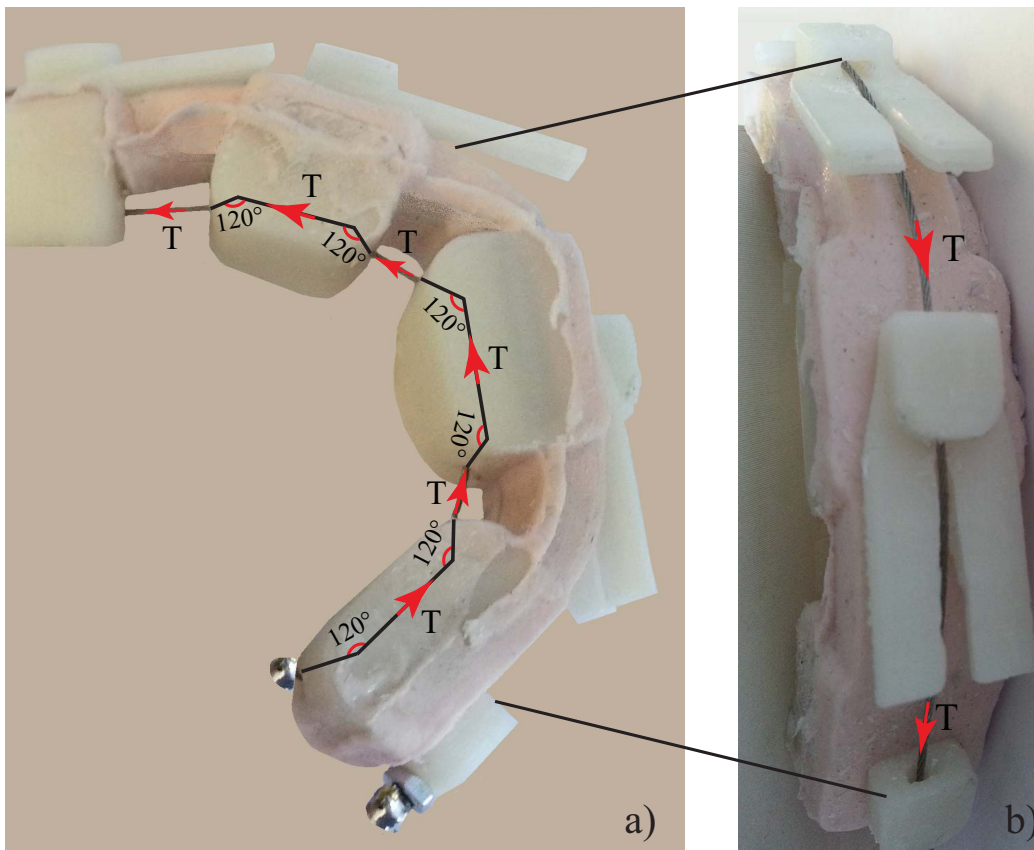


Figure 2.12: Actuation of the finger

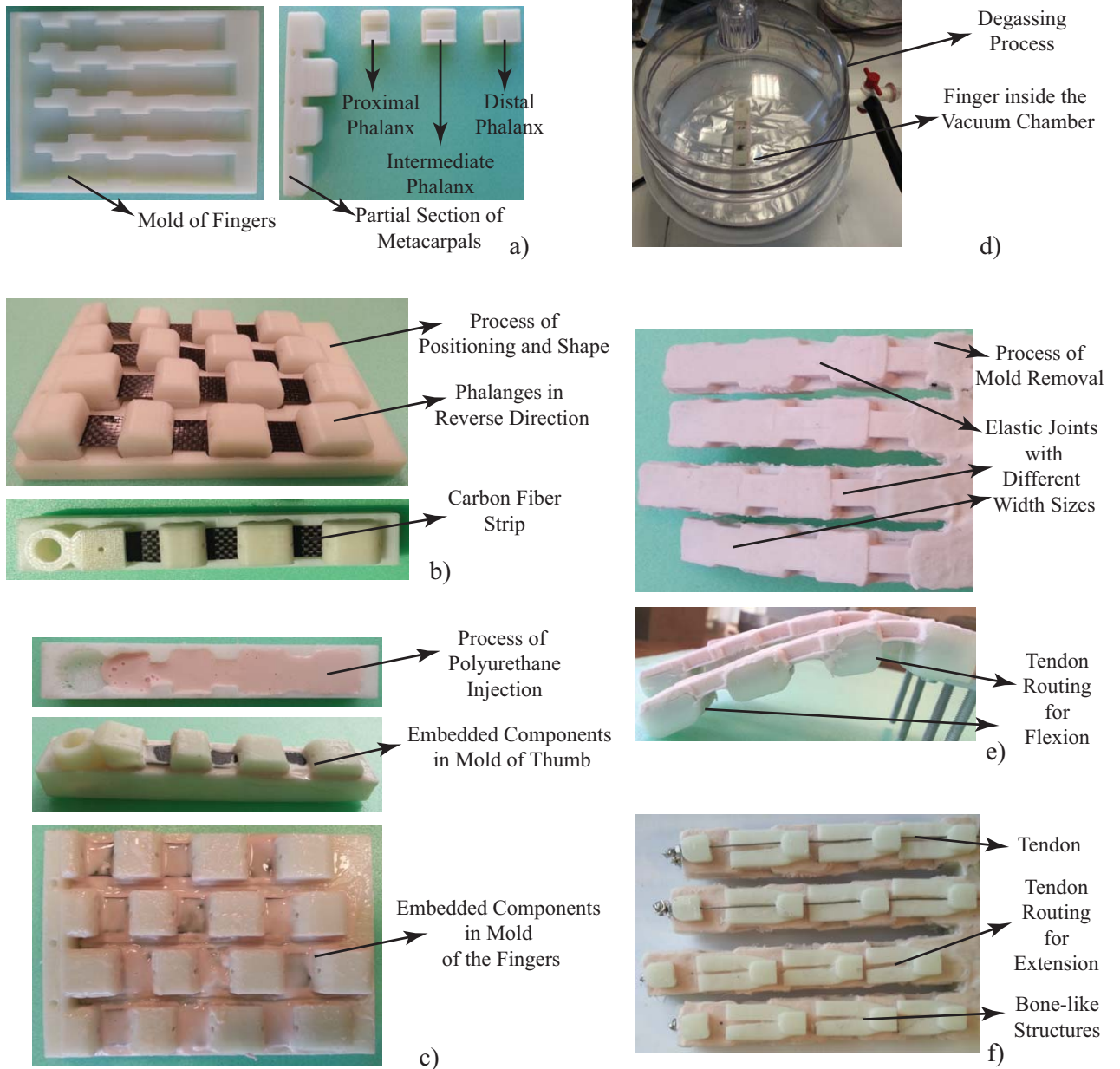


Figure 2.13: Fabrication process of the elastic joint fingers

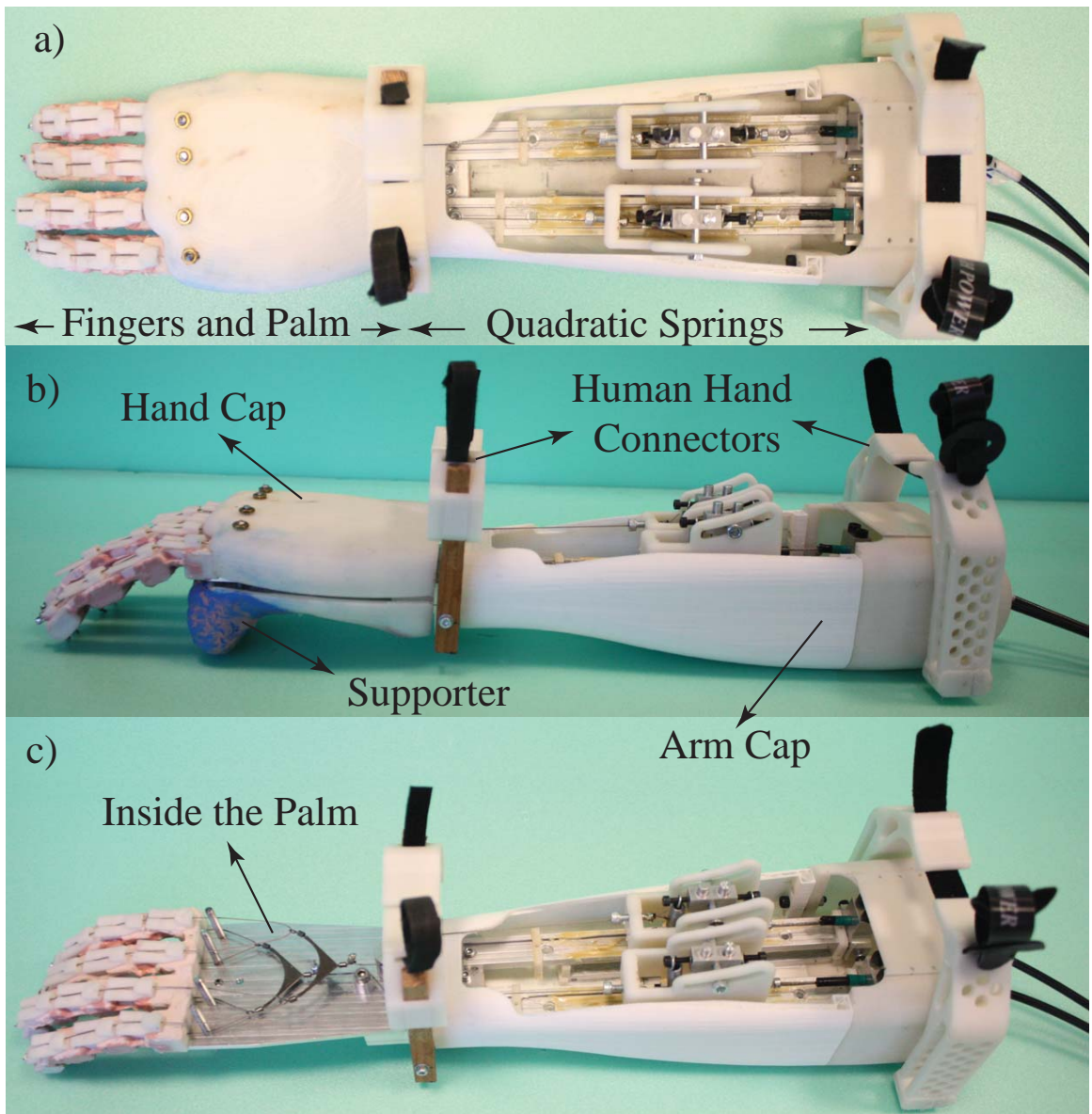


Figure 2.14: Assembly of hand prosthesis viewed from different perspectives  
 (a) Top View of the Hand Prosthesis (b)Rear View of the Hand Prosthesis  
 (c) The View of Inside of The Hand

# Chapter 3

## 3 sEMG-based Tele-Impedance Control of the Transradial Hand Prosthesis

Today's successful innovative designs and engineering solutions are inspired by biological systems and realized by imitating design in nature. For instance, the perfect design concept of human is unrivaled in adaptation to the varying conditions, especially performing tasks that require physical interaction with the environment. The significant factors behind such adaptability are based on the humans's capability on the prediction of the after-effect of the actions and expertly regulation of their impedance depending on the environment/task conditions. For example, during the execution of some tasks requiring the use of tools, such as writing, need high precision for accurate performance, humans adjust their fingers to become quite stiff to present the control performance of a high-precision positioning. This achievement can also be consistently realized while interacting with soft/fragile objects, e.g., humans regulate their fingers to become more compliant while manipulating an egg.

Humans' achievements in adaptation to the dynamics of the environment through the capacity of impedance modulation shed light on the fields of robotics. Many robots responsible for such tasks requiring the physical interaction with the environment have been developed utilizing the idea of

impedance regulation of humans. Software based modulation of compliance through the impedance/admittance control methods draws a considerable interest by the robotic fields, while in recent years hardware based modulation becomes prominent and is realized by the special mechanisms enabling stiffness regulation. The performance benefits of impedance modulation during the control of prosthetic limbs has been underlined in the literature [34,35]. More recently, a systematic study has been conducted and experimental results have indicated that the design of prostheses with user-selectable, task-dependent impedance modulation enhances the user performance using a both (virtual) prosthetic arm and a real physical system [8–10].

Today, unfortunately, the commercially available hand prostheses do not represent the similar characteristics of stiffness regulation that humans have. Otto Bock’s Sensor Hand [13], The Bebionic Hand (RSL Steeper) [14], Motion Control Hand [16] and Touch Bionics’ i-Limb Ultra [15] are successful at position or velocity control executed proportional to sEMG signals. These hands are commonly configured with tactile and force sensors to enable amputee auto-grasp feature and preserve physically interacted object against slip. Since all of these hand prosthesis are produced in stiff form and work under position/velocity control, they represent successful performance on non-contact tasks or a set of predefined tasks for which the mechanical impedance of the device is optimized, whereas such prostheses struggle while physically interacting and adapting with the un structured environment. Prosthetic hands in rigid form under position/velocity control are not appropriate for the tool use and dexterous contact manipulation, with unknown, possibly fragile, environments.

The idea of integrating impedance modulation into prosthetic limbs has

been first proposed and experimented in [33–35]. In these studies, sEMG signals are utilized to obtain estimations for impedance and velocity references to be used in the adaptive impedance control of Boston elbow prosthesis in a crank-turning tasks. Since the Boston elbow prosthesis is structured in rigid form, estimated impedance references could not be effectively transferred to the prosthesis due to the controllable bandwidth of the actuators. Besides, the Boston elbow prosthetic device appears rigid outside of the bandwidth region. Moreover, including software based impedance modulation into systems necessitates non-stop use of actuators, which results in more energy consumption. Alternatively, in [36], the drawback of the bandwidth limitation is reduced to a certain extent integrating series elastic actuation (SEA) in the design of elbow prosthesis and its impedance is modulated through the amputee’s sEMG signals. With this design, impedance modulation ability is still limited owing to the actuator bandwidth. Nevertheless, prosthetic design with SEA provides compliance into design and keeps its output impedance low above the control bandwidth. Thanks to the hardware based integration, device robustness, reliability and safety are improved, especially on the condition of impact with the environment. However, controlling the interaction forces with SEA requires continuous use of actuators and is energetically inefficient as in the software based impedance regulation. In [59], they proposed a variable stiffness actuation (VSA) to modulate stiffness of a prosthetic wrist in a concept of a simulation study. VSA provides opportunity to modulate desired impedance in hardware environment and the actuators are only in use during the modulation and/or joint rotations. Hence, proposed mechanical concept provides energy efficiency. Moreover, the desired impedance can be enforced over the whole frequency spectrum, including frequencies well

above the controllable bandwidth of the actuators.

In the literature, sEMG signals have also been utilized for the impedance modulation of robotic manipulators. In particular, sEMG signals measured from an antagonist muscle pairs are employed for the estimation of impedance and velocity references to be used in the adaptive impedance control of the elbow prosthesis in [34,35]. In these studies, prosthetic limb's position and stiffness control using the relevant muscle groups of amputee's intact musculature may not provide optimal functionality and performance as the impedance regulation is realized intentionally, which necessitates high concentration since the muscle groups are not physically interacted with the task. In [59], sEMG signals measured from the agonist and antagonist muscle pairs of forearm conditioned to obtain the variance of the windowed sEMG signals which are mapped to the stiffness and position control references performed in a simulated VSA wrist. As in the case of [34,35], this study requires intentional regulation of impedance utilizing unattached muscle groups, which diverges amputee's concentration away from the task. In addition, the technique utilized in this study provides position and impedance modulation under soft and stiff conditions of muscles, whereas it is not experimented under condition of the isometric co-contraction. Moreover, the approach causes some artifacts since joint direction affected by the instantly varying stiffness reference. A series of experiments conducted in [60] indicates that joint stiffness of a human limb can be estimated through superposition of the absolute value of antagonistically arranged relevant muscle torques. This approach is utilized in the studies [61,62] to estimate impedance and position of a rigid body manipulator utilizing the co-contraction activity of antagonistic muscle pairs placed in forearm, and the control approach is called *tele-impedance*

*control.*

In this dissertation, we propose a variable stiffness hand prosthesis design and its human-machine interface based on sEMG signals. VSA mechanisms are designed to serve as an antagonistically arranged artificial muscles which are responsible for the impedance and position modulation of the hand. This mechanism can regulate impedance and position itself independently under quasi-static conditions [51], and also be can opportunisticly placed anywhere on the forearm. Mimicking the working principle of an antagonistically arranged muscle groups can be approximated by using spring elements moving on a designed second order surface [52]. Although VSA mechanisms are preferred in some robotic hands [18, 38], to the best of our knowledge, no such VSA applications have been noticed in hand prostheses. VSA mechanism provides opportunities since the desired impedance level is regulated in hardware and hence is not restricted by the bandwidth of the actuators. Moreover, passively modulation of impedance by VSA mechanisms provides energy efficiency since the actuators are in use during the position and/or impedance regulation of joint. Tele-impedance control of a VSA hand prosthesis utilize muscle activity, namely sEMG signals, hence the user is naturally incorporated into the control architecture. In this dissertation, we utilize the experimentally verified stiffness estimation technique in the study of [60] to produce desired impedance level of an amputee at each instance of time. Estimated impedance level by means of sEMG is mapped to the impedance range of the VSA mechanisms in hand prosthesis as reference value in control architecture. Besides, position control references for the variable stiffness transradial hand prosthesis is estimated utilizing muscular activities of the chest and shoulder muscles and mapped to the angular open and close range

of fingers.

The human based part of the proposed human-machine interface composed of four channels of sEMG signals is responsible for supplying the both position and impedance references to be used in the variable stiffness transradial hand prosthesis control. In particular, it is a common preference in the literature that position control of the variable stiffness transradial hand prosthesis is modulated by the conditioned sEMG signals measured from chest for closing action and shoulder or opening action. Rather than other approaches utilizing sEMG signals for impedance regulation, the impedance modulation is realized employing the impedance of the *intact* portion of the limb, i.e. upper arm. In this way, while the proposed human-machine interface requires amputee to intentionally control the position of the variable stiffness transradial hand prosthesis, impedance regulation takes place automatically based on the instantaneous impedance of the intact portion of the limb. This study [11] emphasizes the fact that proposed approach enables the amputee to conduct natural impedance modulation from task to task or during execution of a single task without requiring amputees' attention. This special property brings together with the other advantages; such as the proposed control interface does not necessitate long training periods, does not interfere with the control of intact body segments, and provides amputee with easiness in use. Moreover, it is verified in the literature [5] that energetic interactions with environment affects the determination of the impedance levels by the intact neuromuscular system. Hence, realizing impedance regulation of the prosthesis to imitate the intact portion of the limb assures to be more reasonable control strategy with respect to the requiring the amputee to determine and control the proper impedance using dysfunctional

muscles that lack feedback, since these muscles are not properly coupled to the task/environment.

### **3.1 Tele-Impedance Control of a Variable Stiffness Transradial Hand Prosthesis**

Prosthetic hand can be opportunistically controlled over the currently available ones if the issue of adaptation to changing physical conditions is taken into consideration with the contribution of variable mechanical impedance property. This study proposes a prosthetic hand with the antagonistic VSA to realize impedance regulation in the perspective of mechanical design. Therewith, a tele-impedance control architecture is also presented to provide natural impedance control of VSA prosthetic hand for an amputee, under the lead of human neuro-musculoskeletal system.

Simultaneous and independent position and impedance control architecture of the antagonistic VSA hand prosthesis through sEMG signals is presented in Figure 5.3. The control of both position and impedance of the hand prosthesis is represented in two modules. In the first module of Figure 5.3, required reference signals for the control of both impedance and position are estimated through filtered and conditioned sEMG signals. Concerning the realistic scenario, for the transradial upper extremity amputees, muscle groups inside the hand and forearm are not appropriate for the EMG measurement. Hence, for the position reference of the prosthetic's fingers, sEMG signals are measured from the different regions of the chest, concurrently for the impedance reference, sEMG signals are recorded from the upper arm. The second module depicts the closed loop control of the VSA hand prosthesis to guarantee convergence of the actual position and impedance values of

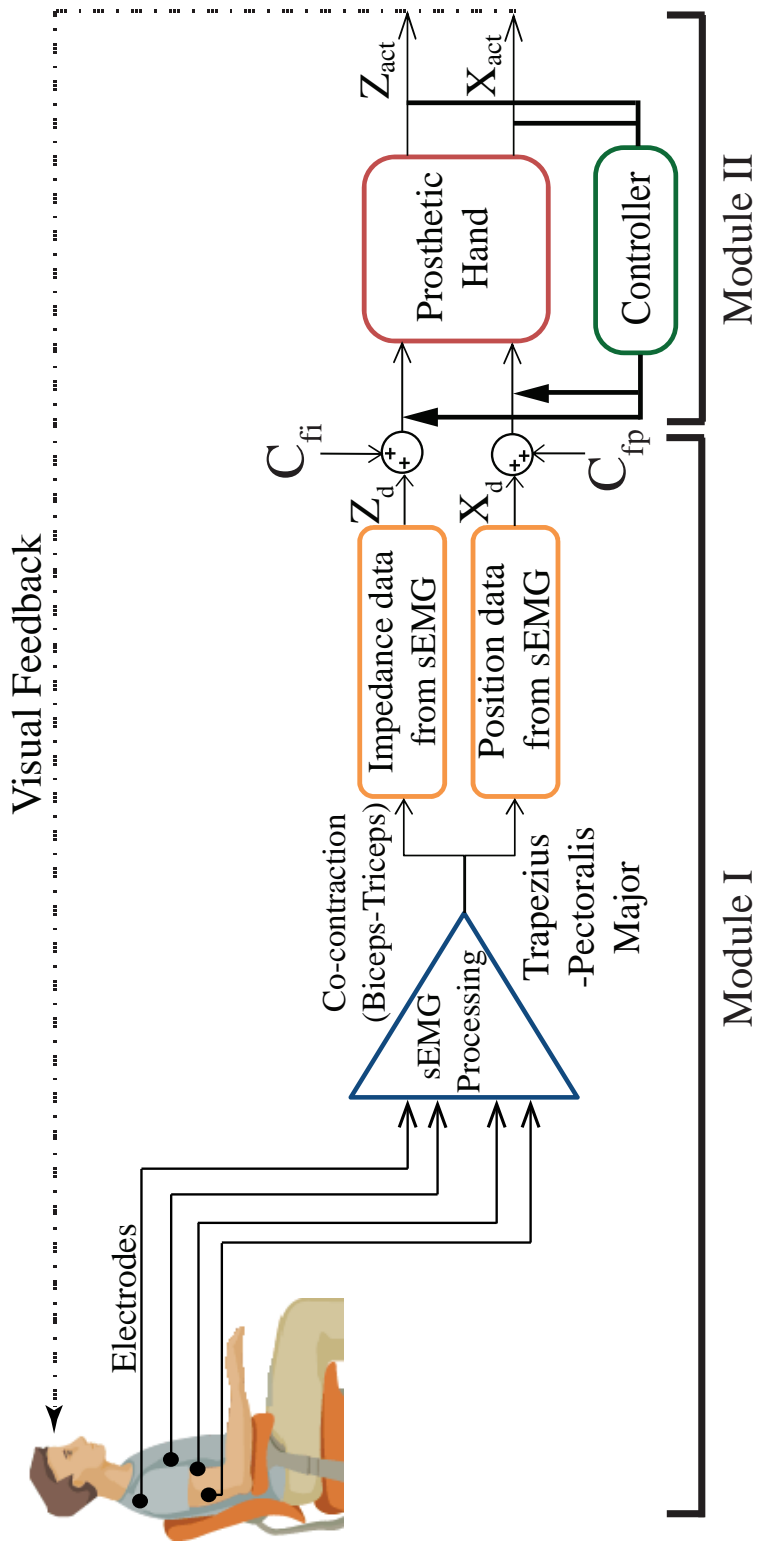


Figure 3.1: The control interface of the VSA prosthetic hand: In the first module, raw sEMG signals are measured from the intact forearm and relevant groups within the remaining thumb musculature and a series of filters are applied. In the second module, the desired position and stiffness levels are estimated from the filtered sEMG signals. Finally, the closed loop position and stiffness control of the variable stiffness prosthetic hand is handled by the third module.

the fingers to the estimated references. Overall control architecture is closed through the visual feedback, which helps amputee modulate his/her sEMG signals to match the task requirements. Stiffness estimation of the finger joint is an indispensable part of tele-impedance control architecture. Hence, in the first place, joint stiffness model and its estimation procedure through sEMG signals are discussed. Secondly, conditioning of sEMG signals as well as the data flow recorded during the experiments and also responsible muscle groups are detailed. Finally, fatigue effect on sEMG signals as a result of muscle tiredness are discussed and the reason of compensation of the muscle fatigue in the control loop is explained.

## **3.2 Joint Stiffness Model**

Muscles are responsible for several physical effects on limb joints of humans, e.g. force generation, stiffness regulation, position changes. All these variations play an important role in adapting unstructured environment. For example, the mechanical impedance of a human hand is adjusted by the ability of co-contraction and reflexive reactions. The varying in co-contraction level and reflex gains modulate the impedance level of muscles and also joint of limbs. Adapting mechanical impedance of the joints is crucial in control of movement under both static and dynamic conditions.

Literature experimentally showed that multi-joint arm movements have a direct impact on characterization of joint stiffness [63–65]. These studies design subject-based experiments in which disturbance forces are applied along multiple directions. Subject controls his/her arm when holds an computer controlled manipulator to perform reaching movement from one point to another. Deviations of the subject’s limb from the undisturbed trajectory

and perturbation forces are recorded simultaneously, thus stiffness of limb joint is estimated. Nevertheless, this technique is successful at characterization of limb impedance, it is not appropriate for the real-time use with prosthetic devices, owing to the requirement of instantly changing stiffness information. A feasible alternative method to estimate limb impedance performs utilizing the property of sEMG signals. A method in the latter case, called index of muscle co-contraction around the joint (IMCJ) [60], concerns the co-contraction level of antagonistic muscle groups around a joint. In this study, IMCJ method is preferred to estimate the stiffness of intact forearm.

Earlier studies in literature [66–68] employ the IMCJ method to investigate mechanical characteristics of the musculoskeletal system. It is observed from these studies that muscle tension is related with the rectified sEMG signals. This relationship is influential to extract the muscle moments produced by the agonist and antagonistic muscle groups are computed by multiplication of rectified sEMG signals belonging to each muscle group with its corresponding moment arm. Hence, the joint torque is estimated as the difference between the agonist and antagonistic muscle moments, which is equivalent to the difference between a weighted function of flexion and extension muscle tensions [60] as expressed in Eqn. (3.1).

$$\tau = \sum_{i=1}^k [\kappa_i \cdot agon(sEMG_i) - \lambda_i \cdot anta(sEMG_i)] \quad (3.1)$$

Here,  $\tau$  denotes the joint torque of the limb, while  $agon(sEMG)$  and  $anta(sEMG)$  represent the muscle activity of the agonist and antagonist muscles, respectively. Here,  $agon(sEMG)$  and  $anta(sEMG)$  are normalized with respect to maximum voluntary contraction level of responsible muscle groups. These signals are pre-processed, in other words, they are full-wave

rectified and averaged after the measurement of raw sEMG signals. Symbols  $\kappa$  and  $\lambda$  capture the effect of the Jacobian, the moment arms that convert muscle activity to muscle tension, that is, instead of multiplying the average of measured force by the Jacobian matrix, their effects are represented by these coefficients. The product of each muscle group activity with the relevant coefficients is referred to as a weighted muscle tension or muscle torque.

Some studies in literature has reported that muscle moment and muscle stiffness are correlated [66, 69, 70]. In the light of this relation, similarly, joint torque and joint stiffness can be linked each other [66, 67]. All these concerned, it is proposed in [60] such that human joint stiffness can be estimated by superpositioning the absolute values of the generated muscle torques. Considering this relationship, it has been proposed that human joint stiffness can be estimated through superposition of the absolute values of the generated muscle torques [60]. Accordingly, using the indices of  $\kappa$  and  $\lambda$  estimated in Eqn. (3.1), joint stiffness is estimated as in Eqn. (3.2).

$$S = \sum_{i=1}^k [|\kappa_i|.agon(sEMG_i) + |\lambda_i|.anta(sEMG_i)] \quad (3.2)$$

Here,  $S$  denotes the IMCJ at a joint. A remarkable result can be deduced from the Eqn. (3.1) and Eqn. (3.2) that if both agonist and antagonist muscle torques increase simultaneously, the joint torque is not produced, while the joint stiffness level is raised.

The command input for the position control of the hand prosthesis is generated utilizing directly proportional relationship between rectified sEMG signals and joint angle. In other words, increase in the amplitude range of

the rectified sEMG signal is interpreted for the hand prosthesis as a rise in the open-angle measure, or vice versa. One of the main goal in the control architecture is to realize the control of position and stiffness independently but simultaneously. However, while the muscles responsible for position control are contracted, other muscle groups are also contracted involuntarily. The other undesirable condition is the contamination of electrocardiography (ECG) signal into the muscle responsible for opening the fingers, pectoralis major. ECG contamination is removed from the useful sEMG signal both placing the electrode different line level with contamination zone and also adding some bias term to the sEMG signal until ensuring the suppression of the ECG signal effect. Pectoralis major and trapezius muscles are quite efficient muscles in terms of ease in production of sEMG signal. Since they enclose very large area on the chest and shoulder regions respectively, maximal contraction is not necessary during the position control of fingers. In particular, normalized sEMG signal represented in the Eqn. (3.3) is realized by %70 maximal voluntary contraction (MVC) instead of %100 MVC. This solution also provides another benefit during the simultaneous control of position and impedance. Less than maximum contraction for the upper level angular changes of fingers preserves the involuntarily contractions of biceps and triceps muscles.

$$sEMG_{normpos} = \frac{sEMG_{position} - sEMG_{bias}}{sEMG_{\%70MVC}} \quad (3.3)$$

According to IMCJ method, muscle torque is produced based on a linear time-invariant process. Hence, the constants  $\kappa$  and  $\lambda$  in Eqn. (3.1) can

be estimated through the experiments under the condition of isometric contractions. Nonetheless, at any rate of muscular activities, muscle tension is nonlinearly related with muscle length and muscle velocity. In addition, it is reported in [69] and [70], when the limb joint is non-stationary, the length of moment arms corresponding to the muscle groups alters. Due to the fact that muscle stiffness varies as a function of muscle length and velocity, the relation between the sEMG signals and dynamic joint stiffness is nonlinearly affected by these factors. Moreover, conditioning sEMG signals utilizing many signal processing techniques cannot perfectly decontaminate sEMG signals from the environmental noise and motion artifacts. Thus, it is inevitable to estimate stiffness with some error using IMCJ method.

Fortunately, some of the studies [8, 36] interested in human-subject experiments regarding variable stiffness prosthesis proved that subjects would prefer to arrange the impedance level of the prosthesis's joint roughly, instead of precisely. This helps people adapt/learn the execution of daily activities by altering the impedance level rather than fine tuning it. In the light of these studies, it is remarkable to emphasize that modulation of impedance in a coarse manner is quite necessary and sufficient to increase the performance and efficiency level of the hand prostheses owing to realization of matching the mechanical properties of hand to requirement of the environment/task. Hence, stiffness estimation using IMCJ method from intact forearm suffices the control of VSA prosthetic hands.

### **3.3 Stiffness Estimation through sEMG Signals**

Indices in Eqn. (3.1) discussed in Section 3.2 are estimated by performing a series of experiments. This procedure is executed with the participation

of a healthy student of Sabancı University (32-year-old female). Before the experiment, participant is guided by a learning period to be experienced about the task. The participant did not present any motor and sensory impairment. The participant signed informed consent forms approved by the University Research Ethics Council of Sabancı University. This experiment is configured by mimicking the realtime experimental condition of hand and arm posture attached to hand prosthesis. During the experiment, subject's arm configuration in space is determined to be the same orientation as in the case of real-time experiments and use of hand prosthesis. This is the appropriate solution to disregard impedance variation caused by the different orientation of arm in space.

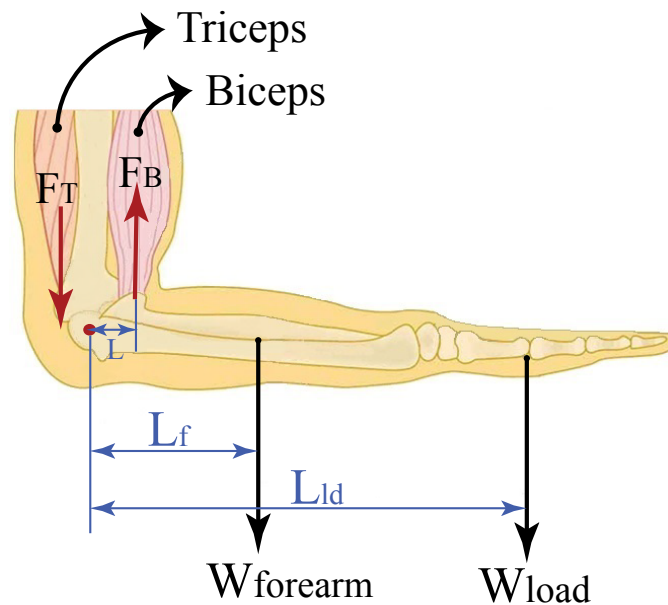


Figure 3.2: Biomechanical system with the pivot at the elbow joint

According to the experimental idea visualized in Figure 3.2, elbow angular position is required to be kept at  $90^\circ$  such that forearm and upper arm

are perpendicular to each other. This condition is provided when the antagonistic muscle groups on upper arm are isometrically contracted. From the biomechanical point of view, it is visualized in Figure 3.2 that muscles are not isotonicly but isometrically contracted in order not to change the palm level and exert forces to set the joint angle at desired level. This experimental procedure reflects the similar condition with that of an amputee who lost his/her arm from below elbow level (a.k.a. transradial amputee) is able to use their muscle groups in upper arm.

The task of the experiment is grasping a dumbbell while positioning the arm at the same level, namely the forearm is configured horizontally while the upper arm is perpendicular to the forearm and palm is facing down. Experiment is repeated for five different load conditions. Participant begins with lifting her forearm when hand is free of load and continues with lifting the dumbbell with increasing load level (0.5kg, 1kg, 1.28kg, 2.26kg, 2.76kg, 3.76kg). Each condition has 20 trials and each trials last 20 seconds. The first 500 samples of each trials are omitted from the data to exclude signal outliers owing to initialization and motion artifacts. Net torque applied on elbow joint is calculated in the Eqn.(3.4). Here,  $W_{load}$  and  $W_{forearm}$  denote the weight of the load grasped by hand and weight of the forearm respectively while  $L_{ld}$  and  $L_f$  are the moment arm of the load and moment arm of the center of gravity of the forearm with respect to the elbow joint.

$$\tau_{elbowjoint} = W_{load}L_{ld} + W_{forearm}L_f \quad (3.4)$$

During the execution of experiment, sEMG signals are also recorded from

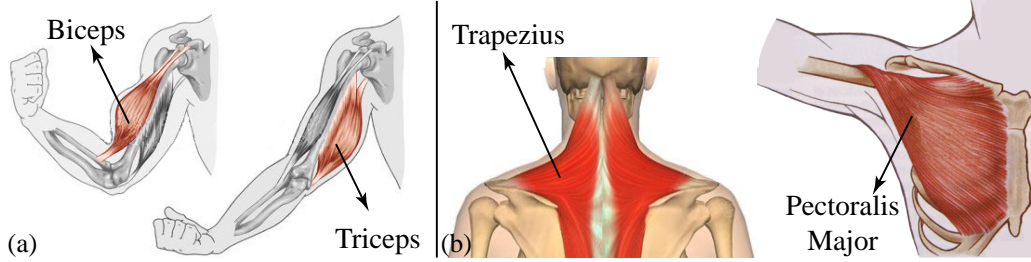


Figure 3.3: The biceps and triceps muscles are employed for the stiffness regulation in (a), while trapezius and pectoralis major muscles are employed for position estimation in (b).

the biceps and triceps antagonistic muscle groups of the subject as shown in Figure 3.3(a). sEMG signals are measured through the surface electrodes of a sEMG signal acquisition device(Delsys-Bagnoli-8) with the sampling rate of 1000Hz. Required signal conditioning for sEMG signals in Eqn. (3.1) is depicted in Figure 3.4 and also a sample signal set obtained from the experiment is illustrated in Figure 3.5. Measured sEMG signals sampled at 1kHz (using NI USB 6251 DAQ Device) are filtered against inherent and environmental noises, and also motion artifacts with the aid of a Butterworth band-pass filter of 20 Hz low cut-off frequency and 500 Hz high cut-off frequency. In order to extract the relation between joint torque and sEMG signals, filtered signal is conditioned with a full-wave rectifier. In order to obtain more smoothed ripple from the rectified signal envelope detector and moving window method are implemented. As a final conditioning, sEMG signal is normalized to correlate the right hand side of the Eqn. (3.1) with the computed torque level in Eqn. (3.4).

The indices in Eqn. (3.1) are estimated by using vectors  $agon(sEMG)$ ,  $anta(sEMG)$  and  $\tau$  in multiple linear regression method. In linear model

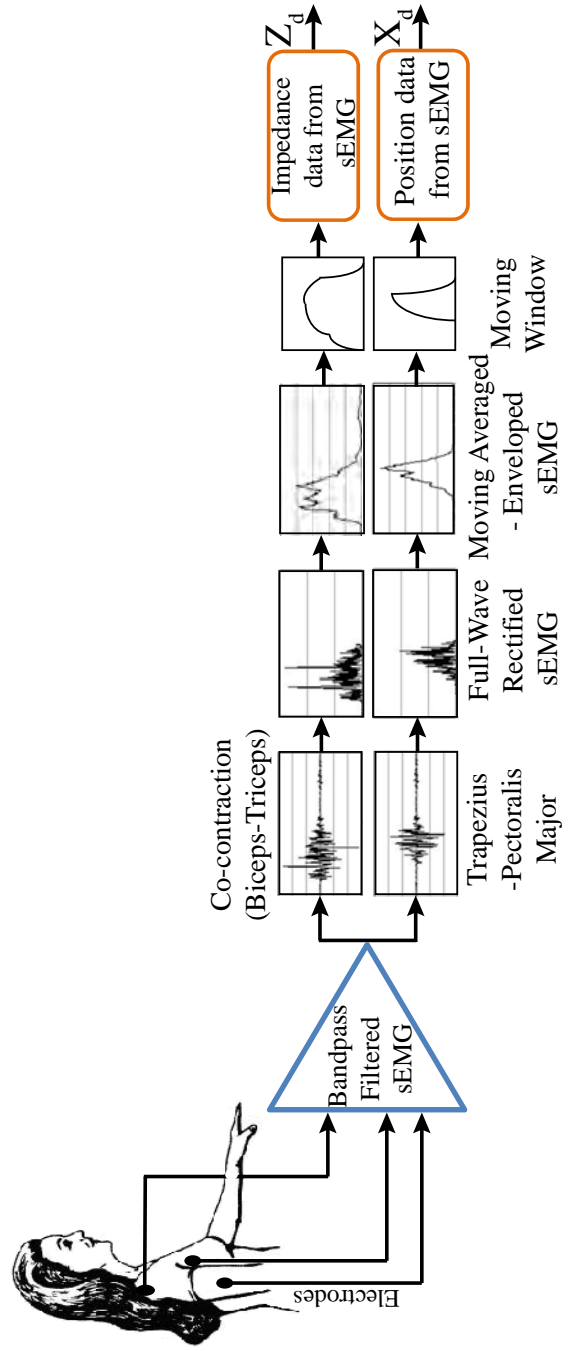


Figure 3.4: sEMG signal flow: Raw sEMG signals are bandpass filtered and full wave rectified. Then, these signals are averaged with 0.5 second moving window and an envelope detector is employed.

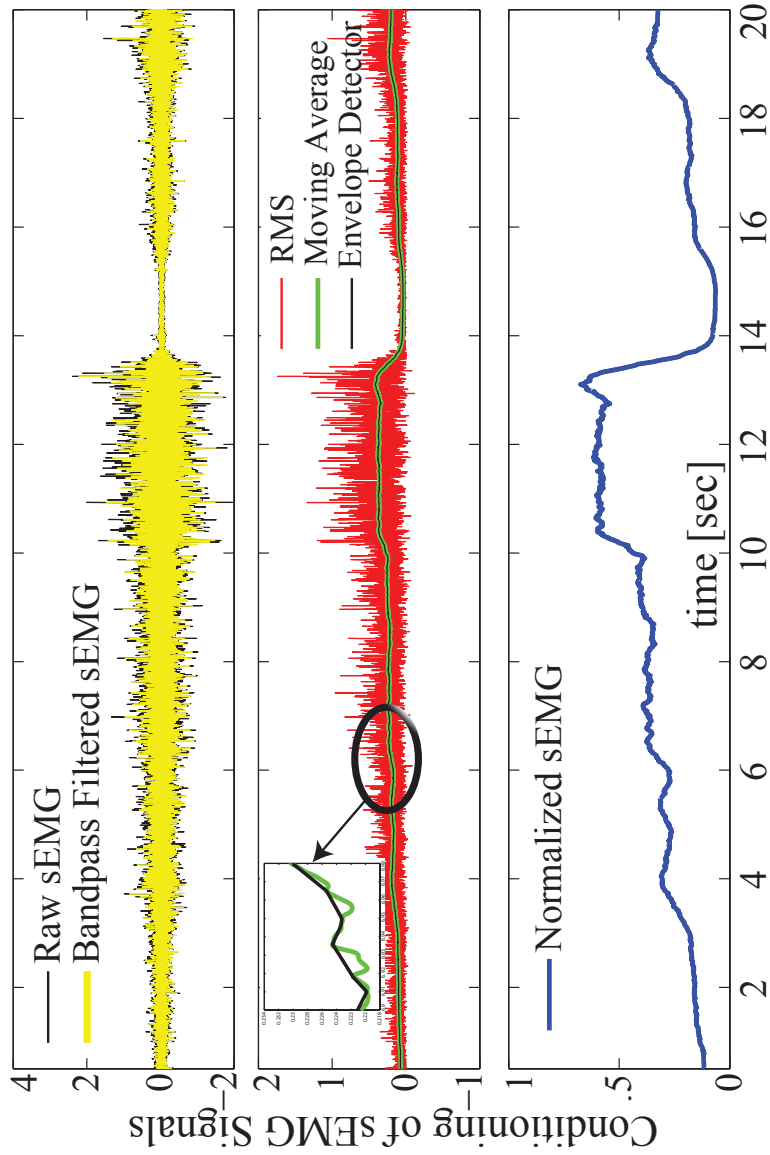


Figure 3-5: Signal processing of raw sEMG signals: On the top graph, the effect of bandpass filtering is presented. The graph in the middle shows rectified (red), moving averaged (green), enveloped (black) sEMG signals. The graph at the bottom depicts the normalized sEMG signal.

(Eqn. (3.5)), regression coefficients are computed with 95% confidence bounds. In Eqn. (3.5),  $x$  and  $y$  denote the vector data of  $agon(sEMG)$ ,  $anta(sEMG)$  respectively, besides  $m$  and  $n$  represent the indices,  $\kappa$  and  $\lambda$  required to be estimated.

$$f(x, y) = mx - ny \quad (3.5)$$

The estimation results are presented in Table 3.1. The quality measures for estimated indices are represented by statistical measures  $R^2$  and root mean square error (RMSE). The result of linear regression method analysis is represented in Figure 3.6. As seen that quality of linear fitting is also statistically represented by  $R^2$  is very close to one, while RMSE is accepted to be zero.

Table 3.1: Estimation Results of Impedance Parameters

$m$	$n$	R-square	RMSE
1,8612	1	0,9938	0,02941

### 3.4 Compensation against Muscle Fatigue

Muscle fatigue can be expressed as a decline in the level of amplitude of sEMG, namely reduction in producing the ability of force by active muscle groups during a ceaseless muscle activity [71]. The reason of muscle fatigue encompasses the metabolic, structural and energetic alternations in muscles owing to insufficient oxygen level and inadequate blood circulation responsible for supply of nutritive substances and also decrease in the efficiency of the nervous system. In particular, the potential reason of muscle fatigue is

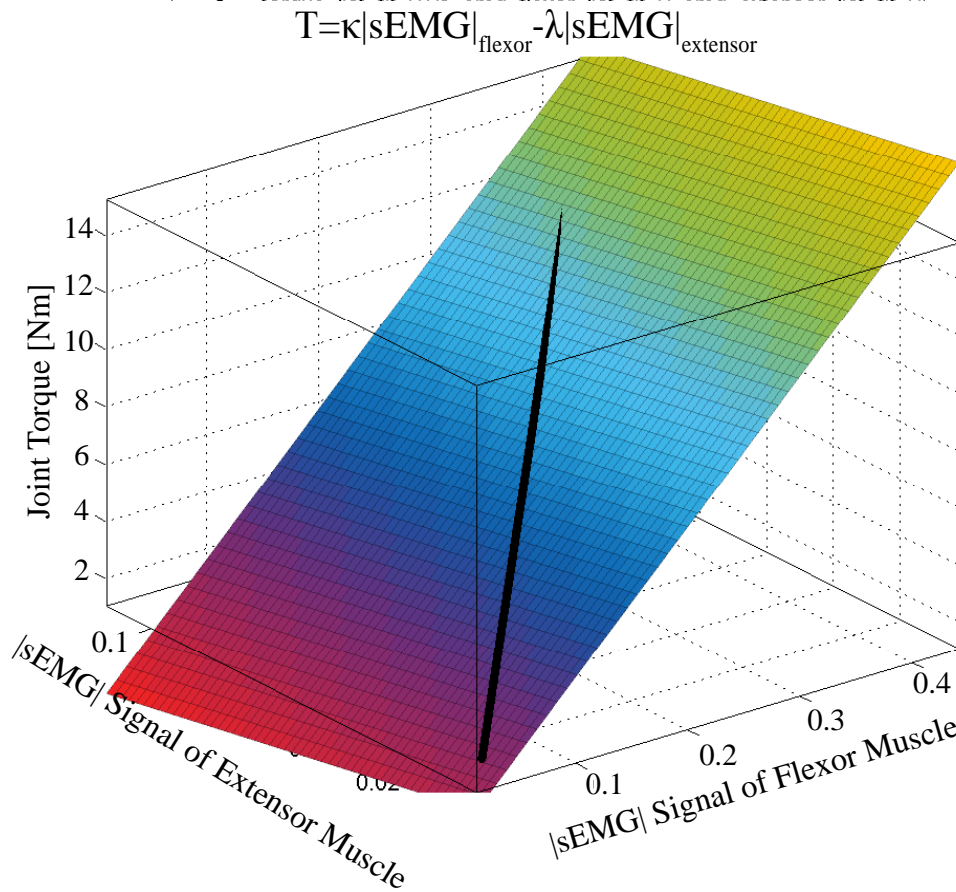


Figure 3.6: Result of linear regression analysis to estimate the indices of  $\kappa$  and  $\lambda$

classified under three groups, central fatigue, fatigue of the neuromuscular junction and muscle fatigue [72].

The assessment of muscle fatigue is a very important research topic, especially, in the field of sEMG based control of prosthetics, neuromuscular rehabilitation and the applications of functional electrical stimulation (FES) systems. In the literature, many approaches have been proposed to estimate the muscle fatigue. Simplest way is to identify onset time of the muscle fatigue by measuring time while a subject is performing an activity, i.e.

grasping a load at defined level under isometric contraction. This method is known as mechanical manifestation of muscle fatigue [73]. Despite the simplicity of this method, results are affected by the motivation of the subject during the experiment and his/her compliance to task conditions [74]. Besides, this method does not only provide continuous information during the experiment and does not provide information about the fatigue level of specific muscle group. Muscle fatigue can also be identified by controlling the lactate concentration in muscle by taking blood samples at certain time intervals. However, rarely taking samples does not give an insight into real-time variations in muscle fatigue. Real-time monitoring of biomechanical and physiological changes in a particular muscle fatigue during a predefined task condition is feasible with measurements of the myoelectric signals on the surface of the skin [75]. Although this method has disadvantages, such as exact positioning of surface electrodes on desired muscles is not precisely realizable and cross-talk of the myoelectric signals produced by the neighboring muscles overlaps on the target sEMG signal, it can provide uninterrupted recordings of muscle fatigue data, while an individual is performing an experimental task.

A large number of studies have been performed using signal-based quantitative criteria of muscle fatigue, mostly in static, but also in dynamic conditions. The non-invasive nature of this technique makes it prominent in many fields, such as biomechanics, physiology, and ergonomics. There are numerous classical and modern signal processing methods and techniques suitable for application in sEMG-based muscle fatigue evaluation [76]. These methods are classified based on their defined domain, as time domain, frequency domain, time-frequency and time-scale representations, and other methods

such as fractal analysis and recurrence quantification analysis. Our intention is not to enlist and explain all related methods in detail but instead to provide succinct description of a relevant method appropriate for integration into our real-time tele-impedance control design.

During our experiments, muscle performance decreases as a function of time and has an undesired effect on hand prosthesis control. In particular, when the level of muscle fatigue increases, sEMG-based impedance and position reference inputs are deteriorated. To illustrate, muscle fatigue problem is demonstrated in Fig 3.7. Here, the green line represents the envelope of the RMS method applied sEMG signals to emphasize the RMS variation during the time. The objective is to estimate muscle fatigue behavior as a function of time and include in the control architecture as a compensation factor in estimated reference input. Most commonly used feature in time domain to represent muscular effort and fatigue is methods responsible for amplitude modulation on sEMG. As a time-domain feature, root-mean-square(RMS) value is used to estimate behavior of muscle fatigue [77]. RMS of the sEMG signal is defined by Eqn. (3.6).

$$RMS = \sqrt{\left(\frac{1}{N}\right) \sum_{i=1}^N x_i^2} \quad (3.6)$$

In Eqn. (3.6),  $x_i^2$  is the  $i^{th}$  sample of the signal, and N is the number of samples in the time interval.

In order to estimate fatigue behavior, an experimental procedure is arranged. During the experiment, human arm posture mimics its experimental condition in the real-time tele-impedance control of prosthesis. During the experiment, subject is requested to realize sustained isometric contractions.

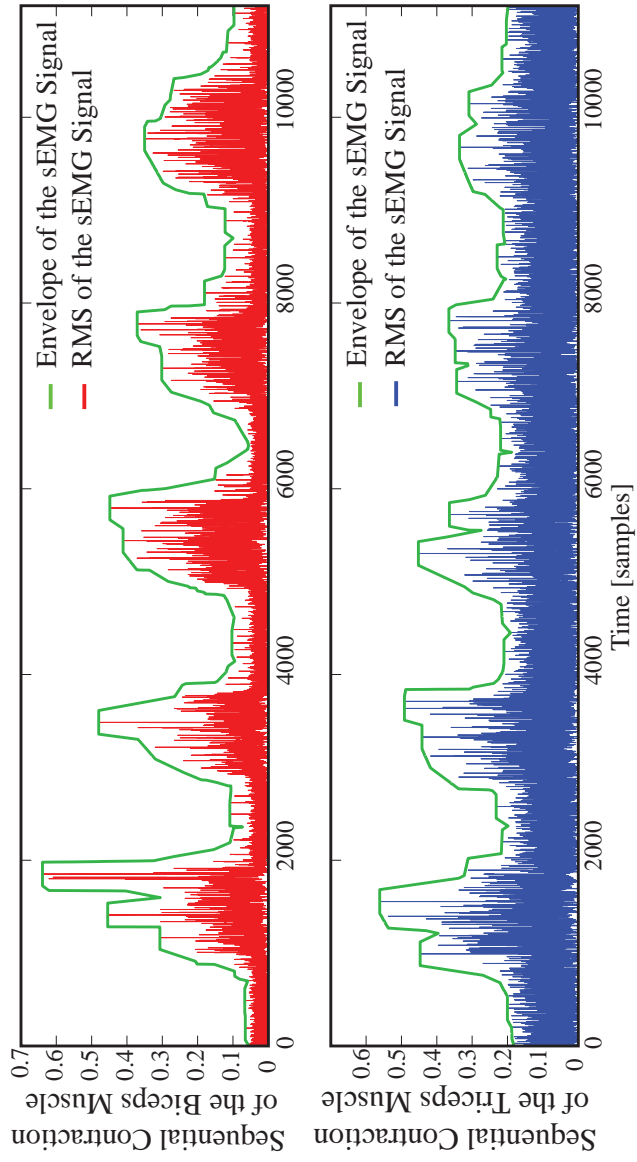


Figure 3.7: Experimental results of average fatigue characteristics of biceps and triceps muscles

The experiment includes 10 sessions and each session lasts 30 seconds. In each session, this procedure is repeated sequentially for 5 times.

The fatigue behavior from the sEMG data is estimated through 3 sequential conditioning stages. Firstly, it is band-pass filtered between 20-500 Hz to omit the undesired signals overlapped on the sEMG during the measurement, e.g. electronic noise, motion artifacts, ECG cross-talks, power-line interference. Secondly, filtered signal is normalized to make comparisons in each session accurately. Finally, RMS method is applied on sEMG signals to extract the time-dependent features. The experimental results in Fig. 3.8 present the fatigue characteristics of biceps and triceps muscles as a function of time. Each trial in x-axis represents the time interval of the muscle contraction. As in this figure, a linear fit is obtained using the data cloud. The equations of the linear fit expresses in Eqns. (3.7) and (3.8) are employed during the work hours of the prosthesis to compensate for the decrease in RMS amplitude due to the fatigue. Here,  $C_b$  and  $C_t$  in Eqns. (3.7) and (3.8) represent compensation factors of fatigue for the muscles of biceps and triceps, respectively as a function of time. As depicted in Figure 5.3, the time dependent compensation factors are included in a summation term to obtain the stiffness and position reference estimations, which are not influenced by the fatigue effect.

$$C_b = -0,0118t + 0,143 \quad (3.7)$$

$$C_t = -0,0037t + 0,12 \quad (3.8)$$

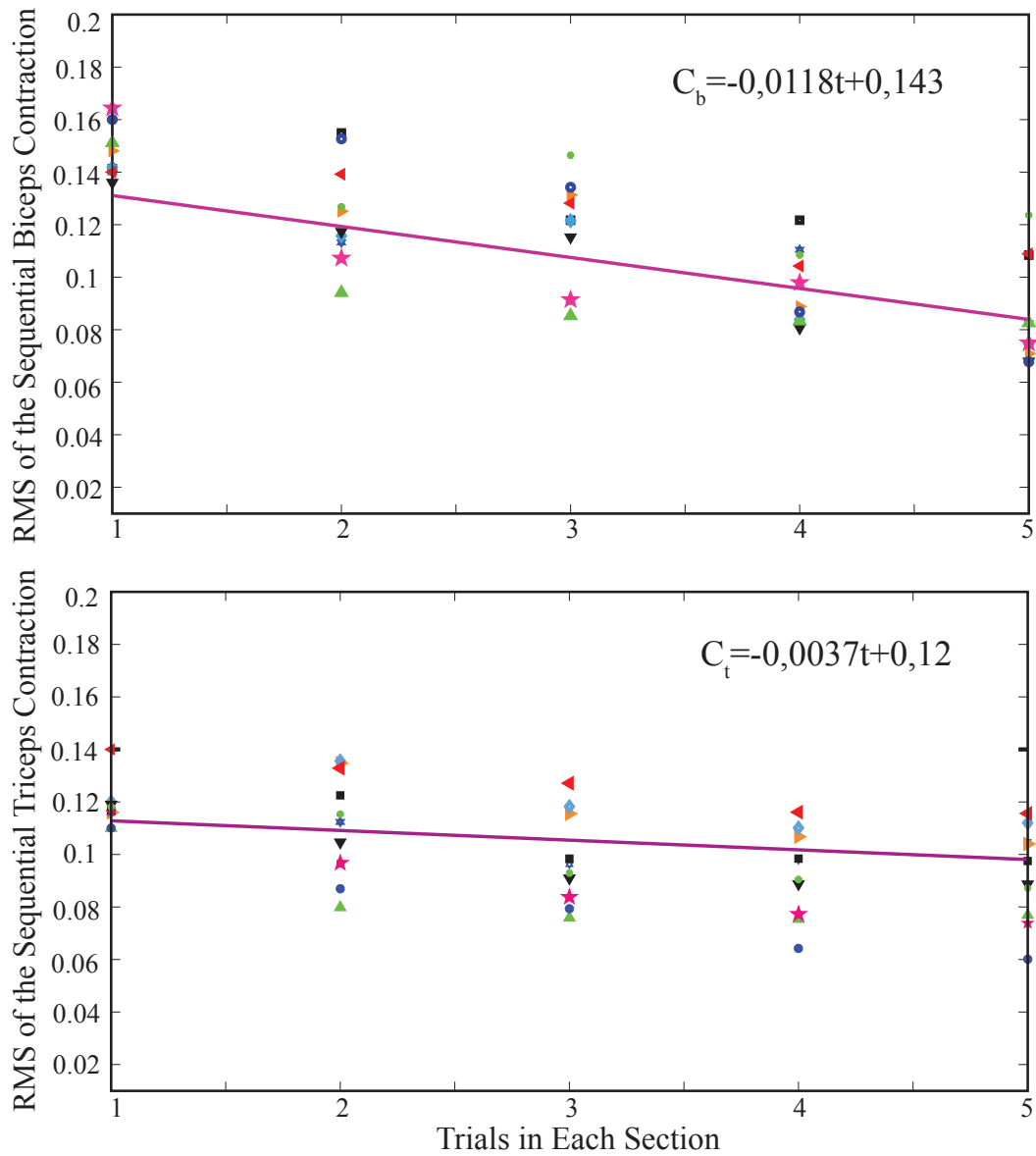


Figure 3.8: Experimental results of average fatigue characteristics of biceps and triceps

# Chapter 4

## 4 Experimental Evaluation of the Variable Stiffness Transradial Hand Prosthesis

In this chapter, the objective is to demonstrate independent position and impedance modulation of the prosthetic hand by means of two sets of experiments. In the first case, it is shown that when position of the hand is set to a certain constant value, device stiffness can vary without affecting its position. The second case represents the capability of position modulation of hand when the stiffness is set at a desired constant value. Each experiment is realized with the contribution of human and without the contribution of human, namely commanded by a PC work-station.

In addition to these studies, a different set of illustrative experiment is also performed to demonstrate compliance and proposed control performance of the variable stiffness hand prosthesis. In the studies mentioned in this chapter, thumb is not included in the design and all tasks are performed using the four fingers.

### 4.1 Setup and Experimental Procedure

The experiment is grouped into two classes. In the first place, mechanical sufficiency is tested providing by the control input through a PC work-station.

Capability of independent control of position and stiffness is validated by means of defined tasks to PC. Secondly, human is interacted with the hand prosthesis and gives reference inputs to the control architecture using sEMG signals. In the second part of the experiment, the objective is representing the feasibility of independent control of position and stiffness provided by the reference control inputs of human.

In the first case, hand prosthesis is attached to the human forearm as depicted in Figure 5.1 (a). A linear actuator (ServoTube Linear Actuator, Copley Controls) combined with precision position encoder is placed just under the four fingers. Shaft of the linear actuator is controlled by giving a ramp input reference signal with a small constant slope to exert slowly raised force on fingers. Both brushed DC motors (Maxon motor) with harmonic drives of VSA and a linear actuator are communicated with a PC workstation through DAQ card (Quanser-Q8 USB). During the study, both linear actuator and DC motors are controlled by a PD controller with gains empirically adjusted to minimize steady-state error and display no overshoot.

In the first task, the aim is observing the position deviation of environment (shaft stroke of the linear actuator) with respect to the initial position level of the shaft after contacting with fingers. This experiment includes three subsections. In each section, stiffness of fingers are set at various levels, i.e. at low, intermediate and high levels, position of the fingers are set at  $0^\circ$ , and the response of fingers to the shaft motion is observed. During the experiment, for instance, hand's stiffness is modulated at a previously defined level and simultaneously ramped force input is applied by the linear motor to the fingers. Position deviation of the shaft and applied force level during the experiment are recorded. Their slope provides an estimate for

the finger stiffness. The experimental results for this task are presented in Figure 4.2. This figure is arranged according to order of increasing stiffness value. In each graph, the best linear fit of the each trial and also their average with blue line are represented. As seen in the figure that first graph has very small slope with respect to the other two graphes. The interval value of stiffness represented in the second graph is not an exact middle value, just an intermediate value. The slopes of each figure expressed in statement (4.1) is obtained from the blue line.

$$k_3 = 0,53 < k_2 = 2,7 < k_1 = 9,1 \quad (4.1)$$

In the second task, the objective is again observation of the position deviation of environment when ramp force input is continuously applied to the fingers. The difference arises from keeping the stiffness level of the fingers same at all three experiments, but changing the position level of the fingers to three different values of  $0^\circ$ ,  $(\frac{\pi}{6})^\circ$ ,  $(\frac{\pi}{3})^\circ$ . When stiffness is set at a constant level, ramped force input is simultaneously exerted on fingers. For three different position conditions of fingers, the relation between the applied force on finger surfaces and their position deviation with respect to the initial condition provides an estimate about simultaneously modulation of finger's stiffness. The experimental results of this task are shown in Figure 4.3. Each figure include the results of all trials and their average value with blue line. As seen that average value of each slope is almost same in three graphes and their value are expressed in the statement (4.2).

$$k_1 = 0,92 \simeq k_2 = 0,87 \simeq k_3 = 0,94 \quad (4.2)$$

The second experiment differs from the first experiment by integrating the human inside control architecture to supply reference inputs to the system. The purpose of the experiment is to demonstrate the feasibility of the independent control of position and stiffness by human. All other experimental procedures are same with the first experiment explained above. Required stiffness and position reference inputs are estimated as discussed in detail in Section and employed for the control of hand prosthesis. In this experiment, stiffness of fingers are adjusted to three different levels. Each sub-session has one stiffness level, i.e., low, intermediate, high levels. Position of the fingers are controlled to  $0^\circ$ . The results of the first task are presented in Figure 4.4 and it can be observed that average slope of each graph is increasing from left to right depending on the modulated stiffness range of fingers. Their stiffness relations are also presented in statement (4.4).

$$k_3 = 0,51 < k_2 = 2,6 < k_1 = 9,5 \quad (4.3)$$

In the second task of the experiment, desired position level of each fingers are set to  $0^\circ$ ,  $(\frac{\pi}{6})^\circ$ ,  $(\frac{\pi}{3})^\circ$  and keeping the stiffness level constant ( $0^\circ$ ) with the position and stiffness references supplied by sEMG signals, respectively. Under these conditions, position deviation of shaft and applied force to the fingers are recorded. The results representing these recordings are expressed in Figure 4.5.

$$k_1 = 0,92 \simeq k_2 = 0,87 \simeq k_3 = 0,92 \quad (4.4)$$

## 4.2 Illustrative Experimental Results

In the second part of the study, the objective is to demonstrate the capability of prosthesis with some illustrative experiments. This study reveals the necessity of compliance property of fingers and also independent control of position and stiffness modulation of hand. During the study, hand prosthesis is attached to human forearm with its connectors (in Figure 2.14) at two points so that the realistic conditions for an amputee is approximated. As discussed in Section , four different muscle groups are used to control position and stiffness of the hand prosthesis.

The main purpose of the study is to grasp many different three-dimensional objects with various material characteristics, such as fragile, elastic (deformable), rigid structural properties. In Figures 4.6 and 4.7, it can be observed that the hand is capable of grasping different geometry of objects, cylindrical, triangular, square, elliptic, and many complex shapes. Depending on the shapes of objects and grasp orientation of hand in space, only required number of fingers becomes functional as a result of self-adaptiveness and compliance.

Another significant property of hand is presented by modulating hand stiffness depending on the materials of the objects. In Figure 4.8, many different property of objects, such as elastics (e.g., sponge), fragile (e.g. egg) are successfully grasped. The importance of this property comes into the picture while grasping an object without slipping but not deforming the object.

All illustrative examples presented here are available in video format at the link: <http://hmi.sabanciuniv.edu/>

### 4.3 Discussion

Passive compliance includes many benefits for prosthetic hands. Compliance increases the success in grasping of objects of different geometric shapes. Hand with compliant fingers minimizes the magnitude of grasping force at the initial interaction to prevent any initial damage. These advantages are quite significant while grasping an unstructured object in an unknown environment. In addition, the capability of stiffness modulation using variable stiffness actuators (VSA) makes hand prosthesis more dexterous allowing interactions with various types of objects, such as fragile, deformable, rigid ones.

In the sense of hand prosthesis, mechanical success does not suffice to satisfy the requirements of an amputee. It should provide ease in control and require short adaptation phase for successful use. Providing a natural control interface, similar to neuromuscular control of a real hand is a desirable for hand prosthesis. In other words, including natural control idea in hand prosthesis results in less effort to learn its use and requires less concentration and intentional control effort. This strategy is possible by integrating sEMG signals produced by humans into the control architecture of hand prosthesis. Control of VSA integrated hand prosthesis is realized using a natural human-machine interface that utilizes sEMG signals measured from the surface of the upper arm, chest and shoulder. In this control technique, called *tele-impedance control* [11], position and impedance parameters are instantly estimated through sEMG signals and sent to the control module of VSA integrated prosthesis as control references. The control of impedance is realized automatically as if natural control of real arm stiffness and position control of fingers are achieved intentionally.

In this dissertation, the hand prosthesis fabricated using an unsophisticated prototyping technique which reduces the construction complexity and decrease the cost of the fabrication without compromising the benefits of passive joint compliance and robustness. Robustness is a very challenging factor in multifingered robot hands while grasping different category of objects. Their expensive manufacturing and vulnerabilities in unknown environment limit their experimental task contents and decelerates implementation due to the meticulous attention in programming. Our design introduces construction of fingers composed of silicon rubber with ABS material, which outperforms conventional finger construction with metal prototypes and rigid joint structures. In the design, fingers are actuated in both direction, flexion and extension tendons. Force transmission in all mechanism is realized through Bowden cables. Thanks to the Bowden cable based transmission, VSA's are placed any suitable location. VSA mechanisms in and prosthesis play important role in the self-adaptation to unstructured environment. VSA's reflects desired impedance and position levels produced by human biopotential signals to the compliant, underactuated fingers depending on the requirement of environment or properties of grasped object. VSA's provides number of advantages, since they provide fast enough reactions to the unstructured environmental conditions thanks to its passive elements, do not require complex control algorithms with respect to the systems working with active impedance control, outperform in terms of energy efficiency.

In addition, VSA hand prosthesis and its sEMG interface for tele-impedance control enable amputees to control the impedance of the prosthetic hand to appropriately match the requirement of the task at hand. Both desired impedance and position of hand are estimated through the sEMG signals and

employed to control the VSA hand prosthesis. In particular, fingers' impedance regulation is realized through the impedance measurements of the intact upper arm, this control takes place naturally and automatically during the interaction with the environment. Regulation of fingers' position is realized intentionally by the amputee through the estimated position measurements of chest and shoulder muscles. The proposed control interface has number of benefits, since impedance modulation takes place naturally from task to task or performing activities of daily living without requiring attention of the amputees, extra concentration and diminishing their functional ability. Consequently, this approach does not require long-term rehabilitation periods, or interfere with control of intact body segments, and provides amputee with easiness in use.

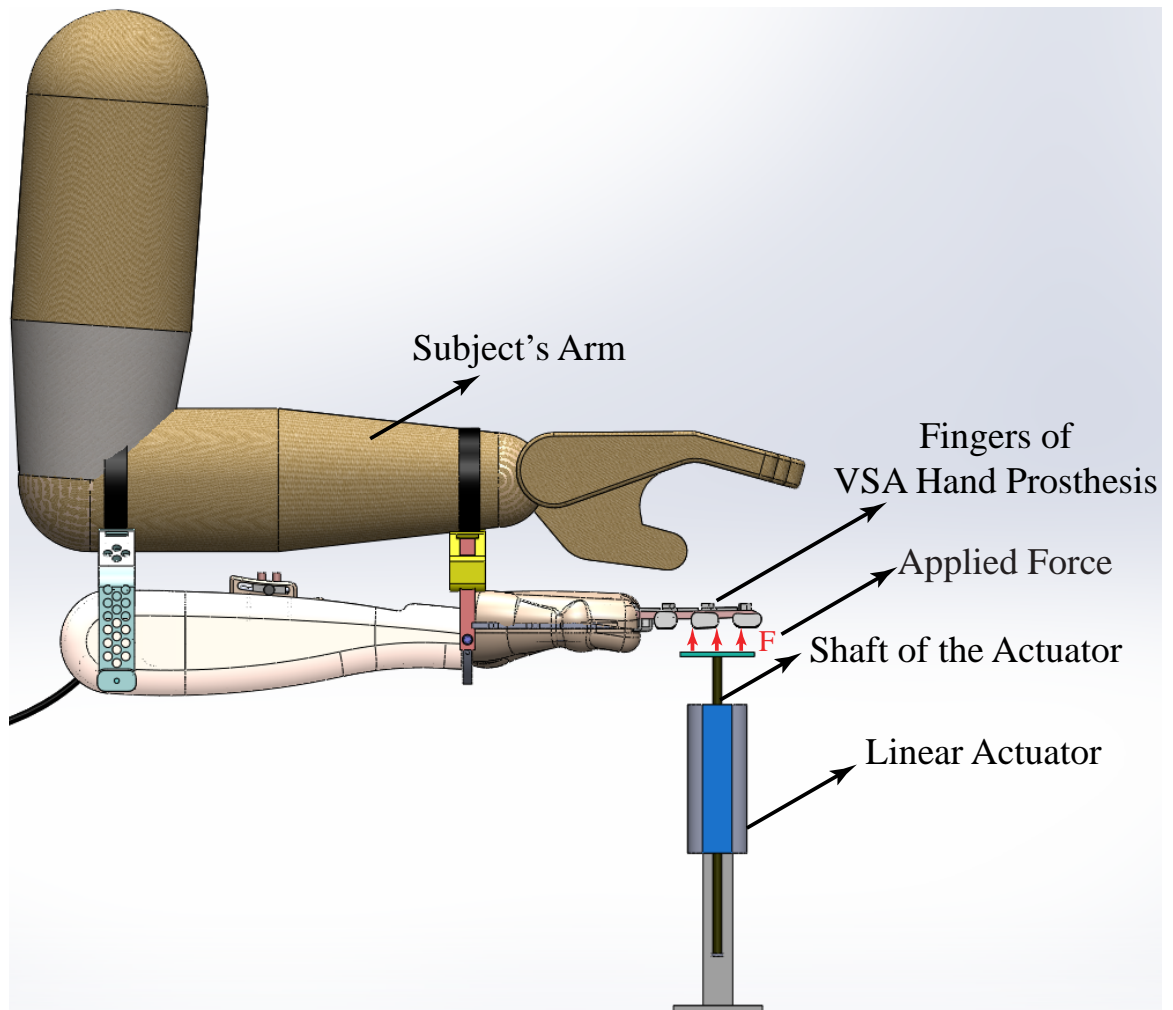


Figure 4.1: Schematic description of the experimental setup

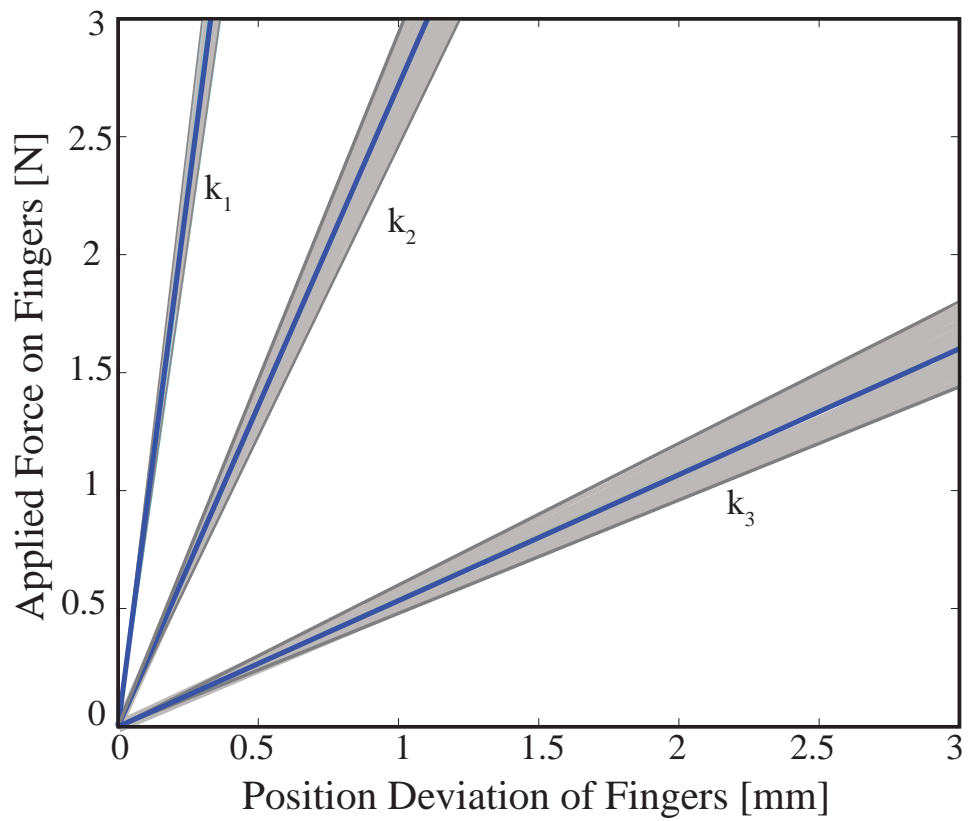


Figure 4.2: Stiffness Modulation of Hand through PC Workstation. Here, gray zone represents the results of each trial. The blue line represents the average value of ten trials.

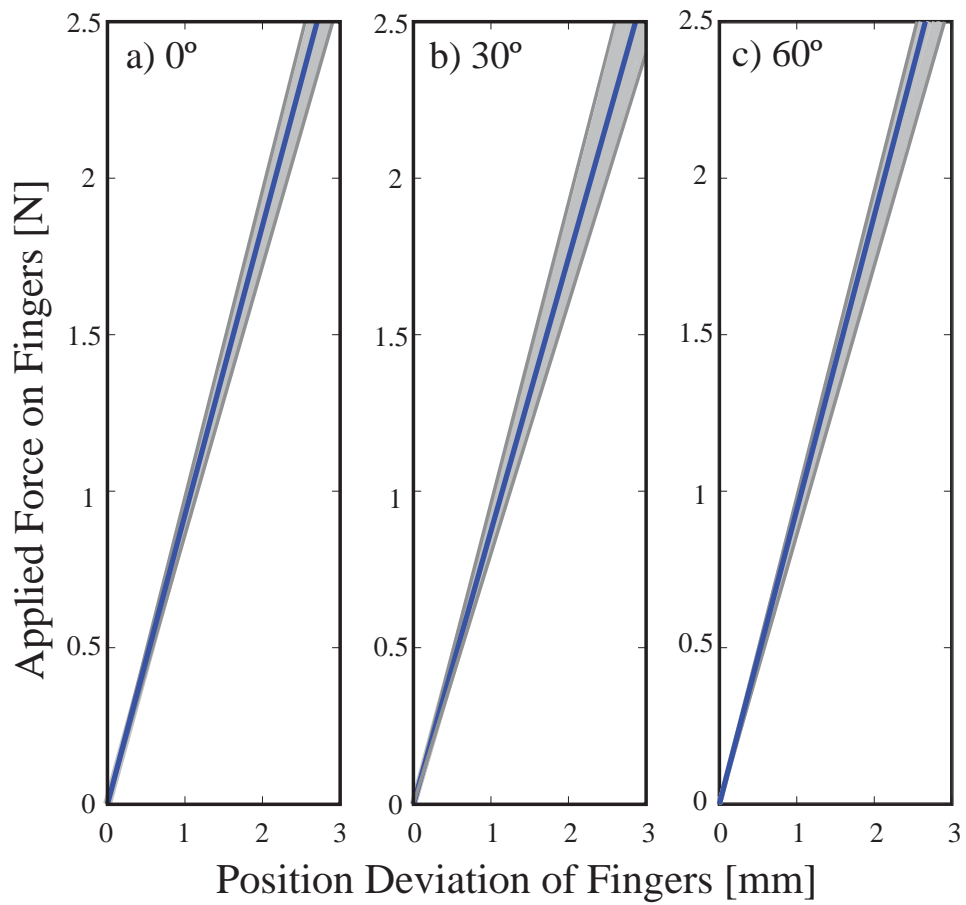


Figure 4.3: Position Control of Hand through PC Workstation. Here, gray zone represents the results of each trial. The blue line represents the average value of ten trials.

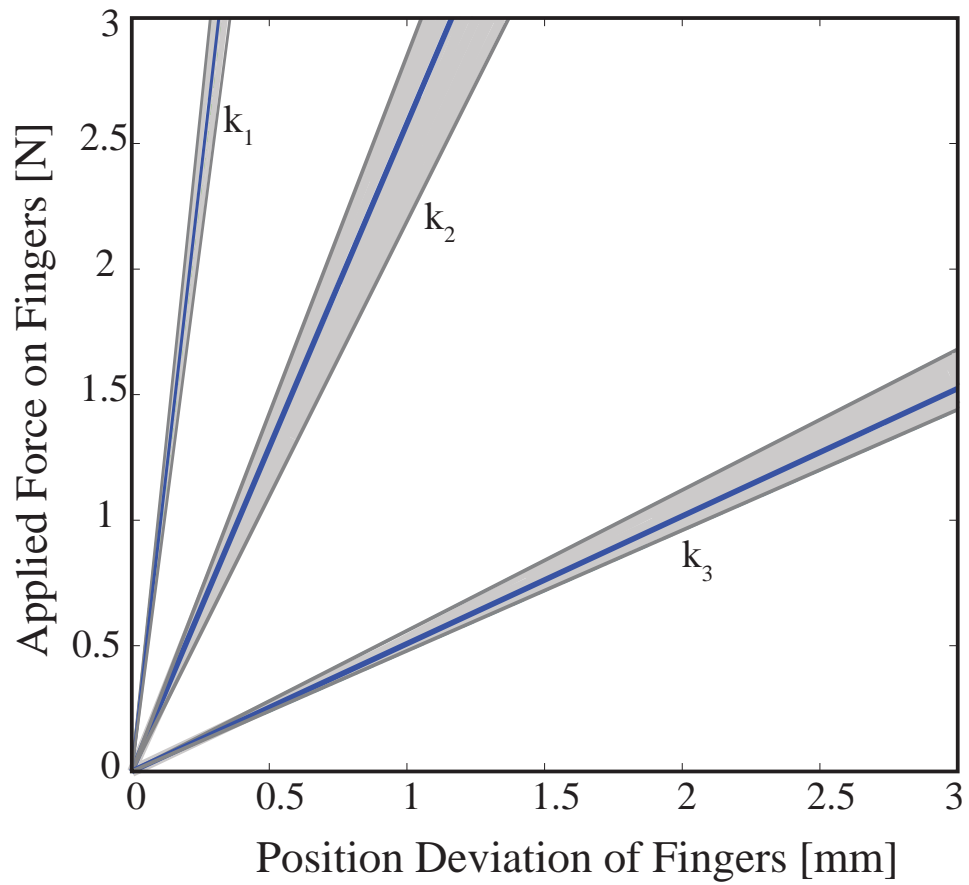


Figure 4.4: Stiffness Modulation of Hand through sEMG Signals. Here, gray zone represents the results of each trial. The blue line represents the average value of ten trials.

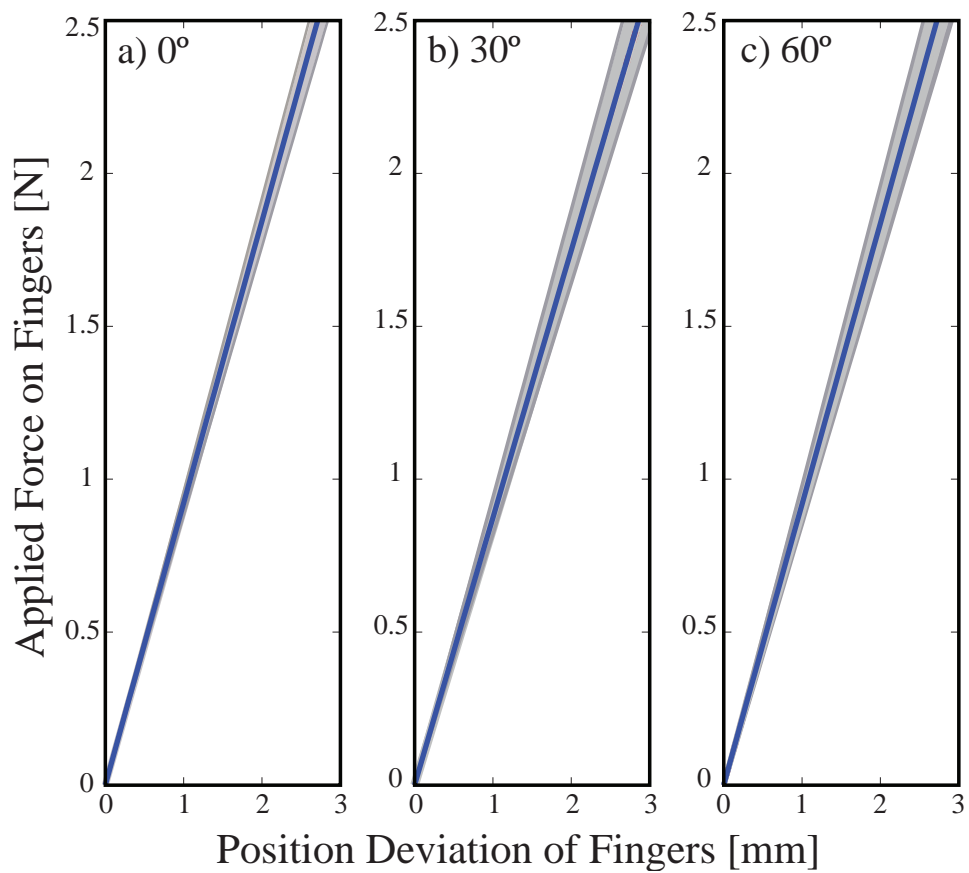


Figure 4.5: Position Control of Hand through sEMG Signals. Here, gray zone represents the results of each trial. The blue line represents the average value of ten trials.

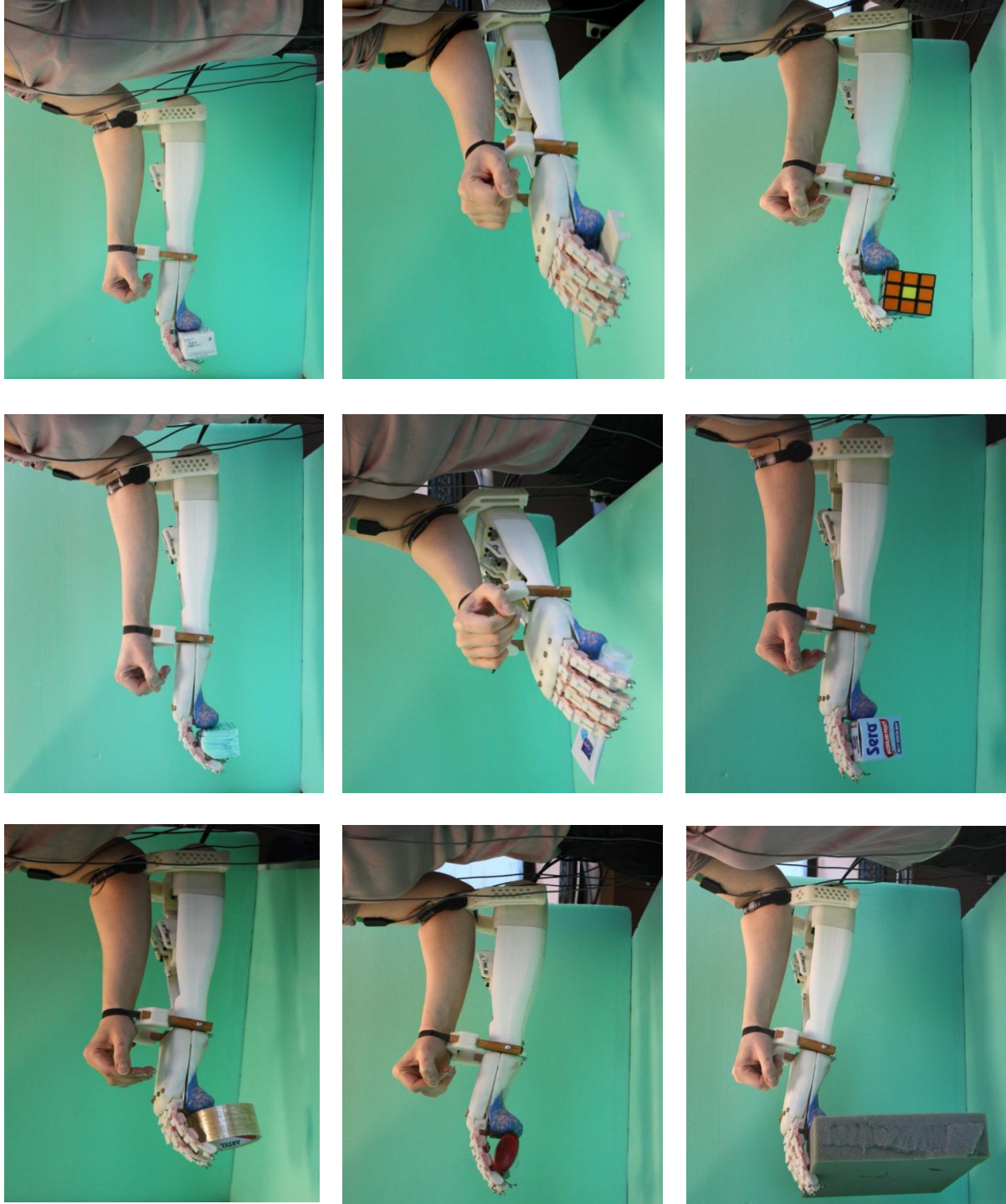


Figure 4.6: Grasping objects with different geometric properties

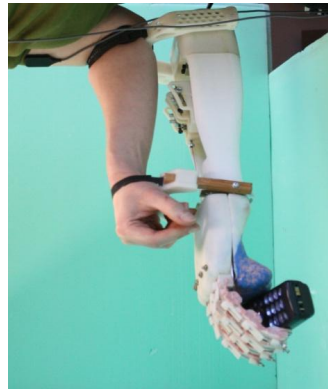
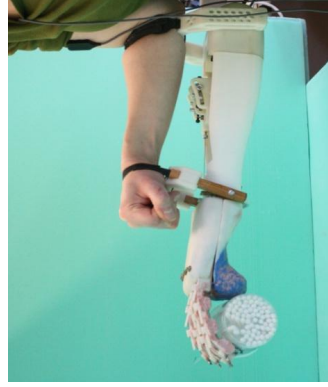
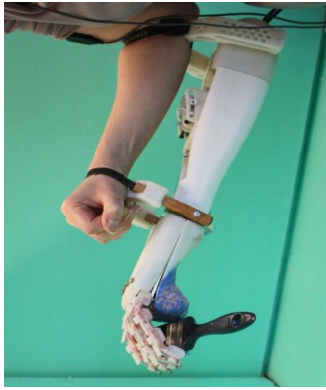
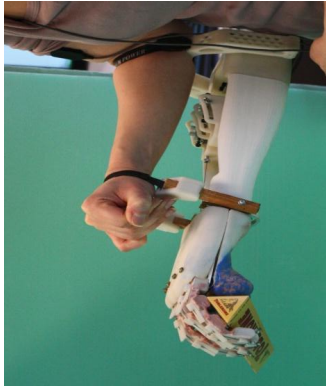
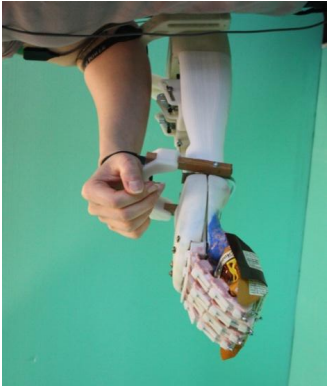
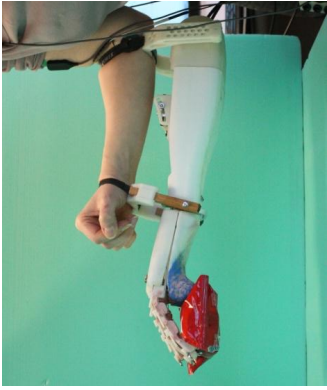
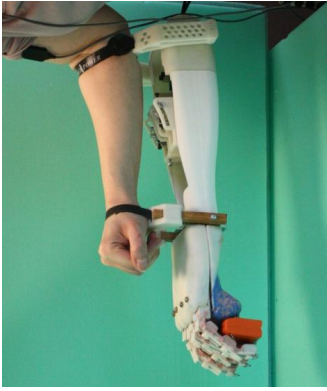


Figure 4.7: Grasping objects with different geometric properties

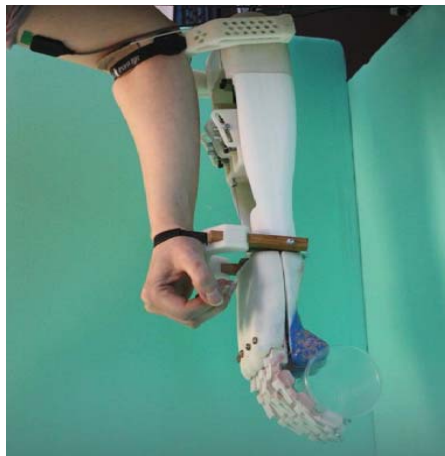
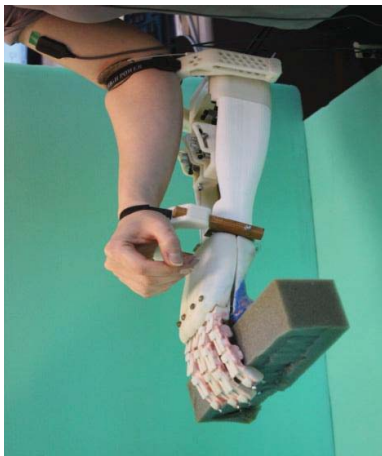
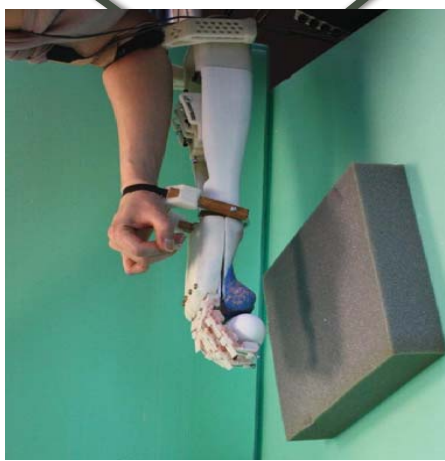
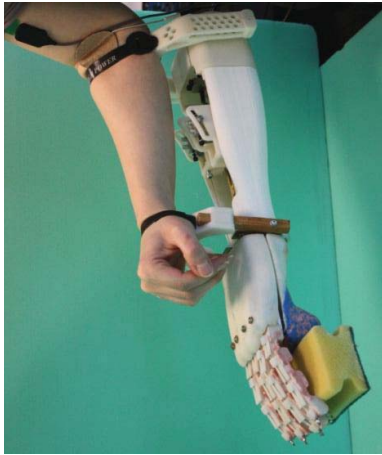
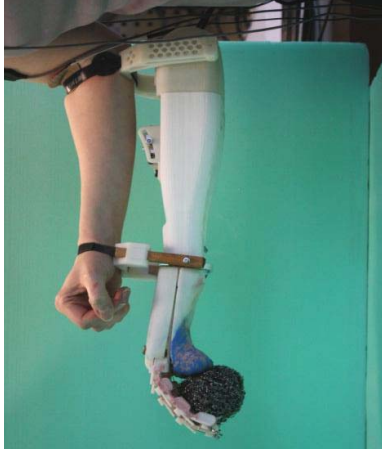


Figure 4.8: Grasping objects with different materials

# Chapter 5

## 5 Human Subject Experiments to Investigate Efficacy of Stiffness Modulation

Several studies conducted on neuromotor control provide evidence that humans have enough capacity to vary their impedance level depending on the requirements of the tasks [1–6]. It is observed in these experiments that humans control the mechanical impedance of their relaxed arm to be kept at low level, for tasks with no prior information in unstructured environment [7]. Besides, humans increase the impedance level of their arms by means of co-contraction of their antagonistic muscle pairs such that they suppress the perturbations or preserve arm stability against disturbances [3]. Humans can also react to the unexpected disturbances by adjusting their arm impedance and this adjustment includes reflexive contributions [78]. The mentioned properties of the neuromusculoskeletal system enable humans to naturally and stably interact with their environment [65, 79]. The ability of impedance variation provides human perform activities with different difficulty levels, from grasping a bouncing ball to holding a child’s hand while walking. Controllability of arm impedance transforms the human arm into a dexterous manipulator since it adapts its dynamics based on the various type of physical interactions.

On the other hand, currently available hand prostheses posses impedance

properties that cannot be controlled during the activities of daily living (ADL). For instance, joint impedance of the body powered prosthesis is set through the impedance of the intact human joint and mechanical design of the prostheses during the operation. Traditional EMG controlled prostheses adjust the joint impedance through the gains of a proportional velocity controller [80]. In these studies, endpoint impedance of the prosthetic limb is influenced by the mechanism between prosthesis and the residual limb of the amputee [36, 81, 82]. Since these prosthetic limbs lack of user-controlled impedance control, their performance stays limited while performing the ADL.

We anticipate that user-controlled impedance increases the dexterity of a prosthesis and improves the amputee’s performance while interacting physically with the environment. In this study, we study the efficacy of the user-controlled impedance on physically attached transradial hand prosthesis. In order to test the necessity of this improvement, physical interactions with the prosthesis are designed to replicate ADL and help us evaluate the usefulness of the impedance regulation with a series of systematic experiments.

## 5.1 State of the Art

The idea of integrating impedance modulation into prosthetic limbs has been first proposed and experimented in [33–35]. In these studies, sEMG signals are utilized to obtain estimations for impedance and velocity references to be used in the adaptive impedance control of Boston elbow prosthesis in a crank-turning tasks. Since the Boston elbow prosthesis is structured in rigid form, estimated impedance references could not be effectively transferred to the prosthesis due to the controllable bandwidth of the actuators. Besides, the Boston elbow prosthetic device appears rigid outside of the bandwidth

region. Moreover, including software based impedance modulation into systems necessitates non-stop use of actuators, which results in more energy consumption. Alternatively, in [36], the drawback of the bandwidth limitation is reduced to a certain extent integrating series elastic actuation (SEA) in the design of elbow prosthesis and its impedance is modulated through the amputee's sEMG signals. With this design, impedance modulation ability is still limited owing to the actuator bandwidth. Nevertheless, prosthetic design with SEA provides compliance into design and keeps its output impedance low above the control bandwidth. Thanks to the hardware based integration, device robustness, reliability and safety are improved, especially on the condition of impact with the environment. However, controlling the interaction forces with SEA requires continuous use of actuators and is energetically inefficient as in the software based impedance regulation. In [59], they proposed a variable stiffness actuation (VSA) to modulate stiffness of a prosthetic wrist in a concept of a simulation study. VSA provides opportunity to modulate desired impedance in hardware environment and the actuators are only in use during the modulation and/or joint rotations. Hence, proposed mechanical concept provides energy efficiency. Moreover, the desired impedance can be enforced over the whole frequency spectrum, including frequencies well above the controllable bandwidth of the actuators. One more research group addressed the systematic study of user-controlled impedance regulation for prostheses. In these studies [8–10], the aim is to identify the characteristics of human impedance modulation while subject is performing a series of pre-defined tasks. It is reported herein that task-dependent impedance enhances user performance during the activities requiring interaction with environment. In this study, however, designed experiments does not

require impedance modulation within each task. Also the tasks limit subject's impedance level at low or high range. In our experiments, impedance variation within a task is allowed and humans are physically connected to the robot, hence our test conditions more closely replicate the actual operating conditions of a prosthetic device.

## 5.2 Overview of the Human Subject Experiments

In this study, a set of human subject experiments is conducted to find an answer to the question: Does human controlled impedance modulation improve the amputee's performance during physical interactions with the environment? The contribution of this study is to closely replicate the conditions of an transradial amputee and investigate his/her physiological requirement, while physically interacting with several (possibly unexpected) condition in the environment and also performing ADL. In order to provide realistic conditions for a healthy volunteer, the transradial hand prosthesis is physically attached to the subject's arm during these experiments. As a result, the interaction forces acting on the transradial hand prosthesis are physically reflected to the subject, as would be the case for an amputee. Moreover, the prosthesis is located with the arm such that subject's focus does not diverge from task during the execution of the designed tasks.

During the experiment, subjects controlled a physical transradial hand prosthesis to interact with a force feedback manipulandum while executing tasks in virtual reality (VR). The working principle of the attached variable stiffness transradial hand prosthesis is coherent with this study. VSAs in the attached prosthesis are designed to serve as antagonistically arranged artificial muscles which are responsible for the impedance and position modulation

of the hand prosthesis.

By means of these systems, subjects completed three one-degree-of-freedom tasks: (1) *Contact force minimization task* in which the aim is to minimize contact forces between the proxy, which represents moving object in the VR, and the variable stiffness transradial hand prosthesis controlled through sEMG signals of the able-bodied subject, (2) *Trajectory tracking task* in which the aim is to minimize the trajectory error between virtual moving object and the variable stiffness transradial hand prosthesis, and (3) *Interaction with a variable impedance environment task* in which the goal is to keep the position of the virtual box at specified level while the mechanical impedance of the virtual environment is randomly changing. All tasks are performed using variable stiffness transradial hand prosthesis. These tasks are intentionally chosen to resemble most common type of interactions and we hypothesize that these tasks would enforce subjects to modulate their impedance and simultaneously the prosthesis impedance to different levels.

### **5.3 Experiment Design**

A human subject experiment is designed in two environments, physical and virtual. Based on the defined task in the virtual environment, subjects perform the experiment using the physical system.

#### **5.3.1 Experiment Setup**

Human subject studies utilize a virtual environment and a force feedback manipulandum. The impedance of the 1 DoF haptic interface is modulated based on impedance control. Besides, the human interacts with the haptic interface through the variable stiffness transradial hand prosthesis. The control

references for the prosthesis are obtained directly through the human muscle activation levels, namely sEMG signals. Both impedance and position modulations of the variable stiffness transradial hand prosthesis are conducted based on the position and stiffness estimations obtained by means of sEMG signals. Overall experimental configuration is depicted in Figure 5.1. Further details of the virtual environment and haptic interface, and variable stiffness transradial hand prosthesis are described in the following sections.

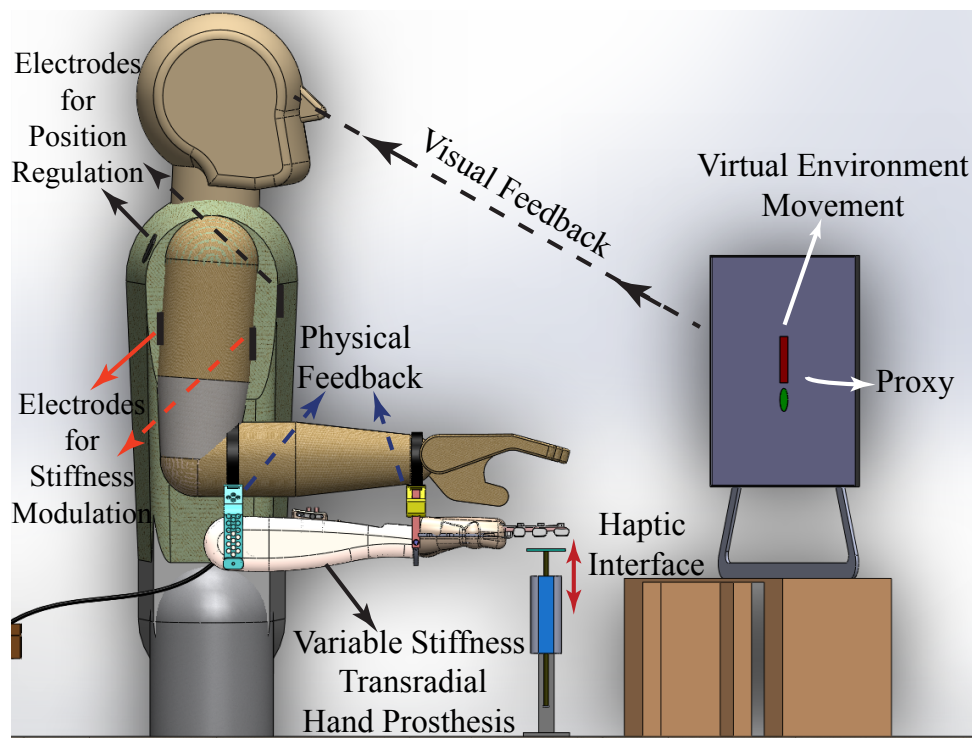


Figure 5.1: Schematic representation of the experimental setup

## A Virtual Environment

1. Hardware: The virtual environment and the 1 DoF haptic interface are represented in Figure 5.1. The haptic interface consists of a direct drive linear motor (ServoTube Linear Actuator, Copley

Controls) combined with precision position encoder, and is placed just under the four fingers. Forces applied by the prosthetic hand is measured by a force sensor (ATI Mini45) and its data transfer to the computer is realized by the NI PCI-6250 DAQ card. Visual feedback is provided via a computer monitor, which is placed in front of the subject in order to display the task in a virtual environment. The movement realized in the virtual environment is coherent with the movement realized by the handle on the shaft. Both of the motions are realized in the vertical direction. The data transfer between linear motor and a PC work-station is realized through a DAQ card (Quanser-Q8 usb). Data are sampled at 500 Hz during the all experiments. The task description is programmed using VRealm Builder, real-time experiment is implemented via MATLAB Simulink environment.

2. Modeling and Control: Subject interacts with the 1 DoF virtual environment through the variable stiffness transradial hand prosthesis as shown in Figure 5.2.

The virtual environment is represented as a point mass  $m$  at position  $x_v$ , while the mechanical impedance of the environment is modeled with a spring with stiffness constant  $k_v$  and a damper with damping constant  $b_v$  connecting the actual position  $x_v$  of the virtual point mass to the desired position  $x_h$  controlled by the subject. This model provides us with opportunity to mimic various kinds of activities in environment in such a way that humans necessitate to change their impedance level. The equation of motion for the virtual environment is expressed in Eqn. (5.1). Here,

$F_{haptic}$  represents the environmental force exerted by the virtual environment. Eqn. (5.1) is an expression of the virtual environment under the influence of external force.

$$m\ddot{x}_v = -b_v(\dot{x}_h - \dot{x}_v) - k_v(x_h - x_v) + F_{haptic} \quad (5.1)$$

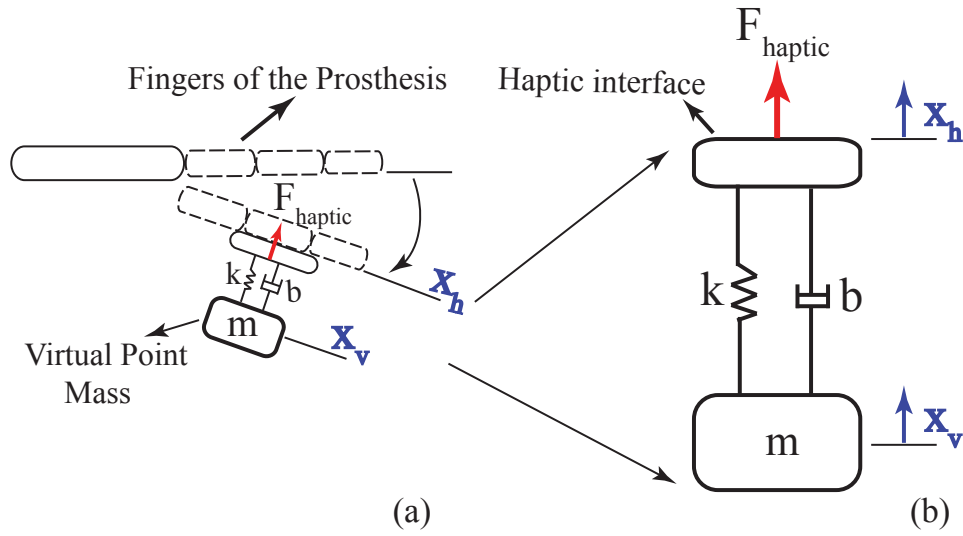


Figure 5.2: a) Schematic representation of the interaction among prosthetic device, haptic interface and virtual environment b) The relation between haptic interface and the virtual environment

## B Physical System (Variable Stiffness Transradial Hand Prosthesis)

1. Hardware: In this study, the haptic interface is manipulated by the variable stiffness transradial hand prosthesis commanded through the sEMG signals. During the experiment, this prosthesis is physically attached to the human's forearm with the mechanical extensions. One of the benefits provided by the mechanical connection is to mimic the condition of an amputee who is a transradial

hand prosthesis wearer. Besides, it integrates all nonlinear effects caused by the hand prosthesis into the experiment results. In addition, concentration of the subject is oriented to the behavior of the transradial hand prosthesis while subject is performing the tasks.

The important property of the hand prosthesis in this study is its mechanical design, namely variable stiffness actuation which enables amputee to vary the impedance level of the fingers and also simultaneously and independently control their position. The required analog inputs to control the the brushed DC motors of the variable stiffness actuator (VSA) are sent to the PC through the DAQ card (Quanser-Q8 USB) with the sampling rate of 500 Hz, real-time implementation is realized via MATLAB Simulink environment. The control references for the VSA mechanisms are obtained through the sEMG signals measured from the surface of the upper arm, and chest and shoulder. The measurement of the sEMG signals are realized through the surface electrodes of a sEMG signal acquisition device (Delsys-Bagnoli-8) with the sampling rate of 1000Hz.

## 2. Tele-Impedance Control:

This prosthetic hand with the antagonistic VSA realizes the impedance regulation in hardware. A tele-impedance control architecture is also preferred to provide natural impedance control of the variable stiffness transradial prosthetic hand for an amputee, under control of human neuro-musculoskeletal system.

Simultaneous and independent position and impedance control

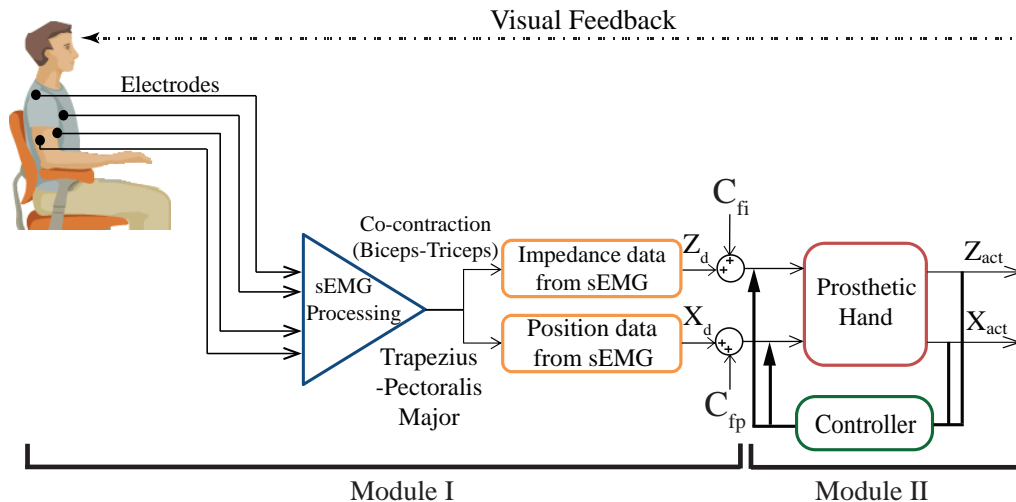


Figure 5.3: The control interface of the VSA prosthetic hand: In the first module, raw sEMG signals are measured from the intact forearm and relevant groups within the remaining thumb musculature and a series of filters are applied. In the second module, the desired position and stiffness levels are estimated from the filtered sEMG signals. Finally, the closed loop position and stiffness control of the variable stiffness prosthetic hand is handled by the third module.

architecture of the antagonistic variable stiffness transradial hand prosthesis through sEMG signals is presented in Figure 5.3. The control of both position and impedance of the hand prosthesis is achieved by two modules. In the first module of Figure 5.3, required reference signals for the control of both impedance and position are estimated through filtered and conditioned sEMG signals. Concerning the realistic scenario, for the transradial upper extremity amputees, muscle groups inside the hand and forearm are not appropriate for the EMG measurement. Hence, for the position reference of the prosthetic's fingers, sEMG signals are measured from the different regions of the chest, concurrently for the impedance reference, sEMG signals are recorded from the up-

per arm. The second module depicts the closed loop control of the VSA hand prosthesis to guarantee convergence of the actual position and impedance values of the fingers to the estimated references. Overall control architecture is closed through the visual feedback, which helps amputee modulate his/her sEMG signals to match the task requirements.

### 5.3.2 Tasks

Subjects execute three simple tasks in two categories. The first task, the contact force minimization task, aims to minimize contact forces acting on the haptic interface by hand prosthesis. The second task, the trajectory tracking task, aims to follow the trajectory of virtual object while random perturbations are applied. In the third task, the interaction with a variable impedance environment task, the aim is to preserve the initial condition of a virtual object while environmental conditions are changing and the perturbations are applied. We hypothesize that performing each task requires different impedance levels. In particular, contact force minimization is performed with low level impedance and trajectory error minimization is realized with high impedance level, whereas interaction with a variable impedance environment requires adaptation of impedance levels during the task. In literature, some systematic studies are performed [8–10], however the observed cases are limited to reveal the requirement for adaptive impedance variation. Besides, in our experiments, humans are physically connected to the robot, hence our test conditions more closely replicate the actual condition of a prosthetic device requirement.

**A Contact Force Minimization:** In this task, while a virtual object is moving in one dimensional trajectory the variable stiffness transradial hand prosthesis is manipulating the haptic interface to minimize the contact force applied on the hand. This task is very similar to the holding someone’s hand while walking as represented in Figure 5.4. In the experimental scenario, virtual moving object represents end effector of the haptic interface that prosthetic device is interacting with. The dynamic equation of the virtual moving object is expressed in Eqn. (5.2). In this equation, the mechanical impedance of the virtual object is introduced by a stiffness with spring constant,  $k_v$  and a damper with damping constant  $b_v$ , and the desired trajectory of the virtual moving object is represented by  $x_v$ .  $x_h$  is the position level representing the combined condition of prosthetic device and the manipulandum. Force generated by the virtual environment ( $F_{haptic}$ ) is a result of the mechanical impedance of the moving object. During the experiment, in the first three cases, stiffness level is predefined by the PC and position control is realized through sEMG signals. In the last case, both position and impedance levels of the fingers are modulated independently and simultaneously through sEMG signals.

$$F_{haptic} = -b_v(\dot{x}_h - \dot{x}_v) - k_v(x_h - x_v) \quad (5.2)$$

In Eqn. (5.2), it is seen that the effect of environmental force on dynamics can be reduced if the actual trajectory of the moving object becomes very close to the desired trajectory of the moving object. However, in this task, the desired position of the object is unknown to the subjects

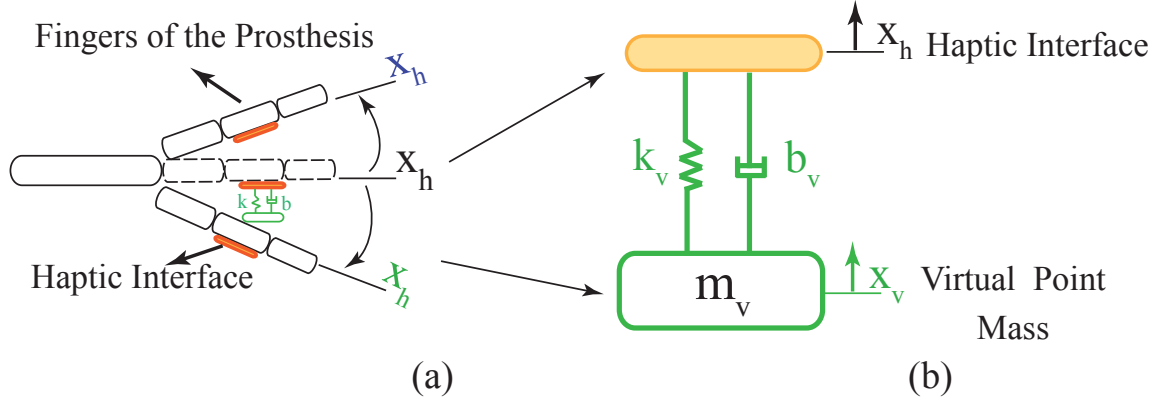


Figure 5.4: Representation of the Contact Force Minimization Task (a) Interaction between the hand prosthesis and haptic interface (b) Representation of physical (haptic interface) and virtual environment

during the study, the impedance parameters between subject and virtual moving mass can be minimized to make the task more easier. The task provides no a priori knowledge for the subjects by randomizing the desired trajectory of the moving object.

The desired trajectory is expressed in Eqn. (5.3).

$$x_{d2} = a_1(\sin \kappa_1 t + \psi_1) + a_2(\sin \kappa_2 t + \psi_2) + bias \quad (5.3)$$

Here,  $t$  represents the time and  $\psi_1$  and  $\psi_2$  are randomized between  $[0, 2\pi)$ . Besides,  $a_1$ ,  $a_2$  and  $\kappa_1$ ,  $\kappa_2$  are determined based on range of motion and maximum speed of the variable stiffness transradial hand prosthesis and they are selected as 5, 5, 0.06, 0.012 respectively.

**B Trajectory Tracking Task:** In this task, while a virtual mass objects is moving randomly in vertical axis, human is commanded to prosthetic

device to follow the trajectory presented in the monitor. The model of the task is represented in Figure 5.5. As depicted in Figure 5.6, the task is following the trajectory changing randomly as a function of time. Simultaneously, at random times force perturbations act by haptic interface and are presented with green balls. The trajectory defined by the sum of different characteristics of sinusoids with blue color is a random trajectory produced by the Eqn. (5.4) and a sample of it is presented in Figure 5.5. Here,  $t$  presents the time and  $\psi_1$  and  $\psi_2$  are randomized between  $[0, 2\pi)$ . During task, random force perturbations are applied to the virtual moving object at random time intervals. The frequency and amplitude of the trajectory are determined during the trial period of the experiment. It is based on range of motion and speed of the prosthetic device. During the experiment, in the first three cases, stiffness level is predefined by the PC and position control is realized through sEMG signals. In the last case, both position and impedance levels of the fingers are modulated independently and simultaneously through sEMG signals.

$$x_d = a_1(\sin(\kappa_1 t + \psi_1)) + a_2(\sin(\kappa_2 t + \psi_2)) + bias \quad (5.4)$$

**C Interaction with a Variable Impedance Environment Task:** In this task, the aim is preserving the position level of the moving object at the defined level while the mechanical impedance of the environment is randomly varying. While performing the task, moving object and also its haptic interface are perturbed. While hand prosthesis is exposed the perturbation, subject gives an appropriate command to keep the

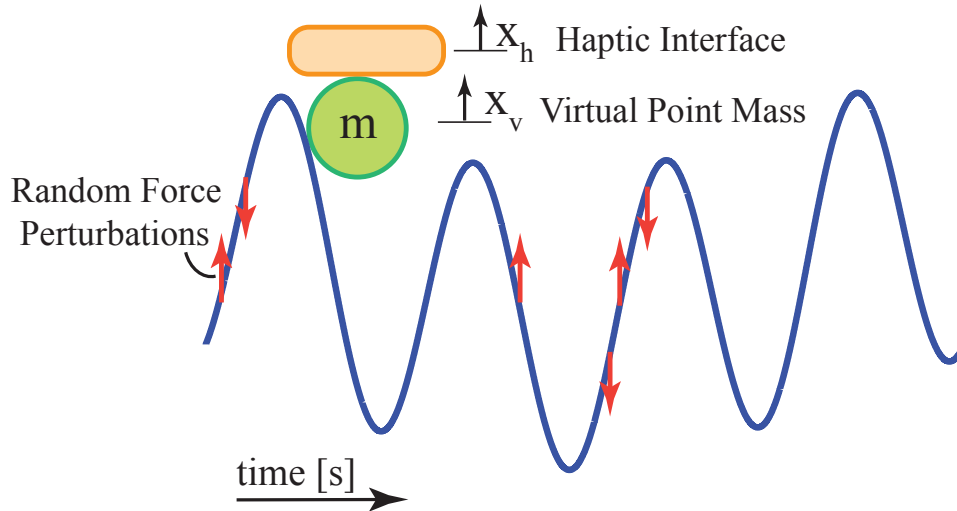


Figure 5.5: The Model of the Trajectory Tracking Task

box at predefined level under the varying environmental conditions. We hypothesize that this task requires continuous adaptation of the prosthetic device to the varying environmental conditions. Adaptation to the environment is realized by modulating the impedance level of the prosthesis through the sEMG signals. During the experiment, fingers of the prosthesis are attached to the haptic interface in order to control the position level of the virtual point mass presented in Figure 5.8 at desired level. During the experiment, in the first three cases, stiffness level is predefined by the PC and position control is realized through sEMG signals. In the last case, both position and impedance levels of the fingers are modulated independently and simultaneously through sEMG signals.

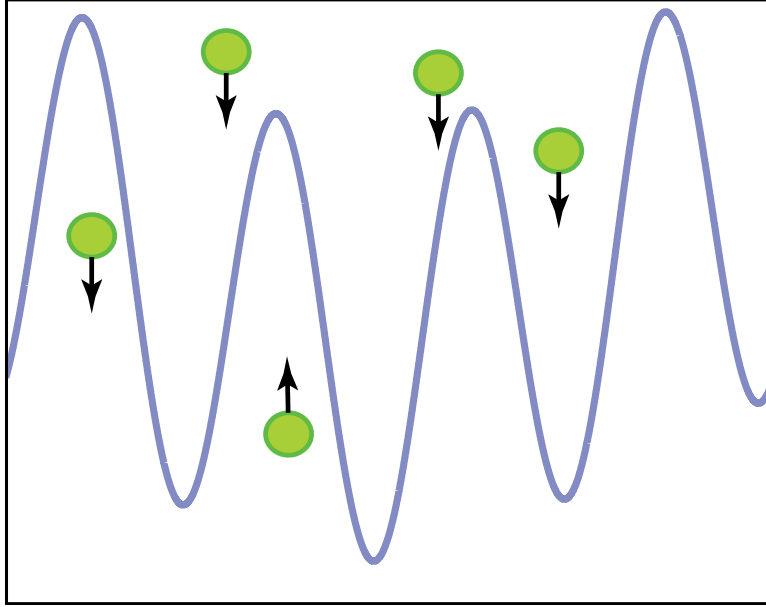


Figure 5.6: Representation of the Trajectory Tracking Task in Virtual Environment

### 5.3.3 Experimental Procedure

Before the experiment, participants are guided by a training period to get experienced about the tasks. In particular, it is informed that subjects are responsible for providing necessary sEMG commands to modulate impedance automatically and position levels of the prosthetic device intentionally while following the task displayed on the monitor. The experiment is conducted with the participation of healthy students of Sabancı University. Participants did not present any motor and sensory impairment. The participant signed informed consent forms approved by the University Research Ethics Council of Sabancı University.

At the beginning of the experiment, the variable stiffness transradial hand prosthesis and the virtual environment are calibrated and initialized. The

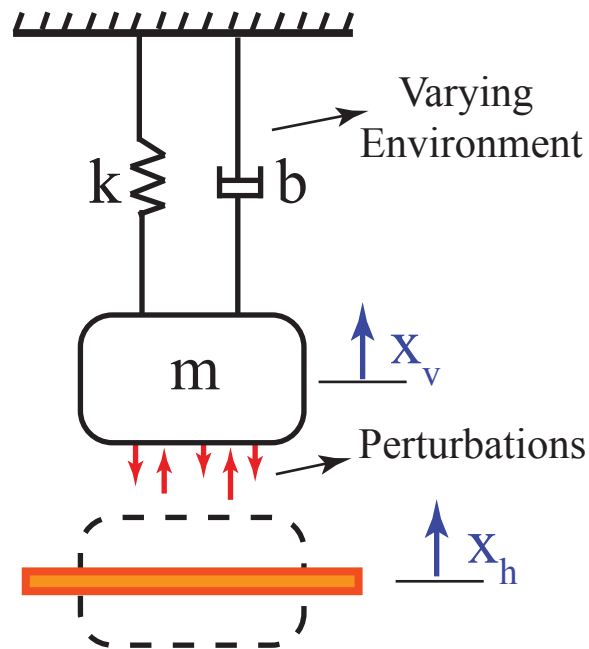


Figure 5.7: The Model of Interaction with a Variable Impedance Environment Task

calibration ensures the task in the virtual environment is properly presented to the subject and finger's position and stiffness are adjusted to be at relax hand posture. Besides, since participant's arm posture affects the arm impedance, at the beginning of the each session subject's forearm is arranged to be perpendicular to the upper arm. For each three task, participant is reminded about their responsibilities. In order to minimize the fatigue effect, participants are relaxed for 30 to 60 seconds between subsessions and this break is also increased upon the subject's request. Experimental procedure for each task is represented in Figure 5.9. Human subject experiments have 4 sessions. Each subsession in the experiment is composed of five trials and each trial lasts 15 seconds. This procedure is repeated five times by giving 1 hour break between each subsession to guarantee the subject's freshness.

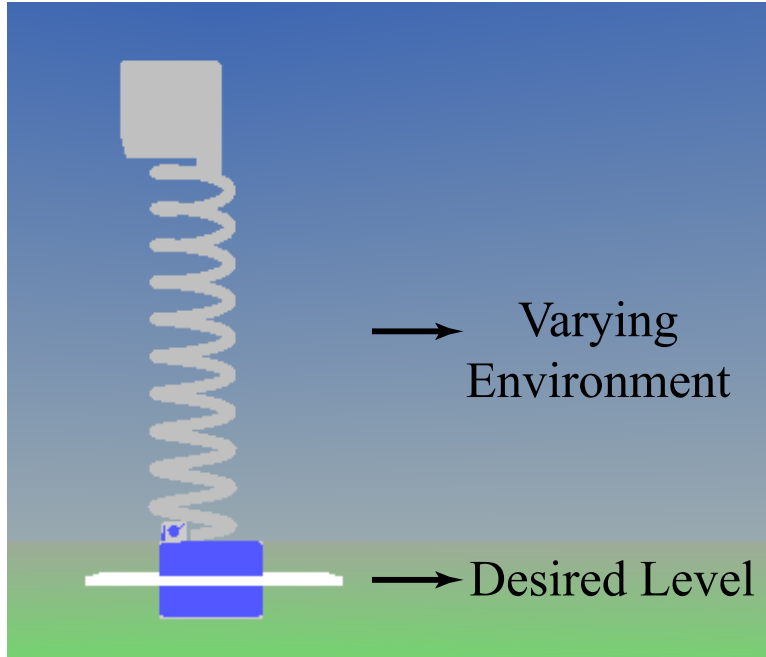


Figure 5.8: Representation of the Interaction with a Variable Impedance Environment Task in Virtual Environment

In order to investigate the effect of human dependent impedance modulation on prosthetic devices, experiments for each tasks are conducted in two categories. In the first category, the impedance is adjusted by a PC workstation to pre-set levels, and human merely supplies the position reference command to the prosthetic device. In this category, the impedance is regulated to three different, i.e., low, intermediate, high levels. For instance, position of the fingers are adjusted through sEMG signals of the subject while the impedance level of the prosthetic hand is predefined to low level through the command input supplied by the PC workstation. At first, when the stiffness level is conducted to be set to low, the fingers are compliant, participant is performing the task by commanding the position reference input only. This procedure is repeated for the intermediate and high stiffness

levels for the fingers as well. In the second category, both impedance and position modulation of hand prosthesis are realized through the sEMG signals provided by the participants. In this category, impedance modulation is realized automatically while the position regulation takes place intentionally. The idea behind executing the tasks in two categories is to compare the human based control effect on the task performance with respect to the fixed impedance levels.

For the contact force minimization task, subjects are required to control the interactions with the haptic interface to minimize contact forces between prosthesis and the end effectors. For the trajectory tracking task, subjects are asked to overlap the mid point of the red cylinder to the green ball controlling the physical proxy of the red cylinder. For the interaction with a variable impedance environment task, subjects are expected to perform the positioning of the box at desired level using the physical proxy of the box. All tasks are executed with manipulation of the variable stiffness transradial hand prosthesis physically attached to the participant's forearm. Before performing the tasks, subjects gain experience about the execution of the tasks and the control of hand prosthesis by practicing the training session. The number of training for each task is based on the learning period of the subject and differs among subjects. Training period is repeated for the each session, LS, IS, HS, VS. Subjects are informed to complete the training period before each session. During the experiment, the order of tasks is randomized between subjects.

## **5.4 Preliminary Results**

This section presents the experimental results with their statistical analysis.

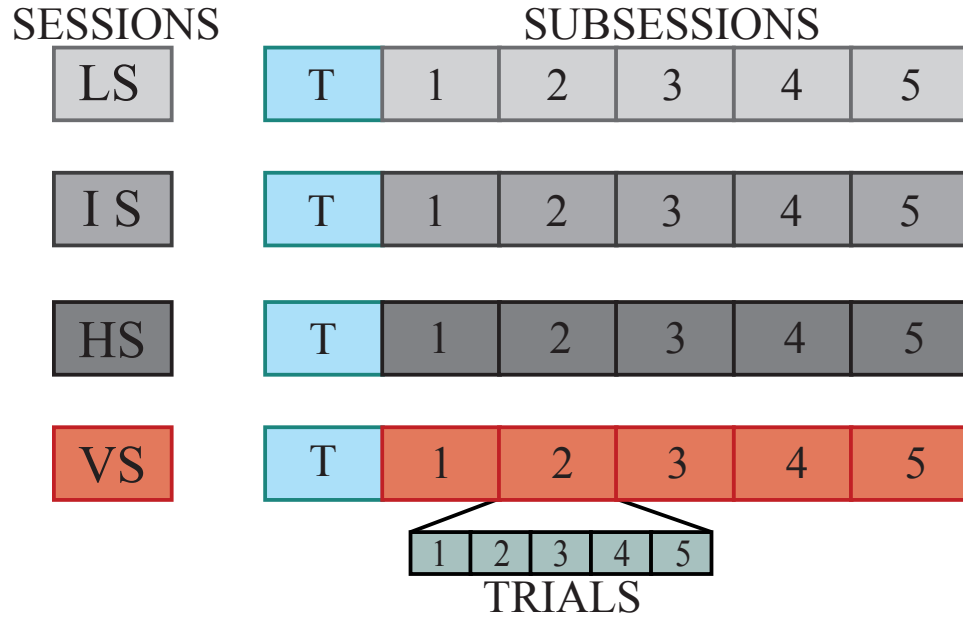


Figure 5.9: Schematic representation of the experiment design. Experiment consisted of 4 sessions: Low Stiffness (LS) Level, Intermediate Stiffness (IS) Level, High Stiffness (HS) Level, and Varying Stiffness (VS) Level. Capital T represents the task training period before each session. Each session contains 5 subsessions, while each subsession has 5 trials.

#### 5.4.1 ANOVA Results of The Experiments

The experiment consists of three factors, namely the tasks and cases modes and the subsessions, thus for the statistical analysis, a repeated measures ANOVA is employed to verify the tested hypotheses. The task mode is analyzed as a between-subject factor, with three different tasks of contact force minimization, trajectory tracking, the interaction with a variable impedance environment. Moreover, the case factor is also analyzed as a between subjects factor with four different cases, predefined low level, intermediate level, high level cases, and sEMG based variation cases. Five subsessions are analyzed as a within-subject factor. Summary of ANOVA results over the performance

Table 5.1: Summary of significance measured by ANOVA for average RMS values

Effect	Significance
Tasks	$F(2,9)=4.938, p < 0.05$
Cases	$F(3,8)=4.536, p < 0.05$
Subsessions	$F(4,36)=0.494, p > 0.05$

error metric is listed in Table 5.1. The results reveal a significant main effects of tasks and cases on the experiments and no significant effects of subsession or interactions.

#### 5.4.2 Contact Force Minimization Performance

Figure 5.10 represents the performance results of the subject in one-degree-of freedom experiment with visual feedback. As seen that, subject shows the best performance when the fingers' stiffness are adjusted at lower level (low). The performance metric is expressed by the RMS values of the net contact force acting on the haptic interface. Performance results indicates that performance of hand prosthesis with human based impedance modulation is very close the performance of low level regulation predefined by the pc workstation. In order to represent statistically significance between cases of the task, paired ttest analysis is realized. Ttest analysis represents statistical significance between the pairs of low-intermediate levels, low-high levels, intermediate-high levels, intermediate-sEMG, high-sEMG at  $p < 0.01$ , while

all other pairs are found to be not significant.

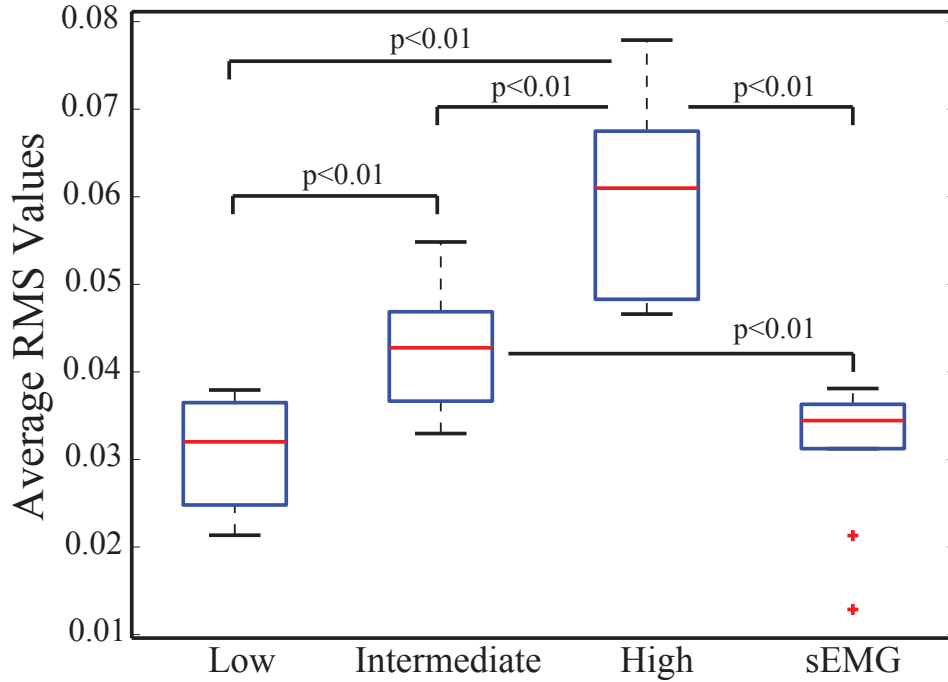


Figure 5.10: Box Plot of the Contact Force Minimization Task Performance

### 5.4.3 Trajectory Tracking Task Performance

Figure 5.11 represents the performance results of the subject in one-degree-of freedom experiment with visual feedback. As seen that, subject shows the best performance when the fingers' stiffness are predefined at high level (high). Besides, performance results indicates that performance of hand prosthesis with human based impedance modulation is very close the performance of high level regulation adjusted by the pc workstation. The performance metric represented by the RMS value of trajectory error of the haptic interface. The paired ttest analysis shows the statistical significance between pairs of low-intermediate levels, low-high levels, low level-sEMG,

intermediate-high levels, high level-sEMG at  $p < 0.01$ , while all other pairs are found to be not significant.

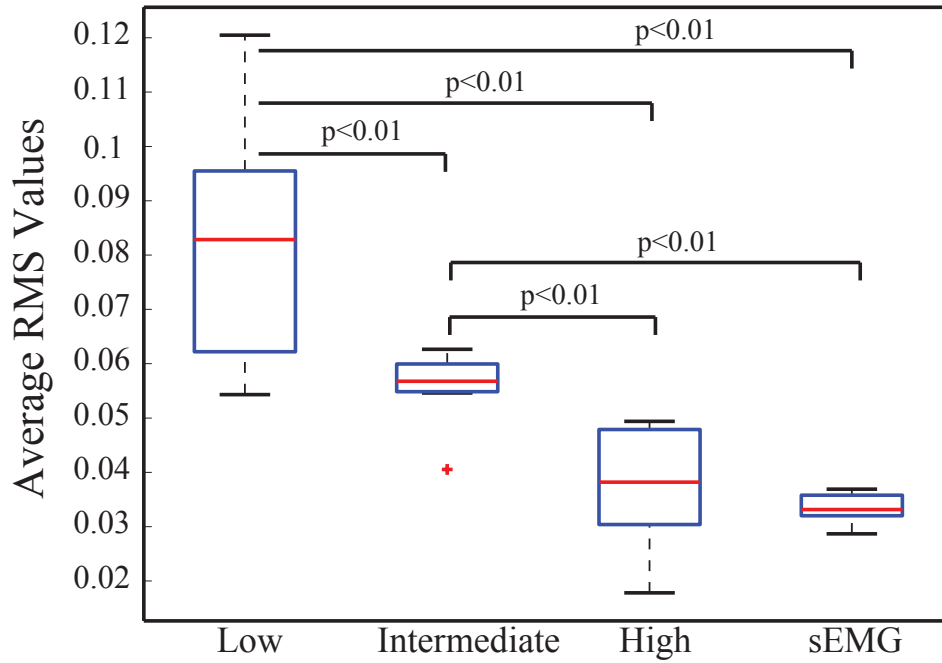


Figure 5.11: Box Plot of the Trajectory Tracking Task Performance

#### 5.4.4 Interaction with a Variable Impedance Environment Task Performance

Figure 5.12 represents the performance results of the subject in one-degree-of freedom experiment with visual feedback. As seen that, subject shows the best performance when the impedance modulation is realized by the human. Since impedance modulation could not be adapted when the mechanical impedance of hand prosthesis is set at a constant level. The mechanical impedance of the variable stiffness transradial hand prosthesis should be varying and adaptable when the mechanical impedance of the virtual environment is

randomly changing. Hence, it is only possible when the impedance modulation of the device is realized by the participant. The performance metric is represented by the RMS error between the defined position level and actual position of the virtual box. The paired ttest analysis shows the statistical significance between pairs of low level-sEMG, intermediate level-sEMG, high level-sEMG at  $p < 0.01$ , while all other pairs are found to be not significant.

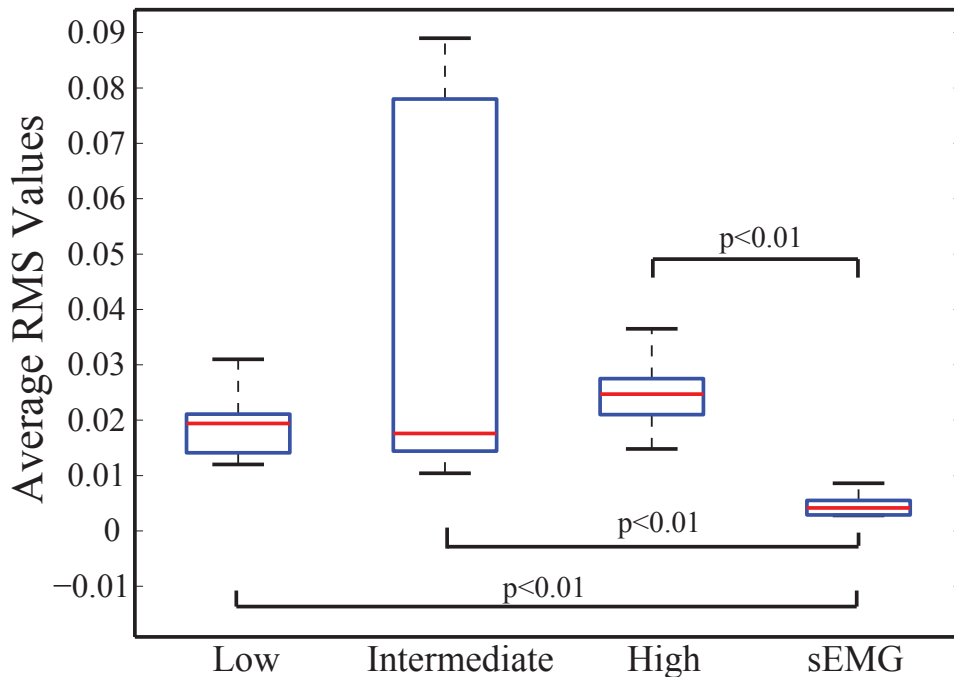


Figure 5.12: Box Plot of the Interaction with a Variable Impedance Environment Task Performance

## 5.5 Discussions

These experiments are designed to reveal the requirement for different level of impedance adjustment and suggest potential advantageous of human-modulated impedance of prosthetic device. The one of important contri-

bution of this study is to observe the varying impedance task on human-impedance modulation and pc-impedance adjustment in three levels. The second remarkable factor affecting the experiment results directly is to connect the prosthetic limb physically to human arm to perform the defined tasks.

Experiments are categorized in two sections to compare the human based impedance control with the pc based impedance control. In pc based control, the impedance modulation is adjusted by the command inputs supplied by the pc workstation. In this category, each task is performed by modulating the fingers' impedance at low, intermediate and high levels separately. While setting the impedance of the fingers to a constant level, position of the hand prosthesis is controlled through the sEMG signals. Integrating this category to the experiments provides us with the understanding the requirement of human based modulation in prosthetic limbs. In the second category of the experiment, both position and impedance of the prosthetic limb are modulated through the sEMG signals while human is performing the tasks. The results indicate that each task requires respective impedance level. Hence there is no optimum impedance level for hand prostheses.

For contact force minimization task, best performance is realized when the impedance level of the hand prosthesis are adjusted to a low level. Human-modulated impedance level also supports this result and sEMG estimation levels indicates the low impedance level as well. In the first category of he the trajectory tracking task, the high level impedance of the hand prosthesis provide best performance while subject is executing the task. for the second category of the experiment, while impedance is also modulated by the subject, the desired level is regulated at high level during the task perfor-

mance. The result of the two tasks shows that the impedance level of the hand prosthesis should not be designed at a constant level owing to satisfy best performance for each task simultaneously. In the interaction with a variable impedance environment task, the environmental conditions are unknown by the subject and hence subject has no prior information about appropriate impedance level for the task. In the first category of this experiment, the impedance of the hand prostheses are adjusted to three different impedance levels in each session. Since the environmental conditions are changing during the experiment, hand impedance level can not be matched with the task requirements. The result does not indicate the appropriate impedance level for the hand prosthesis. When the impedance is modulated by the user continuously during the second category of the experiment, the necessary impedance level for the hand is provided by the subject depending on the environmental conditions. The results also show that the best performance of the interaction with a variable impedance environment task is represented by the human-modulated impedance level through the sEMG signals.

The experimental results suggest that designing hand prosthesis with human-modulated variable impedance property provides effective and high performance use of these devices. The amputees can control the impedance level of the prosthesis in a natural way through the sEMG signals and determine the appropriate impedance level to improve the performance in various environmental conditions.

# Chapter 6

## 6 Conclusions and Future Works

In this work, design, manufacturing, and tele-impedance control of a variable stiffness transradial hand prosthesis is presented. In addition, the benefits of the user-based impedance modulation in hand prosthesis design are demonstrated by means of the human-subject experiments. The proposed variable stiffness transradial hand prosthesis is capable of modulation of impedance and position of fingers and its compliant fingers can easily adapt unstructured environments. Hence, depending on the environmental conditions, hand can regulate its stiffness and transmit stiffness level of the VSA to the compliant fingers. For instance, when the tasks require stiff interactions with the prosthetic hand, VSA increase their stiffness level by changing the position of the linear springs on the expanding contour.

The control of the variable stiffness transradial hand prosthesis were conducted through the sEMG signals. The muscle groups were chosen based on the condition of the transradial amputees. The position control of fingers was executed through the muscles placed under shoulder and chest. Besides, the impedance control of the fingers was realized through the intact muscle groups placed under the upper arm. For this control, position and stiffness references were estimated through the sEMG signals using the idea of the working principle of the antagonistic muscle groups. The position of the

fingers were regulated intentionally through the contraction of the muscles placed under the chest and shoulder. The stiffness modulation was automatically realized through the muscles placed under the upper arm. Subjects did not exert extra effort while modulating the impedance of the hand prosthesis. The stiffness and position modulation of the variable stiffness transradial hand prosthesis were validated with a series of human subject studies. It is demonstrated that stiffness can be easily adjusted to three different levels, while position is kept constant at a given reference value. Similarly, position was controlled to three different references while the impedance is kept constant. The working principles of the variable stiffness transradial hand prosthesis and finger compliance were also demonstrated with illustrative experiments. It is shown that, the variable stiffness transradial hand prosthesis can achieve successful grasps for objects of various geometry and different materials.

In the final part of the study, we hypothesized that human-based impedance modulation improves an amputee's performance during ADL. In order to investigate the validity of this hypothesis, we executed a series of experiments with a healthy volunteer. In these experiments, different category of tasks were presented to subject. During the study, the variable stiffness hand prosthesis was physically attached to the forearm of the volunteer. The physical coupling of the prosthetic device and the human arm enabled integration of physical interactions experienced by amputees to be integrated in the experiment. In addition, consistent placement of the prosthesis provided proper hand-eye coordination. Experimental results provided evidence that designing prosthesis with human based impedance modulation can significantly improve performance level of the amputees while interacting with the

various kind of tasks and/or unstructured environment.

Future works include integration of tactile feedback to variable stiffness transradial hand prosthesis to provide direct feedback to amputee and conducting experiments on larger set of volunteers involving transradial amputees to test efficacy of the proposed approach.

## References

- [1] E. J. Perreault, R.F. Kirsch, and P.E. Crago. Multijoint dynamics and postural stability of the human arm. *Experimental Brain Research*, 157(4):507–517, 2004.
- [2] F. Popescu, J.M. Hidler, and W.Z. Rymer. Elbow impedance during goal-directed movements. *Experimental Brain Research*, 152(1):17–28, 2003.
- [3] D.W. Franklin, E. Burdet, R. Osu, M. Kawato, and T.E. Milner. Functional significance of stiffness in adaptation of multijoint arm movements to stable and unstable dynamics. *Experimental Brain Research*, 151(2):145–157, 2003.
- [4] D.W. Franklin and T.E. Milner. Adaptive control of stiffness to stabilize hand position with large loads. *Experimental Brain Research*, 152(2):211–220, 2003.
- [5] D.W. Franklin, U. So, M. Kawato, and T.E. Milner. Impedance control balances stability with metabolically costly muscle activation. *Journal of Neurophysiology*, 92(5):3097–3105, 2004.
- [6] D.W. Franklin, M. Kawato, U. So, and T.E. Milner. Interacting with our environment: Impedance control balances stability and metabolic cost. In *IEEE Engineering in Medicine and Biology Society*, volume 2, pages 1440–1443, Sept 2003.

- [7] N. Hogan. Skeletal muscle impedance in the control of motor actions. *Journal of Mechanics in Medicine and Biology*, 02(03n04):359–373, 2002.
- [8] A. Blank, A.M. Okamura, and L.L. Whitcomb. Task-dependent impedance improves user performance with a virtual prosthetic arm. In *IEEE International Conference on Robotics and Automation (ICRA)*, pages 2235–2242, May 2011.
- [9] A. Blank, A.M. Okamura, and L.L. Whitcomb. User comprehension of task performance with varying impedance in a virtual prosthetic arm: A pilot study. *4th IEEE RAS EMBS International Conference on Biomedical Robotics and Biomechatronics*, pages 500–507, 2012.
- [10] A. Blank, A.M. Okamura, and L.L. Whitcomb. Task-dependent impedance and implications for upper-limb prosthesis control. *International Journal of Robotics Research*, 3(6):827–846, 2013.
- [11] E. Hocaoglu and V. Patoglu. Tele-impedance control of a variable stiffness prosthetic hand. In *IEEE International Conference on Robotics and Biomimetics (ROBIO)*, pages 1576–1582, 2012.
- [12] M. Yoshikawa, Y. Taguchi, S. Sakamoto, S. Yamanaka, Y. Matsumoto, T. Ogasawara, and N. Kawashima. Trans-radial prosthesis with three opposed fingers. In *IEEE/RSJ International Conference on Intelligent Robots and Systems (IROS)*, pages 1493–1498, Nov 2013.
- [13] Ottobock, 2014.
- [14] bebionic, 2014.

- [15] Touch Bionics Inc., 2014.
- [16] Motion Control Inc., 2014.
- [17] Liberating Technologies Inc., 2014.
- [18] Shadow Robot Company Ltd., 2014.
- [19] Meka Robotics, H2 Compliant Hand, 2014.
- [20] Meka Robotics, G2 Compliant Gripper, 2014.
- [21] Twendy-One, 2014.
- [22] Prensilia S.r.l., 2014.
- [23] W. Townsend. The barretthand grasper - programmably flexible part handling and assembly. *Industrial Robot: An International Journal*, 27(3):181–88, 2000.
- [24] Robotiq. Two-finger adaptive robot gripper, 2014.
- [25] B. et al. Rubinger. Self-adapting robotic auxiliary hand (sarah) for spdm operations on the international space station. In *I-SAIRAS, Quebec, Canada*, 2001.
- [26] Ottobock. Electric greifer, 2014.
- [27] Schunk. Schunk sdh hand, 2014.
- [28] S. M. Jimmy and G. Giuseppina. Robotic hands: Design review and proposal of new design process. In *Proceedings of World Academy of Science: Engineering & Technology*, pages 85–90, 2007.

- [29] A. Bicchi. Hands for dexterous manipulation and robust grasping: a difficult road toward simplicity. *IEEE Transactions on Robotics and Automation*, 16(6):652–662, Dec 2000.
- [30] B. Siciliano and O. Khatib, editors. *Springer Handbook of Robotics*. Springer, 2008.
- [31] T. Feix, R. Pawlik, H. Schmiedmayer, J. Romero, and D. Kragic. A comprehensive grasp taxonomy, June 2009.
- [32] I.M. Bullock and A.M. Dollar. Classifying human manipulation behavior. In *IEEE International Conference on Rehabilitation Robotics (ICORR)*, pages 1–6, June 2011.
- [33] C. Abul-Haj and N. Hogan. An emulator system for developing improved elbow-prosthesis designs. *IEEE Transactions on Biomedical Engineering*, BME-34(9):724–737, Sept 1987.
- [34] C. Abul-Haj and N. Hogan. Functional assessment of control systems for cybernetic elbow prostheses. i. description of the technique. *IEEE Trans. Biomed. Eng.*, 37(11):1025–1036, 1990.
- [35] C. Abul-Haj and N. Hogan. Functional assessment of control systems for cybernetic elbow prostheses. ii. application of the technique. *IEEE Trans. Biomed. Eng.*, 37(11):1037–1047, 1990.
- [36] J. W. Sensinger and R. F. Weir. User-modulated impedance control of a prosthetic elbow in unconstrained perturbed motion. *IEEE Trans. Biomed. Eng.*, 55(3):1043–1055, 2008.

- [37] M. Grebenstein, M. Chalon, G. Hirzinger, and R. Siegwart. Antagonistically driven finger design for the anthropomorphic dlr hand arm system. In *10th IEEE-RAS International Conference on Humanoid Robots (Humanoids)*, pages 609–616, Dec 2010.
- [38] S. Wolf, O. Eiberger, and G. Hirzinger. The DLR FSJ: Energy based design of a variable stiffness joint. *IEEE International Conference on Robotics and Automation*, pages 5082–5089, May 2011.
- [39] Guanglin Li and T.A. Kuiken. EMG pattern recognition control of multifunctional prostheses by transradial amputees. In *Annual International Conference of the IEEE Engineering in Medicine and Biology Society (EMBC)*, pages 6914–6917, Sept 2009.
- [40] C. Castellini, P. van der Smagt, G. Sandini, and G. Hirzinger. Surface EMG for force control of mechanical hands. In *IEEE International Conference on Robotics and Automation (ICRA)*, pages 725–730, May 2008.
- [41] Jun-Uk Chu, Inhyuk Moon, Yun-Jung Lee, Shin-Ki Kim, and Mu seong Mun. A supervised feature-projection-based real-time EMG pattern recognition for multifunction myoelectric hand control. *IEEE/ASME Transactions on Mechatronics*, 12(3):282–290, June 2007.
- [42] Domenico Prattichizzo, Monica Malvezzi, Marco Gabiccini, and Antonio Bicchi. On the manipulability ellipsoids of underactuated robotic hands with compliance. *Robotics and Autonomous Systems*, 60(3):337–346, 2012.

- [43] L. Birglen and C.M. Gosselin. On the force capability of underactuated fingers. In *IEEE International Conference on Robotics and Automation (ICRA)*, volume 1, pages 1139–31145, Sept 2003.
- [44] T. Laliberte, L. Birglen, and C. Gosselin. Underactuation in robotic grasping hands. In *Machine Intelligence and Robotic Control*, volume 4 of 3, pages 1–11, 2002.
- [45] Y. Kamikawa and T. Maeno. Underactuated five-finger prosthetic hand inspired by grasping force distribution of humans. In *IEEE/RSJ International Conference on Intelligent Robots and Systems (IROS)*, pages 717–722, Sept 2008.
- [46] Y.J. Shin, Keun-Ho Rew, Kyung-Soo Kim, and Soohyun Kim. Development of anthropomorphic robot hand with dual-mode twisting actuation and electromagnetic joint locking mechanism. In *IEEE International Conference on Robotics and Automation (ICRA)*, pages 2759–2764, May 2013.
- [47] Young June Shin, Ho Ju Lee, Kyung-Soo Kim, and Soohyun Kim. A robot finger design using a dual-mode twisting mechanism to achieve high-speed motion and large grasping force. *IEEE Transactions on Robotics*, 28(6):1398–1405, Dec 2012.
- [48] A.M. Dollar and R.D. Howe. A robust compliant grasper via shape deposition manufacturing. *IEEE/ASME Transactions on Mechatronics*, 11(2):154–161, 2006.

- [49] A.M. Dollar, L.P. Jentoft, J.H. Gao, and R.D. Howe. Contact sensing and grasping performance of compliant hands. *Autonomous Robots*, 28(1):65–75, 2010.
- [50] R.R. Ma, L.U. Odhner, and A.M. Dollar. A modular, open-source 3d printed underactuated hand. In *IEEE International Conference on Robotics and Automation*, May 2013.
- [51] C. English and D. Russell. Mechanics and stiffness limitations of a variable stiffness actuator for use in prosthetic limbs. *Mechanism and Machine Theory*, 34(1):7–25, Jan. 1999.
- [52] S. A. Migliore, E. A. Brown, and S. P. DeWeerth. Novel nonlinear elastic actuators for passively controlling robotic joint compliance. *Journal of Mechanical Design*, 129(4):406–412, 2007.
- [53] A. Howe, D. Thompson, and V. Wright. Reference values for metacarpophalangeal joint stiffness in normals. *Annals of the Rheumatic Diseases*, 44:469–476, July 1985.
- [54] F. Touvet, N. Daoud, J.P. Gazeau, S. Zeghloul, M. A. Maier, and S. Es-kiizmirli. A biomimetic reach and grasp approach for mechanical hands. *Robot. Auton. Syst.*, 60(3):473–486, March 2012.
- [55] K.B. Shimoga and A.A. Goldenberg. Soft materials for robotic fingers. In *IEEE International Conference on Robotics and Automation*, volume 2, pages 1300–1305, May 1992.
- [56] M.R. Cutkosky, J. Jourdain, and P. Wright. Skin materials for robotic fingers. In *IEEE International Conference on Robotics and Automation*, volume 4, pages 1649–1654, Mar 1987.

- [57] S. Plagenhoef, F.G. Evans, and T. Abdelnour. Anatomical data for analyzing human motion. *Quarterly for Exercise and Sport*, 54:169–178, 1983.
- [58] Paolo de Leva. Adjustments to zatsiorsky-seluyanov’s segment inertia parameters. *Journal of Biomechanics*, 29(9):1223–1230, 1996.
- [59] S. Rao, R. Carloni, and S. Stramigioli. Stiffness and position control of a prosthetic wrist by means of an emg interface. *IEEE EMBS*, pages 495–498, 2010.
- [60] R. Osu, D W. Franklin, H. Kato, H. Gomi, K. Domen, T. Yoshioka, and M. Kawato. Short- and long-term changes in joint co-contraction associated with motor learning as revealed from surface EMG. *J Neurophysiol*, 88:991–1004, 2002.
- [61] A. Ajoudani, N.G. Tsagarakis, and A. Bicchi. Tele-impedance: Preliminary results on measuring and replicating human arm impedance in tele operated robots. *IEEE International Conference on Robotics and Biomimetics*, pages 216–222, Dec. 2011.
- [62] A. Ajoudani, N.G. Tsagarakis, and A. Bicchi. Tele-impedance: An approach for skill based body machine interface. *International Workshop on Human-Friendly Robotic*, 2011.
- [63] H. Gomi and M. Kawato. Equilibrium-point control hypothesis examined by measured arm stiffness during multijoint movement. *Science*, 272(5258):117–120, 1996.

- [64] E. Burdet, R. Osu, D. W. Franklin, T. Yoshioka, T. E. Milner, and M. Kawato. A method for measuring endpoint stiffness during multi-joint arm movements. *Journal of Biomechanics*, 33(12):1705–1709, 2000.
- [65] E. Burdet, R. Osu, D. W. Franklin, T. E. Milner, and M. Kawato. The central nervous system stabilizes unstable dynamics by learning optimal impedance. *Nature* 414, pages 446–449, June 2001.
- [66] H. Gomi and R. Osu. Task-dependent viscoelasticity of human multi-joint arm and its spatial characteristics for interaction with environments. *Journal of Neuroscience*, 18:8965–8978, Nov. 1998.
- [67] I. W. Hunter and R. E. Kearney. Dynamics of human ankle stiffness: variation with mean ankle torque. *Journal of Biomechanics*, 15(10):747–752, 1982.
- [68] J. V. Basmajian and C. J. De Luca. *Muscles Alive*. Baltimore, MD: Williams and Wilkins, 1985.
- [69] D.K. Kuechle, S. R. Newman, E. Itoi, B.F. Morrey, and K N. An. Shoulder muscle moment arms during horizontal flexion and elevation. *Journal of Shoulder and Elbow Surgery*, 6(5):429–439, 1997.
- [70] W.M. Murray, S.L. Delp, and T.S. Buchanan. Variation of muscle moment arms with elbow and forearm position. *J Biomech*, 28(5):513–525, 1995.
- [71] M.R. Al-Mulla, F. Sepulveda, and M. Colley. A review of non-invasive techniques to detect and predict localised muscle fatigue. *Sensors*, 11(4):3545–94, Mar 2011.

- [72] R. Merletti, A. Rainoldi, and D. Farina. *Myoelectric Manifestations of Muscle Fatigue*, pages 233–258. John Wiley & Sons, Inc. Hoboken, New Jersey, 2005.
- [73] NK. Vollestad. Measurement of human muscle fatigue. *Journal of Neuroscience Methods*, 74(2):219–227, Jun 1997.
- [74] RM. Enoka and J. Duchateau. Muscle fatigue: what, why and how it influences muscle function. *Journal of Physiology*, 586(1):11–23, Jan 2008.
- [75] CJ. De Luca. Myoelectrical manifestations of localized muscular fatigue in humans. *Crit Rev. Biomed. Eng.*, Feb 1984.
- [76] M. Cifrek, V. Medved, S. Tonkovic, and S. Ostojic. Surface emg based muscle fatigue evaluation in biomechanics. *Clinical Biomechanics*, 24(4):327–340, Mar 2009.
- [77] M. Bilodeau, S. Schindler-Ivens, DM. Williams, R. Chandran, and SS. Sharma. Emg frequency content changes with increasing force and during fatigue in the quadriceps femoris muscle of men and women. *Journal of Electromyography and Kinesiology*, 13(1):83–92, Feb 2003.
- [78] R. Shadmehr and SP. Wise. *The Computational Neurobiology of Reaching and Pointing*. Cambridge, MA: MIT Press, 2005.
- [79] D.W. Franklin, E. Burdet, KP. Tee, R. Osu, CM. Chew, T.E. Milner, and M. Kawato. Cns learns stable, accurate, and efficient movements using a simple algorithm. *Journal of Neuroscience*, 28(44):3099–08, 2008.

- [80] P. Parker, K. Englehart, and B. Hudgins. Myoelectric signal processing for control of powered limb prostheses. *Journal of Electromyography and Kinesiology*, 16(6):541–548, 2006.
- [81] M.B. Silver-Thorn. In vivo indentation of lower extremity limb soft tissues. *Rehabilitation Engineering, IEEE Transactions on*, 7(3):268–277, Sep 1999.
- [82] YP1 Zheng, AF. Mak, and AK. Leung. State-of-the-art methods for geometric and biomechanical assessments of residual limbs: a review. *Journal of Rehabilitation Research & Development*, 38(5):487–504, Sep-Oct 2001.